# Fixing the Standard Model: From Dark Matter to the Baryon Asymmetry of the Universe

Seyda Ipek

A dissertation
submitted in partial fulfillment of the
requirements for the degree of

Doctor of Philosophy

University of Washington

2015

Reading Committee:

Ann Nelson, Chair

Steve Sharpe

Anna Goussiou

Program Authorized to Offer Degree:
Physics

University of Washington

**Abstract**

Fixing the Standard Model: From Dark Matter to the Baryon Asymmetry of the Universe

Seyda Ipek

Chair of the Supervisory Committee:
Professor Ann Nelson
Department of Physics

Since its foundation in the 20th century, the Standard Model has been immensely powerful in explaining many particle physics phenomena. With the discovery of the Higgs boson at the LHC, the Standard Model seems to be complete. However, there are many observations that we cannot explain within the Standard Model. After giving an introduction to the Standard Model, I focus on two questions that require beyond the Standard Model physics in this thesis: **1)** What is the particle nature of dark matter? **2)** Why is there a matter–antimatter asymmetry in the Universe?

## TABLE OF CONTENTS

## LIST OF FIGURES

## LIST OF TABLES

## ACKNOWLEDGMENTS

I thank first and foremost my advisor Ann Nelson for her time and effort as she helped me with my graduate work. She always had time for physics and quite often for a beer or two. Our conversations were mostly confusing moments for me while I struggled to comprehend her patient explanations of the same question I asked for the $n^{\text{th}}$ time. But asked her I did, and as this thesis is proof, it paid off.

I would also like to thank the members of the Particle Theory group, past and present, for being the best colleagues one could hope for. Max Hansen has always been a supportive friend and a knowledgable physicist to discuss, for example, details of dimensional regularization. Jakub Scholz was not only a great officemate but also a helpful mentor in physics and in life. Bridget Bertoni's attention to details has always pushed me to understand a subject in a deeper level. David McKeen's door was always open when I had a question about probably something I had asked Ann about but had not understood the answer to.

Coming from Turkey, half a world away from USA, I cannot thank enough to everyone who made Seattle home for me. Ahmet Keles made my transition as smooth as possible and has always helped me whenever he could. Fellow graduate students and my first roommates here, Chengeng Zeng and Spencer Williams, has been dear friends since we all moved to Seattle in 2010. My most sincere gratitude however goes to Paul Janos, alpha-housemate of 5249, collector of everything-stained-glass, life advisor to name a few of his qualifications, for providing a 'home' for me, in every sense of the word possible. I also cannot thank enough to my many housemates over the years, especially for putting up with my loud laughs and morning cheer. I thank Matthew Blosser, not just a roommate but also one of the best scientists I met, for introducing me to the amazing world of crosswords and for many *fun* discussions we had about physics, politics, ethics, etc. (It is not an exaggeration to say he has opinions about stuff.)

I also would like to thank my family, in Turkish if I may. Sevgili ailem, bana bütün eğitim hayatım boyunca yardımda bulunduğunuz için ne kadar teşekkür etsem azdır. Annem ve babamın, ben fizikçi olma hayallerimi kovalarken, çektiği sıkıntıların karşılığını alanımdaki en iyi bilim insanlarından biri olarak ödeyeceğimi umuyorum.

I cannot skip acknowledging the amazing staff of College Inn. Thanks for having the best pub in the U District, so close to the physics department!

Last but not least I would like to give my thanks to my thesis committee: Steve Sharpe, Anna Goussiou, Sanjay Raddy, Shih-Chieh Hsu, Marcel den Nijs and Tom Quinn.

Chapter 1

# INTRODUCTION

The Standard Model (SM) is a theory of elementary particles and their interactions via the strong and electroweak (EW) forces. The history of the SM, one can say, starts with the discovery of electron in cathode ray tube experiments by J.J. Thomson, J.S. Townsend, and H.A. Wilson in 1896. The prime-time of the SM was however the 20th century. In 1905 Albert Einstein published his seminal paper describing photon as 'the quanta of light', which brought him the Nobel Prize in 1921. Einstein's theory on the particle nature of photon was confirmed by Robert Millikan almost a decade later. In order to explain the apparent violation of energy, momentum and angular momentum conservation in beta decays, Wolfgang Pauli proposed the existence of a yet undetected neutral particle in 1930. This particle was detected in 1956 by Clyde Cowan and his team and later called the neutrino. Also around this time there were many discoveries of new hadrons. In 1960 Murray Gell-Mann and George Zweig, independently from each other, proposed the quark model to classify the baryons and mesons using a color symmetry. Almost all of the quarks were discovered during 1970s, at Stanford Linear Accelerator (up, down, strange, charm) and at Fermilab (bottom) and attracted many Nobel Prizes. With the observation of the top-quark in 1995 at Fermilab, all SM particles were accounted for but one: the Higgs boson. Higgs mechanism was developed over 1960s by many physicists including the most important contributions from P. Higgs, R. Brout and F. Englert. They had to wait five decades to see the SM completed by the discovery of the Higgs boson at the LHC in 2012. (See Fig. 1.1 for a brief timeline of the SM.)

The SM, with its particle content and gauge interactions explains a plethora of phenomena from the solar cycle to beta decay to particle–antiparticle oscillations. As an example of a very good model, it is important for a model builder to know about the SM and its phenomenology as much as possible. Hence, even though this thesis is about several

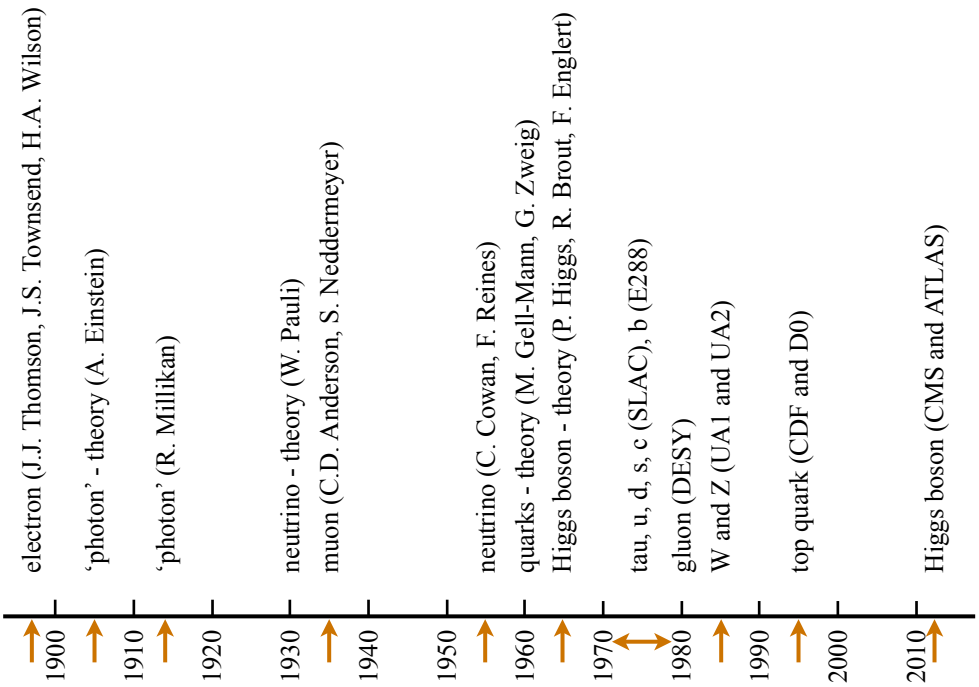


Figure 1.1: A brief history of the Standard Model

beyond-the-SM (BSM) models, I will start with a brief overview of the SM and some of its shortcomings. I will assume my audience to be comfortable with quantum field theory tools and ideas, *e.g.* renormalization, Feynman diagrams, loop calculations, and to have a working knowledge of group theory and thermal field theory, but not necessarily to be familiar with the details of the SM. Unfortunately I cannot give a (even close to) full account of the vast phenomenology of the SM here. I will mainly focus on the parts of the SM that has problems at explaining several observations. It is hoped that this thesis will be read by students who are just entering particle physics research and will pique their interest in the field of BSM physics. The curious reader should refer to [1–3] for more detailed discussions.

### *1.1 Standard Model Particles and Interactions*

Standard Model particles [1] include quarks, leptons, gauge bosons, and the Higgs boson. Interactions between these particles are described by the SM gauge group: $SU(3)_c \times SU(2)_L \times U(1)_Y$. Gauge fields are in adjoint representations of their respective gauge groups and mediate the corresponding interactions. The first gauge group, $SU(3)_c$ where $c$ is for color, corresponds to strong interactions mediated by gluons. Quarks are charged under this color group while leptons are not. $SU(2)_L \times U(1)_Y$ portion of the SM gauge group gives rise to weak and electromagnetic interactions, mediated by $W^{\pm}, Z^0$ and photon respectively, after the electroweak symmetry breaking, which we will discuss later. Here the subscript $L$ is for left-handedness and is there because only left-handed fermion fields are charged (i.e. transform non-trivially) under $SU(2)_L$ and the subscript $Y$ corresponds to hypercharge. Together, these fields include all observed elementary particles and their interactions via the fundamental forces, except for gravity. Table.1.1 shows the SM fields and their charge assignments under the SM gauge group.

Most general renormalizable Lagrangian written with the SM field content gives the SM Lagrangian

$$\begin{aligned}\mathcal{L} = &-\frac{1}{4}G^{\alpha}_{\mu\nu}G^{\alpha\mu\nu} - \frac{1}{4}W^{a}_{\mu\nu}W^{a\mu\nu} - \frac{1}{4}B_{\mu\nu}B^{\mu\nu} - \frac{g_3^2\,\theta_3}{64\pi^2}\epsilon_{\mu\nu\lambda\rho}G^{\alpha\mu\nu}G^{\alpha\lambda\rho} \\ &- \frac{1}{2}\bar{L}\not{D}L - \frac{1}{2}\bar{E}\not{D}E - \frac{1}{2}\bar{Q}\not{D}Q - \frac{1}{2}\bar{U}\not{D}U - \frac{1}{2}\bar{D}\not{D}D \\ &- y_{ij}\,\bar{L}^i\phi\,E^j - \tilde{y}^d_{ij}\,\bar{Q}^i\phi\,D^j - \tilde{y}^u_{ij}\,\bar{Q}^i(i\sigma_2)\phi^*U^j - (D_\mu\phi)^\dagger(D^\mu\phi) + V(\phi) + \text{h.c.}, \qquad (1.1)\end{aligned}$$

where $\alpha = 1, \ldots, 8$ is the $SU(3)_c$ index, $a = 1, 2, 3$ is the $SU(2)_L$ index and $i, j = 1, 2, 3$ are generation indices. Kinetic terms have the covariant derivative $D_\mu = \partial_\mu - ig_3\,\frac{1}{2}\lambda_\alpha G^\alpha_\mu - ig_2\,\frac{1}{2}\sigma_a W^a_\mu - ig_1\,\hat{Y}B_\mu$, where $\lambda^\alpha$ are Gell-Mann matrices that are generators of $SU(3)_c$, $\sigma_a$ are the Pauli matrices that are generators of $SU(2)_L$ and $\hat{Y}$ is the hypercharge operator. Gauge coupling constants $g_i$ are free parameters.

Each term in Eq. 1.1 induces many interactions between the SM particles. It is impossible

[1] Throughout this work *particle* and *field* are used interchangeably unless it is important to distinguish between a field and the particle it creates/annihilates. For an in-depth discussion of what a particle means, the reader is recommended to take a Quantum Field Theory class from Lawrence Yaffe.

| Fields \ Group | $SU(3)_c$ | $SU(2)_L$ | $U(1)_Y$ |
|---|---|---|---|
| $Q = \begin{pmatrix} u \\ d \end{pmatrix}_L$ | 3 | 2 | $\frac{1}{6}$ |
| $U = u_R$ | $\bar{3}$ | 1 | $\frac{2}{3}$ |
| $D = d_R$ | $\bar{3}$ | 1 | $-\frac{1}{3}$ |
| $L = \begin{pmatrix} \nu \\ e \end{pmatrix}_L$ | 1 | 2 | $-\frac{1}{2}$ |
| $E = e_R$ | 1 | 1 | $-1$ |
| $G_\mu^\alpha$ | 8 | 1 | 0 |
| $W_\mu^a$ | 1 | 3 | 0 |
| $B_\mu$ | 1 | 1 | 0 |
| $\phi = \frac{1}{\sqrt{2}} \begin{pmatrix} \phi^+ \\ h + v \end{pmatrix}$ | 1 | 2 | $\frac{1}{2}$ |

Table 1.1: Standard Model fields and their charge assignments under the gauge group $SU(3)_c \times SU(2)_L \times U(1)_Y$. We adopt the first generation notation for fermions, and suppress the generation index where possible. The first block has the quarks where $q_L$ is the $SU(2)_L$ quark doublet and $u_R, d_R$ are the right-handed up- and down-quark singlets. Note that the matrix structure corresponds to $SU(2)_L$ and not to the spinor structure of the fields. The second block contains the leptons, where $\ell_L$ is the $SU(2)_L$ lepton doublet and $e_R$ is the right-handed electron field. Note that there is no right-handed neutrino field. The third block has the gauge fields: $G_\mu^\alpha$, $\alpha = 1, \ldots, 8$, are gluons, different combinations of $W_\mu^a$, $a = 1, 2, 3$, and $B_\mu$ form the $W^\pm, Z$ bosons and the photon after the electroweak symmetry breaking. $\phi$ is the Higgs field with a vacuum expectation value $v$.

to go through each of them in great detail, but let us at least mention what is happening in each line.

1. In the first line of the SM Lagrangian are the field strength terms, $F_{\mu\nu} = [D_\mu, D_\nu]$, that give the kinetic terms and self-couplings for the gauge fields. The last term in this line violates charge-parity ($CP$) symmetry. It induces, for example, a neutron electric dipole moment (EDM). $CP$ violation in the EW sector of the SM is already observed in interesting phenomena. However, we have yet to observe any $CP$ violation in the strong interactions. The upper bound on the neutron EDM is $|d_n| < 2.9 \times 10^{-26} e\,\text{cm}$ [4], which puts an upper bound on the size of this term: $\theta_3 < 10^{-9}$. This small number contradicts the notion of *naturalness* in particle physics. Naturalness in this sense is a widely acknowledged idea that if some free parameter in a model is small, there must be a symmetry that when it is restored, the parameter is zero. This situation where $\theta_3$, a free parameter, is not an $O(1)$ number is called the *strong CP problem*. In 1977 Helen Quinn and Roberto Peccei proposed a solution to this problem by imposing a global $U(1)$ symmetry on the SM that gets spontaneously broken [5]. This symmetry breaking gives rise to a new particle called the *axion*, which is also a dark matter candidate.

2. The second line of the SM Lagrangian has the kinetic terms for fermion fields. Here $Q$ is an $SU(2)_L$ doublet that contains the left-handed up- and down-quarks, and similarly the $SU(2)_L$-doublet $L$ has the left-handed electron and neutrino:

$$Q = \begin{pmatrix} u_L \\ d_L \end{pmatrix}, \quad L = \begin{pmatrix} e_L \\ \nu_L \end{pmatrix} \tag{1.2}$$

   The right-handed fields ($U, D$ and $E$) are $SU(2)_L$ singlets. (Note that there is no right-handed neutrino field.[2]) Fermions interact with the gauge fields via the covariant derivatives.

3. The third line of Eq. 1.1 gives the Higgs field interactions – fermion masses via the Higgs mechanism, Higgs kinetic term, and Higgs self couplings. We will revisit the Higgs potential and EW symmetry breaking when we discuss the problem of producing

[2]This is because we have not observed any right-handed neutrinos yet. However, there are models with right-handed neutrinos, which we will discuss in later chapters.

the baryon asymmetry of the Universe in Section 1.2.2 and again in Chapter 4, so let us give a summary here. The Higgs potential

$$V(\phi) = \lambda \left( \phi^\dagger \phi - \frac{\mu^2}{2\lambda} \right)^2 , \tag{1.3}$$

has a minimum at $v^2 = \frac{\mu^2}{\lambda}$, where $v$ is called the *vacuum expectation value* (*vev*) of the Higgs field $\phi = \frac{1}{\sqrt{2}} \left(\phi^+,\ h + v\right)^{\mathrm{T}}$. The Higgs field expectation value can be gauged fixed to the form $\langle \phi \rangle = \frac{1}{\sqrt{2}}(0,\ v)^T$, which still leaves the gauge invariance of the subgroup $U(1)_{\mathrm{em}}$ (of $SU(2)_L \times U(1)_Y$) explicit. Electromagnetic charge of a particle is $Q = T^3 + Y$, where $T^3$ is the third component of the weak isospin. This mechanism is called *EW symmetry breaking*[3].

All SM particles (save the neutrinos) get their masses through the Higgs field. But most important of all are the gauge bosons, which gets their masses through the Higgs kinetic terms after the EW symmetry breaking: $M_W = \frac{g_2\, v}{2} = 80$ GeV and $M_Z = \frac{M_W}{\cos\theta_W} = 91$ GeV, where $\tan\theta_W = \frac{g_1}{g_2}$ is called the *Weinberg angle*. This mechanism was introduced in 1964 by Peter Higgs [6] and Robert Brout and François Englert [7], independently from each other, explaining how to have massive gauge bosons and predicting a Higgs particle. The Higgs mass, $m_h = \sqrt{2\lambda} v = 125$ GeV, was measured by the LHC experiments CMS [8] and ATLAS [9] in 2012, completing the SM and earning Englert and Higgs the 2013 Nobel Prize[4]. Higgs field also gives mass to fermions through the Yukawa terms: $m_f = \frac{y_f\, v}{\sqrt{2}}$, where $y_f$ is the Yukawa coupling for a fermion $f$. (The careful reader might have noticed the (generation) index structure of the Yukawa couplings in Eq. 1.1. We will explain this in the next section shortly.)

There are 19 free parameters in the SM: Three gauge coupling constants, $g_1, g_2, g_3$; $CP$-violating coupling in the strong sector, $\theta_3$; 9 fermion masses, Higgs mass and self-coupling constant, three mixing angles and one phase in the quark mixing process, which we will discuss shortly. The SM Lagrangian with these parameters gives an amazingly rich

[3] *Symmetry breaking* terminology is misleading when talking about gauge symmetries.

[4] Unfortunately Brout had passed away and the Nobel Prize is not awarded posthumously.

phenomenology. I do not have the means or the space to delve into how the SM explains almost all of our observations regarding particle physics. However, I will discuss one SM process, quark mixing, since it plays a possible role in generating the matter asymmetry of the Universe.

### *1.1.1 Quark Mixing and CP Violation*

The Yukawa couplings $y_{i,j}$ and $\tilde{y}^{u,d}_{ij}$ in Eq.1.1 are not necessarily diagonal in the flavor basis. Lepton Yukawas can be made diagonal by field redefinitions without affecting any other term in the Lagrangian. However the quark sector is more complicated. In order to diagonalize the quark Yukawas we can rotate the up- and down-type quark fields by unitary matrices

$$u_i \to V^u_{ij}\, u_j, \quad d_i \to V^d_{ij}\, d_j, \tag{1.4}$$

such that the mass terms in the Lagrangian changes as

$$\frac{\tilde{y}^u_{ij}\, v}{\sqrt{2}} V^{u*}_{ki} V^u_{jl}\, \bar{u}_k u_l + \frac{\tilde{y}^d_{ij}\, v}{\sqrt{2}} V^{d*}_{ki} V^d_{jl}\, \bar{d}_k d_l \longrightarrow \frac{y^u_i\, v}{\sqrt{2}}\, \bar{u}_i u_i + \frac{y^d_i\, v}{\sqrt{2}}\, v\, \bar{d}_i d_i. \tag{1.5}$$

This rotation of the quark fields also affects the EW sector of the SM. For example, quark–$W$-boson interactions become

$$g_2\, W^+_\mu\, \bar{u}\gamma^\mu(1-\gamma_5)d \longrightarrow g_2\, (V^{u\dagger}V^d)\, W^+_\mu\, \bar{u}\gamma^\mu(1-\gamma_5)d. \tag{1.6}$$

Due to this rotation quark mass eigenstates are not weak-interaction eigenstates. The mass and interaction eigenstates are related via a complex, unitary matrix called the Cabibbo-Kobayashi-Maskawa (CKM) matrix,

$$\begin{aligned} V_{CKM} = V^{u\dagger}V^d &= \begin{pmatrix} V_{ud} & V_{us} & V_{ub} \\ V_{cd} & V_{cs} & V_{cb} \\ V_{td} & V_{ts} & V_{tb} \end{pmatrix} \\ &= \begin{pmatrix} c_{12}c_{13} & s_{12}c_{13} & s_{13}\, e^{-i\delta} \\ -s_{12}c_{23} - c_{12}s_{23}s_{13}\, e^{i\delta} & c_{12}c_{23} - s_{12}s_{23}s_{13}\, e^{i\delta} & s_{23}c_{13} \\ s_{12}s_{23} - c_{12}c_{23}s_{13}\, e^{i\delta} & -c_{12}s_{23} - s_{12}c_{23}s_{13}\, e^{i\delta} & c_{23}c_{13} \end{pmatrix}, \end{aligned} \tag{1.7}$$

where $s_{ij} = \sin\theta_{ij}$. $V_{CKM}$ has three mixing angles, $\theta_{12}, \theta_{13}, \theta_{23}$, and one phase, $\delta$. Precise measurements of the CKM angles is a good test of the SM since any deviations from unitarity is a sign of new physics [10].

Most important feature of the CKM matrix for my graduate research has been the $CP$ violation it brings to the SM. The phase in $V_{CKM}$ is the only observed source of $CP$ violation in the SM[5]. By late 1950s it was shown that weak interactions do not conserve $C$ and $P$ symmetries separately. It was not known if the combination, $CP$ symmetry, was conserved until 1964. J.W. Cronin and V.L. Fitch showed that $CP$-symmetry is violated in neutral kaon, a bound state of strange and down quarks, decays [11]. However at that point, lacking a full knowledge of the quark sector, the source of this $CP$ violation was not understood. In 1973 M. Kobayashi and T. Maskawa [12], building on N. Cabibbo's previous work [13], proposed that if there exists a third generation of quarks, $CP$ violation can be incorporated into the weak interactions via a quark mixing matrix as in Eq. 1.7. Indeed one can show that with only two families of quarks, the phase in $V_{CKM}$ is only an overall phase, and can be rotated away by field redefinitions. In the last few years $CP$ violation has also been observed in $B$- and $D$-meson decays.

Observation of $CP$ violation in the SM has existential importance. If $CP$ is a good symmetry, matter and antimatter behave exactly the same. But we know the Universe is not $CP$ symmetric because there is more matter than antimatter in the cosmos. Then this gives a chance to the SM, a model that explains almost every particle physics phenomenon, to explain the matter asymmetry of the Universe. However, as we will discuss in Section 1.2.2, this $CP$ violation is not enough to produce the observed baryon asymmetry.

## *1.2 Problems with the Standard Model*

The SM gives us an understanding of the interactions of the known elementary particles via the strong, weak and electromagnetic forces. It explains a wide range of physical phenomena, from auroras to Compton scattering. However the SM still has its limitations, and, though definitely not wrong, it is incomplete. Problems of the SM can be loosely divided into

[5]Neutrinos mass eigenstates are also a mixture of flavor eigenstates. There can be $CP$ violation in this mixing. However, there are no observations hinting at that.

two types[6]: **(i)** *Existential problems* that are due to inherent shortcomings of the SM such as the lack of an explanation for the origin of neutrino masses and **(ii)** *ephemeral problems* that are due to *curious*, i.e. with somewhat important statistical significance, unexplained observations at particle detectors such as a forward-backward asymmetry in top–antitop quark production at the Tevatron [14, 15]. Even though ephemeral problems, sometimes also referred to as *detector anomalies*, often go away with further scrutiny by the experimental physicists or by better understanding of SM predictions, this classification does not necessarily make one type of problems more important than the other to work on, as many anomalous observations of varied significance led to the completion of the SM. While as an ephemeral problem of its time I worked on the $t\bar{t}$ forward-backward asymmetry problem [16], my graduate work mostly spanned existential problems of the SM. Hence I will give a summary of these problems (and details of a couple) in this section. These problems, most of them named (since we like to give names to things we do not understand) and not ordered with respect to importance, are listed below.

1. Neutrinos, at least two flavors of them, have masses albeit very small ($< O(\text{eV})$). However there is no right-handed neutrino singlet. Hence, neutrinos cannot get their masses via coupling to the Higgs field, unlike other fermions. There are numerous new physics proposals to explain the neutrino masses, *e.g.* heavy right-handed neutrinos, but none of them has been experimentally verified yet.

2. As explained after Eq. 1.1 the smallness of the $\theta_3$ parameter cannot be explained with any fundamental symmetries of the SM and dubbed *the strong CP problem*. The canonical solution to this problem is given by R. Peccei and H. Quinn and predicts new scalar particles called *axions*. Apart from solving the strong $CP$ problem, axions are also a dark matter (DM) candidate. There are various experiments that are searching for axions, *e.g.* ADMX experiment at the University of Washington.

3. The SM covers a range of scales, even only in the quark sector with up-/down-quark

[6]This classification has its own problems, especially when it comes to situations where an observation fits into both categories, such as indirect signatures of dark matter–SM interactions.

masses of $O$(MeV) and a top-quark mass of 173 GeV. In addition there is no reason why there should be only 6 flavors of quarks or leptons. Collectively, these are called *flavor problems*.

4. The Universe is thought to have gone through an inflationary period of exponential expansion. In most theories this process requires an inflaton particle. The SM does not contain an inflaton.

5. The SM includes only three of the four fundamental interactions; gravity is not emergent from the SM.

6. Furthermore the gravitational scale, $M_{\text{Planck}} \sim 10^{19}$ GeV, is far removed from the weak scale, $O$(100 GeV). This separation of scales is called *the hierarchy problem* since it is not understood why these two scales are 17 orders-of-magnitude different. There are two ways to look at this problem. One is to try to explain why gravity is so weak, *e.g.* with extra dimensions that the graviton, gravitational force carrier, lives in. There are several experiments that are searching for extra dimensions, mostly via testing the inverse-square low. University of Washington hosts the Eöt-Wash group that pioneered the search for macroscopic extra dimensions.

7. Another way to look at the hierarchy problem is to understand why the weak scale is so low. Weak scale is set by the weak boson masses, which are set by the *vev* of the Higgs field. (This is also related to the mass of the Higgs boson, and is framed almost exclusively as "Why is the Higgs mass so small?".) In a way the Higgs mass is not natural since there are no symmetries to protect its mass from getting large quantum corrections, unlike the fermion masses which are protected by a chiral symmetry or photon and gluon masses which are protected by gauge symmetries. This is often called *the naturalness* or *fine-tuning problem*, since it is thought that large quantum corrections to the Higgs mass should be cancelled by some process in a very precise way. Supersymmetry, the most popular new physics model in the last few decades, provides a solution to this problem. Supersymmetry (SUSY) is a generalization of Poincaré

algebra and relates fermions and bosons. In the minimally supersymmetric Standard Model (MSSM), there is a scalar partner for every SM fermion and a fermionic partner for every SM boson. Investigating the loop corrections to the Higgs mass in MSSM, one finds that scalar contributions to the corrections cancel the contributions from their fermion partners to a degree. The largest particle collider experiment, LHC, is searching for supersymmetric particles, but they have not been observed as of 2015[7].

8. The limitations of the SM become even more apparent when we look at our Universe at large. 69% of the energy budget of the Universe is dark energy [17]. This is a mysterious form of energy with negative pressure that is responsible for the acceleration of the Universe. The SM does not include any particles that fits these properties.

9. 26% of the Universe's energy density comes from dark matter, kind of matter that interacts almost only gravitationally, and only 5% is baryonic matter[8]. There is no elementary particles in the SM that can be considered as dark matter. I will discuss what we know about dark matter in more detail in the following section.

10. The baryonic matter in the Universe is dominantly matter, i.e. there is very little antimatter. The baryon asymmetry of the Universe is quantified as $\frac{n_B - n_{\bar{B}}}{s} \simeq 10^{-10}$ where $n_{B,(\bar{B})}$ is the (anti)baryon number and $s$ is the entropy density. Even though the SM violates $CP$ symmetry, hence matter and antimatter interact differently, it still cannot explain why there is so much more matter than antimatter. I will discuss this shortcoming of the SM in Section 1.2.2.

It is hoped that we will find solutions to all of these problems, extending the SM to a complete model, and understand Nature in full. Unfortunately, so far, I only had the chance to investigate a couple of these problems in detail and to offer new physics models to explain them. In the following sections I will discuss our knowledge of dark matter and the SM processes that was thought to explain the baryon asymmetry of the Universe.

---

[7] Or to put it more positively: Only half of the supersymmetric particles have been observed.

[8] In cosmological and astrophysical sense, baryonic matter refers to all the particles in the SM, and not just the baryons.

### *1.2.1 Dark Matter: What We Know*

In 1933, while investigating the Coma galaxy cluster, F. Zwicky realized that the virial mass of the cluster was higher than the luminous mass [18]. He attributed this discrepancy to some matter that did not emit light, and called it *dark matter*. In 1970's and early 80's V.C. Rubin and her colleagues were studying galaxy rotation curves and they showed, first in Andromeda and then also in other galaxies, that the stars in galaxies have similar velocities independent of their distance from the center of the galaxy. One expects the rotational velocities to fall off with an inverse-square law as moving further from the center, if the bulk mass of the galaxy is located at the center (see Fig. 1.2). Rubin employed Zwicky's dark matter (DM) idea, that there is some unaccounted for matter distributed throughout the galaxies, to explain these observations.

In the early 2000's, the evidence for DM started piling in from two directions. First was the NASA mission WMAP (Wilkinson Microwave Anisotropy Probe), launched in 2001 to observe the Cosmic Microwave Background (CMB). CMB is a picture of the Universe when it was about 380.000 years old. About that time the Universe was filled with hot, dense, ionized hydrogen. Photons were trapped in this relativistic fluid and the Universe was *opaque*. When the temperature dropped below $\sim$3000 K, electrons bonded to the hydrogen, and photons could escape. This happened at a redshift of $z \sim 1000$, hence these photons are now in the microwave range. Since the CMB photons were involved in the motion of the relativistic fluid prior to their escape, they give us an idea of what the Universe was going through before the last scattering. (The most recent measurement of the CMB spectrum can be seen in Fig. 1.2.) The most visible feature of the CMB power spectrum is its oscillatory structure. This is an imprint of the acoustic oscillations that the early plasma went through due to the competition between a gravitational potential that was pulling the matter towards overdense regions and photon pressure that pushes everything out. Since DM has very weak interactions with everything else, it tends to just sit at the center of the gravitational well, while the rest of the plasma is going under oscillations. Energies of the photons that escaped this potential depend on how strong the gravitation was when they left. Thus, looking at the relative peak strengths in the CMB spectrum, one can deduce

the amount of DM in the Universe. WMAP was the first experiment to measure the CMB spectrum in detail to find that 24% of the Universe is made up of DM [19]. By now we have much more precise observations by Planck satellite and the DM is measured to fill 26% of the Universe.

A direct evidence for the existence of DM came in 2006 from observation of the merger of two galaxy clusters [20]. Most of the baryonic mass of a cluster is not bound in galactic stars (1%) but is in intracluster plasma (5-15%). When two clusters collide, while the galaxies do not interact much with each other, the plasma experiences a friction and lags behind the galactic mass. X-ray observations of the *bullet cluster* show where the centers of the plasma mass is, as can be seen in Fig. 1.2. If the clusters had only baryonic matter, the gravitational centers would follow the X-ray centers. However weak lensing observations of the same merger show that the gravitational centers of the two clusters are far from the plasma. Hence, it can be concluded that most of the clusters was made up DM and DM did not have any appreciable interactions to slow it down.

Careful reader might have realized that all of these hints of the existence of DM comes from its gravitational interactions with the baryonic matter. So far we have no information regarding the particle nature of DM or any strong evidence for its interactions with the SM or with itself. For astrophysicists this is not a bug but a feature. Non-relativistic (cold) and collisionless DM is fairly good at explaining the CMB, and also gives more or less the right structure in the Universe. But this is a nagging issue for particle physicists: DM must have been produced with the rest of the matter after the Big Bang, so it must couple to the SM at some level.

As is, the SM does not include any candidates that can be DM. In the past, it was thought that neutrinos could have been DM since they interact so little with everything else. However, neutrinos are too light. The structure in the Universe would be different if particles like neutrinos were DM. For example, structures on larger scales, *e.g.* superclusters of galaxies, would have formed before structures on smaller scales, *e.g.* galaxies. This is contrary to the more bottom-up structure formation that is observed, where small structures form earlier.

The most popular way to describe DM as some sort of particle is to think of it as a

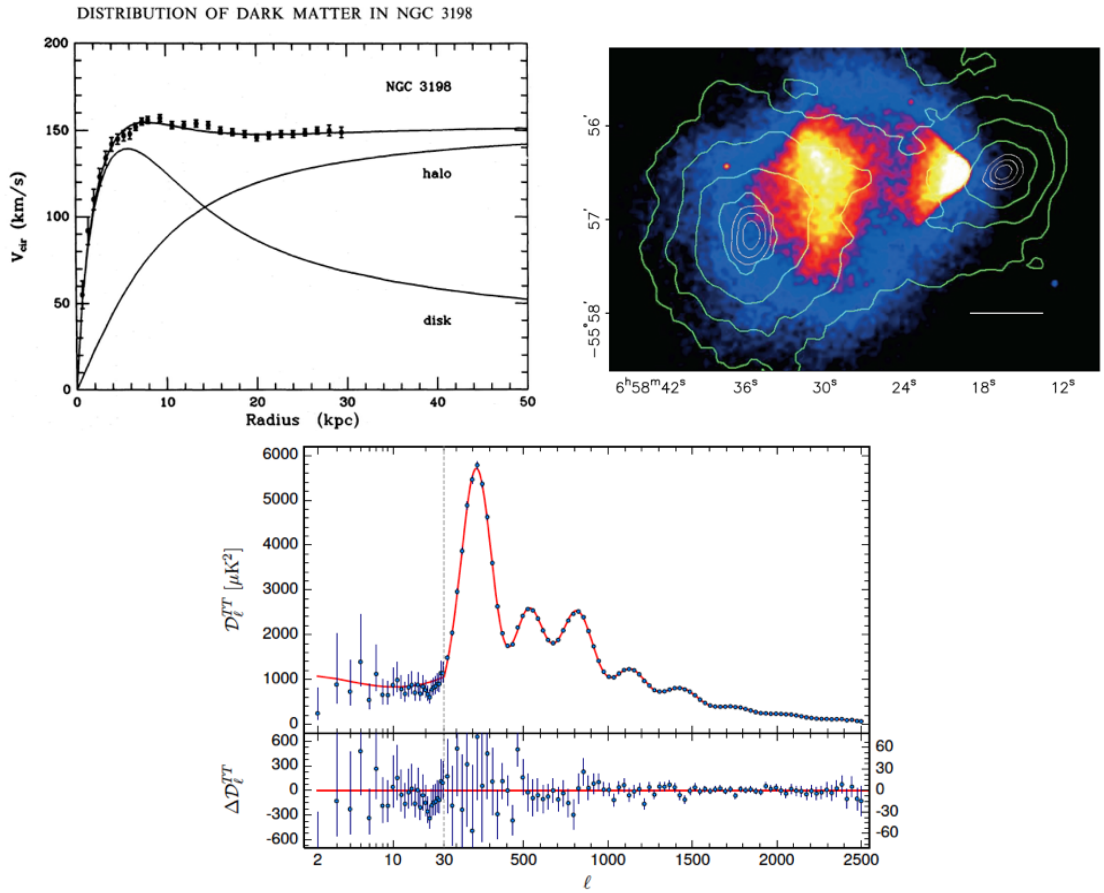


Figure 1.2: Top left: Rotational velocities of stars in the spiral galaxy NGC 3198 [21]. That the velocities do not fall off with the distance from the center of the galaxy was the first hint for DM. Top right: Color image of a cluster merger (called *bullet cluster*) [20], with the white bar indicating 200 kpc. Intracluster plasma, slowed down due to its interactions, is seen as bright regions, Gravitational equipotential contours do not follow the hot plasma. This is a clear sign for the existence dark matter, which has at best very minimal interactions with the baryonic matter. Bottom: Power spectrum of the CMB measured by the Planck satellite [17]. Dark matter affects the gravitational potential well that is involved in the acoustic oscillation of the plasma in the early Universe. Amount of dark matter can be inferred from the heights of the peaks in the CMB spectrum.

*weakly interacting massive particles* (WIMP) in the following sense. Massive DM particles and antiparticles were produced thermally in the early Universe. As the Universe expands, it cools. When the temperature drops below the mass of the DM particles, the production stops. After that particles and antiparticles can still annihilate with some cross section $\sigma$. Particle–antiparticle annihilation ceases when the annihilation rate becomes comparable to the expansion rate of the Universe, $n\langle\sigma v\rangle \sim H(T)$ where $n$ is the DM number density, $v$ is the DM velocity and $H$ is the Hubble constant at temperature $T$. This sets the relic density of DM, and requires a cross section $\sigma \sim 10^{-36}$ cm$^2$ for a particle with mass $O(1 - 100\text{GeV})$. These numbers are at the weak interaction scale, and this process is often referred to as the WIMP miracle. (See, for example, [22] for a nice read about DM and other mysteries of the Universe.)

The WIMP miracle sets the model-building ground for many DM models. In addition, since WIMPs live around the weak scale, it is logical to assume they are connected to the SM, which has its own weak sector. Needless to say, there are numerous experiments searching for DM–SM interactions. These searches are usually classified in three groups: **(i)** Direct searches where one looks for interactions of the DM around us with some nuclei in a detector. **(ii)** Indirect detection where decay or annihilation products of DM is searched for. **(iii)** Collider searches where DM production through SM interactions is studied. (See Fig. 1.3.)

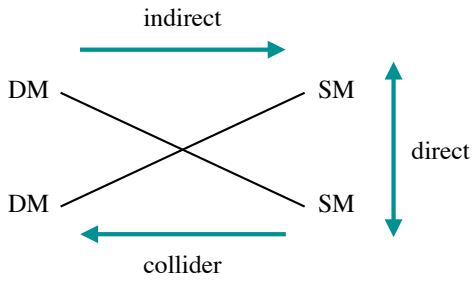


Figure 1.3: Schematic description of DM search methods.

Direct detection and collider experiments have been looking for DM–SM interactions everywhere, but so far we only have upper limits on the interaction strength. However, there are some indirect hints of DM–SM interactions. We will discuss these hints and

possible new physics explanations in Chapters 2-3. We also note that WIMP mechanism is not the only possiblity to get the correct DM density. For example, DM might not be thermally produced or the DM density might be set by some asymmetry.

### *1.2.2 Baryon Asymmetry of the Universe and Electroweak Baryogenesis*

There are more baryons than antibaryons in the Universe[9]. There are two separate measurements of this asymmetry. First one is from the CMB. As described in the previous section, acoustic oscillations of the relativistic fluid leaves its imprint on the CMB power spectrum. The relative heights and places of the peaks in the CMB power spectrum depends on the net baryon density of the Universe. Second method to measure the baryon asymmetry is to measure the abundances of light nuclei, such as deuterium and lithium [23]. These elements were formed at $T \sim 1$ MeV, and their abundance depends strongly on the amount of baryons that were present at the time. Both of these measurements give a baryon asymmetry to entropy ratio of

$$\eta \equiv \frac{n_B - n_{\bar{B}}}{s} \simeq 10^{-10}, \tag{1.8}$$

where $s$ is the entropy density of the Universe, and $B(\bar{B})$ is the (anti)baryon number. $\eta$ is the canonical measure of the baryon asymmetry since it does not change as the Universe expands as long as there are no processes that produce a large amount of entropy.

How did this baryon asymmetry come to be? In 1967 A.D. Sakharov showed that three conditions must be satisfied in order to produce a net baryon number in any model of the Universe [24]. **(1) Baryon number cannot be a conserved quantity.** In an inflationary Universe, we assume there was no initial baryon asymmetry to begin with. Since there is a baryon asymmetry now, baryon number must have been violated at some point. **(2) $C$- and $CP$-symmetries must be violated.** These symmetries basically give a way to differentiate matter and antimatter. In the early Universe there must exist some interactions which preferred to destroy antimatter more than matter. **(3) These $B$-,**

[9] I will use *matter–antimatter asymmetry* and *baryon–antibaryon asymmetry* interchangeably. By charge conservation, charged leptons must have the same asymmetry as baryons. This is not so for neutral leptons, i.e. neutrinos. A non-zero neutrino asymmetry would alter the abundances of light nuclei such as $^4$He, and is very interesting. However, we will not discuss this further in the present work.

**$C$- and $CP$-violating processes should happen out of thermal equilibrium.** In a $CPT$-invariant Universe, in thermal equilibrium, any process that produces baryon number would also happen in the opposite direction, destroying baryons, with equal rate.

An immediate question follows: Does the SM satisfy these three conditions, hence explain the baryon asymmetry? The short answer is 'No'. However, it is still important to know how the SM baryogenesis works and does not work because many new physics models are either an extension of EW baryogenesis or employ portions of it that work. Hence let us discuss a longer version of the answer with explanations[10].

**(1) Baryon number is anomalously violated in the SM**. At the classical level the SM Lagrangian in Eq. 1.1 conserves both baryon number[11] and lepton number ($L_n$, $n = e, \mu, \tau$). However, at the quantum level baryon and lepton currents, $j^{B,L}$ are not conserved due to an $SU(2)_L$ anomaly[12]

$$\partial^\mu j^B_\mu = 3\frac{g^2}{16\pi^2} W^{\mu\nu\,a}\widetilde{W}^a_{\mu\nu}, \quad \partial^\mu j^{L_n}_\mu = \frac{g^2}{16\pi^2} W^{\mu\nu\,a}\widetilde{W}^a_{\mu\nu}, \tag{1.9}$$

where $\widetilde{W}^a_{\mu\nu} = \frac{1}{2}\epsilon_{\mu\nu\lambda\rho}W^{\lambda\rho\,a}$. Due to this anomaly a baryon number can be produced between an initial time $t_i$ and a final time $t_f$

$$\Delta B = \int_{t_i}^{t_f} d^4x\; 3\frac{g^2}{16\pi^2} W^{\mu\nu\,a}\widetilde{W}^a_{\mu\nu}, \tag{1.10}$$

where the integral takes integer values for vacuum to vacuum transitions and is the same for lepton number production. We can understand this through a potential as in Fig. 1.4. Different $SU(2)_L$ field configurations have different energies and the maximum energy configuration is called *sphaleron* with $E_{\rm sph} = \frac{2M_W}{\alpha_W} B\left(\frac{m_h}{M_W}\right)$, where $B$ is $O(1)$. The Universe needs to come over this energy barrier in order to change its baryon number. At zero temperature the Universe sits at one of the minima of this potential, and the only way it can change to another minima is through tunneling processes (instantons). The rate for

[10] See [22] for a very nice discussion of baryogenesis.

[11] When I say *baryon number*, most of the time I mean a net baryon number, $B - \bar{B}$. This should be clear from the context.

[12] This anomaly arises because left- and right-handed fields interact differently under $SU(2)_L$ – in fact right-handed fields do not interact with the weak force. The calculation of the anomaly is very similar to the chiral anomaly. For details see, *e.g.*, [3] or various lecture notes from the University of Washington Particle Theory Journal Club.

tunneling is extremely small, $\Gamma \sim \mathrm{e}^{-4\pi/\alpha_W} \sim \mathrm{e}^{-165}$. Hence, baryon number does not change currently. However, at finite temperatures, Universe can be in a sphaleron configuration and can jump over the extremum point. At very high temperatures, the Universe is in an unbroken phase, i.e. Higgs field has zero *vev*, and $M_W = 0$. In this case the sphaleron processes occur very rapidly with $\Gamma_{\rm sph} \simeq 25\,\alpha_W^5 T$. At temperatures close to the EW transition, $T \sim 100$ GeV, the sphaleron rate gets a Boltzmann suppression,

$$\Gamma_{\rm sph} \simeq T \exp\left[-\frac{2M_W(T)}{\alpha_W T} B\left(\frac{m_h}{M_W}\right)\right], \tag{1.11}$$

where $M_W(T) = g_2\langle\phi(T)\rangle$. Comparing this rate with the expansion rate of the Universe, $H \sim \frac{T^2}{M_{\rm Pl}}$ where $M_{\rm Pl}$ is the Planck mass, shows that sphaleron processes switch off after the EW transition, $T \sim 100$ GeV. More detailed calculations give $T = 131.7 \pm 2.3$ GeV [25].

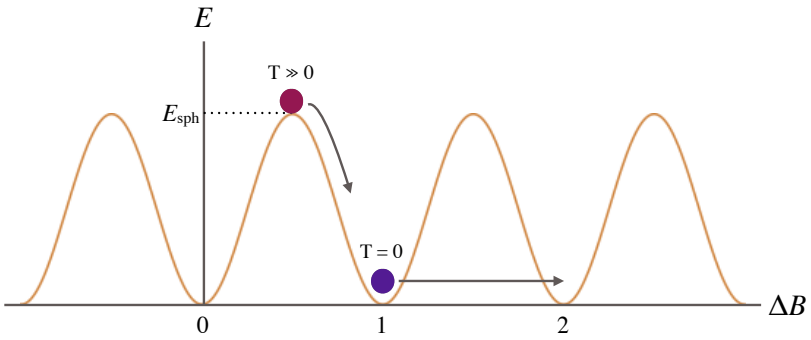


Figure 1.4: Schematic description of baryon number violation via the $SU(2)_L$ anomaly. At zero temperature the Universe needs to tunnel between different minima of this potential to change baryon number. At finite temperatures it can jump over the extremum of the potential.

**(2) The SM has $CP$ violation in the EW sector, but this $CP$ violation is not enough.** In order to retain the $CP$-violation in the CKM matrix in a process, all three generations of quarks must be involved. Hence $CP$ violation is suppressed by not only small mixing angles but also small Yukawa couplings. It is shown that the SM $CP$ violation gives at best $\eta \sim 10^{-20}$ [26, 27].

**(3) There are no out-of-equilibrium processes in the SM.** At a temperature

about 100 GeV, the Hubble rate is $\sim 10^{-14}$ GeV, while the EW processes are happening with a much faster rate of $\sim 1$ GeV. For a process $X$ to happen *out-of-equilibrium*, its rate should be smaller than the Hubble rate at some temperature $T$, $\Gamma_X < H(T)$. It is not obvious what processes can be out-of-equilibrium in the SM. Once upon a time it was thought that the EW phase transition[13] could provide out-of-equilibrium conditions for the baryon asymmetry production, if it was found to be first order [29]. We can see how the SM transition happens with a very simplified picture of what happens as the Universe cools down from $T \gg 100$ GeV to $T = 0$. At high temperatures and in the weak coupling regime, one-loop effective potential of the Higgs field is

$$V(\phi, T) = \lambda \left(\phi^2 - \frac{v^2}{2}\right)^2 + \frac{T^2}{24}\left(\sum_{\text{bosons}} g_i m_i^2(\phi) + \frac{1}{2}\sum_{\text{fermions}} g_i m_i^2(\phi)\right) - \frac{T}{12\pi}\sum_{\text{bosons}} g_i m_i^3(\phi) + O\left(m \log\left(\frac{m}{T}\right)\right), \tag{1.12}$$

where $g_i$ is the degeneracy factor of $i$th particle and

$$m_f = y_f\,\phi, \quad M_W = \frac{g_2}{\sqrt{2}}\phi, \quad M_Z = \frac{\sqrt{g_2^2 + g_1^2}}{\sqrt{2}}\phi.$$

Most important contributions to Eq. 1.12 come from $W/Z$-bosons and the top quark due to their large couplings to the Higgs. Then we can write the potential as

$$V(\phi, T) \simeq \lambda \left(\phi^2 - \frac{v^2}{2}\right)^2 + \alpha\frac{T^2\phi^2}{24} - \beta\frac{T\phi^3}{12\pi}, \tag{1.13}$$

where

$$\alpha = \frac{2}{v^2}\left(6M_W^2 + 3M_Z^2 + 6m_t^2\right), \qquad \beta = \frac{\sqrt{2}}{v^3}\left(6M_W^3 + 3M_Z^3\right). \tag{1.14}$$

At high temperatures, $T \gg m_i$, the minimum of the potential is $\phi = 0$. This corresponds to the unbroken phase, where the SM particles are massless. (This is not quite true since all fields have some thermal value at finite temperature.) As the temperature cools down, the potential starts having other local minima. At some critical temperature $T = T_c$, we expect the global minimum of the potential to be at $\phi \neq 0$ which corresponds to the broken phase. Eventually we have $\phi = v/\sqrt{2}$ at $T = 0$. The structure of this change in the potential, and

[13] For an introduction to phase transitions, with a renormalization group approach, see [28].

hence the order of the phase transition, depends on a competition between the $T^2\phi^2$ and $T\phi^3$ terms in Eq. 1.13. (See Fig. 1.5 for a schematic description of a first- and second-order transition.) It turns out, in the SM, the EW transition is not a first-order phase transition but a crossover.

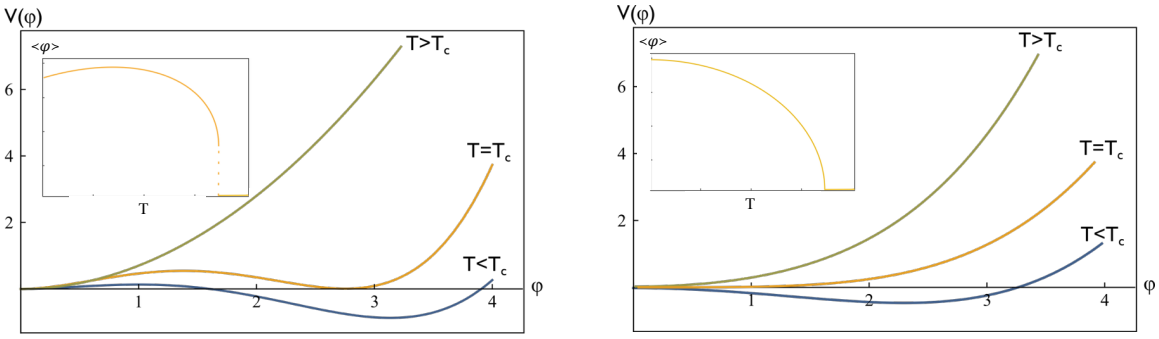


Figure 1.5: Left: Change in the potential energy for a first-order phase transition. The potential acquires two degenerate minima at a critical temperature $T_c$. Below $T_c$ the expectation value of the scalar field $\phi$ changes abruptly (see the inset figure). Right: Potential energy in a second-order phase transition changes continuously. This is also seen in the change in the expectation value of $\phi$.

In a first-order EW phase transition, bubbles of broken phase nucleate, percolate and eventually fill the whole space. This is a highly non-equilibrium process. However, even if the EW phase transition were first order, this is not enough to produce a baryon number. Baryon number violating sphaleron processes should also be out-of-equilibrium right after the phase transition, requiring $\Gamma_{\rm sph}(T_c) \lesssim H(T_c)$. Using $\Gamma_{\rm sph}$ in Eq. 1.11, this non-equilibrium condition turns into an upper bound on the Higgs expectation value right after the critical temperature,

$$\frac{\sqrt{2}\phi_c}{T_c} \gtrsim 1, \tag{1.15}$$

where $\phi_c$ and $T_c$ is found from minimizing the potential in Eq. 1.13

$$T_c = \left(\frac{6m_h^2}{6M_W^2 + 3M_Z^2 + 6m_t^2}\right)^{1/2}, \qquad \phi_c = \frac{\beta}{16\pi\lambda}T_c. \tag{1.16}$$

Remembering that the Higgs mass $m_h = \sqrt{2\lambda}v$, Eq. 1.15 gives an upper bound on $m_h$,

$$m_h^2 < \frac{1}{2\pi}\frac{1}{v}\sum_{\text{bosons}} g_i m_i^3 \simeq (60\text{ GeV})^2. \tag{1.17}$$

Of course this is not true, since we know the Higgs mass is 125 GeV. The easiest way to fix this problem is to extend the SM to add more bosons that couple to the Higgs field, so that they will elevate this upper bound by contributing to the right-handside of this inequality. In MSSM this is done by the supersymmetric partner of top-quark, stop. However, MSSM EW baryogenesis is also under heavy scrutiny due to experimental constraints in the supersymmetric sector [**?** ].

Finally let us give a sketch of how EW baryogenesis would have worked in an ideal Universe since at least parts of it are employed in many new physics models. At high temperatures the Higgs field has zero expectation value and the Universe is in the symmetric phase ($SU(2)_L \times U(1)_Y$ symmetry is not broken). As the Universe cools down the Higgs potential acquires a global minima at $\langle\phi\rangle \neq 0$. (Let us assume this change happens via a first-order phase transition.) The Universe responds to this change in a way much like boiling water: It creates bubbles inside which Higgs field is in the broken phase. Outside the bubbles is still the unbroken phase. Since the free energy of the broken and unbroken phases are different, there is a surface tension and smaller bubbles collapse under this pressure. Larger bubbles start expanding and they eventually fill up the whole Universe. As the bubbles expand fermions interact with the bubble wall and are either transmitted or reflected. Due to the $CP$-violation in the quark mass matrix, particles and antiparticles are reflected at different rates. The built-up of antiparticles outside the bubble wall is quickly washed out by sphaleron processes that happen very fast in the symmetric phase. Sphaleron processes inside the wall are slower, and they can happen out of thermal equilibrium (only if the Higgs mass were less than 60 GeV, or if there is some new physics). Hence the baryon number inside the wall is retained. See Fig. 1.6 for a schematic description.

### *1.3 Layout*

In Chapter 2, we will discuss a UV complete WIMP model that explains the Galactic Center gamma ray excess, based on [30].

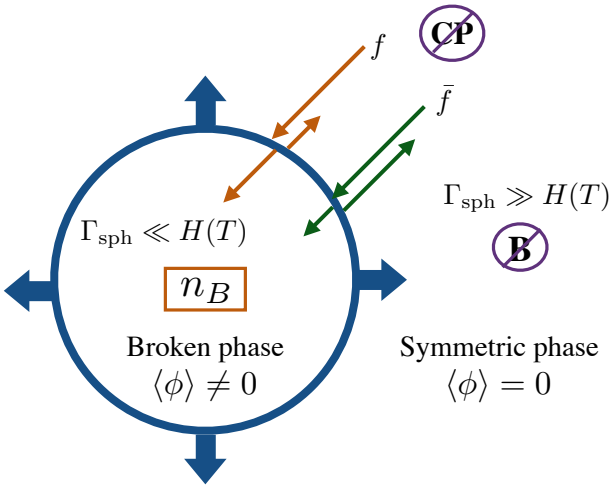


Figure 1.6: Schematic description of bubble wall expansion and EW baryogenesis. See text for details.

In Chapter 3, we will describe an asymmetric DM model that has neutrino interactions to discuss its consequences on both neutrino physics and the small scale structure of the Universe, based on [31].

In Chapter 4, we discuss EWBG with a two Higgs doublet model, and constraints on the $CP$ violation that might exist in the Higgs sector, based on [32].

In Chapter 5, we will introduce a supersymmetric model that exhibits pseudo-Dirac gluino oscillations. Possible $CP$ violation in these oscillations can be observed as a same-sign dimuon asymmetry and could play a role in producing the baryon asymmetry of the Universe. This will be based on [33] and also ongoing work.

Chapter 2

# DARK MATTER: HINTS FROM THE GALACTIC CENTER

Evidence for an excess of gamma rays with $\mathcal{O}$(GeV) energy coming from the center of our galaxy has been steadily accumulating over the past several years. Recent studies of the excess in data from the Fermi telescope have cast doubt on an explanation for the excess arising from unknown astrophysical sources. A potential source of the excess is the annihilation of dark matter into standard model final states, giving rise to gamma ray production. The spectrum of the excess is well fit by 30 GeV dark matter annihilating into a pair of $b$ quarks with a cross section of the same order of magnitude as expected for a thermal relic. Simple models that can lead to this annihilation channel for dark matter are in strong tension with null results from direct detection experiments. We construct a renormalizable model where dark matter-standard model interactions are mediated by a pseudoscalar that mixes with the CP-odd component of a pair of Higgs doublets, allowing for the gamma ray excess to be explained while suppressing the direct detection signal. We consider implications for this scenario from Higgs decays, rare $B$ meson decays and monojet searches and also comment on some difficulties that any dark matter model explaining the gamma ray excess via direct annihilation into quarks will encounter.

## *2.1 Introduction*

One of the prime unanswered questions about our Universe is the nature of dark matter (DM). Evidence for DM is overwhelming, coming from a diverse set of observations, among them galactic rotation curves, cluster merging, and the cosmic microwave background (see, e.g. [34] and references therein). So far, dark matter has not been observed nongravitationally, yet the fact that a thermal relic with weak-scale annihilation cross section into standard model (SM) final states would have an energy density today that is compatible with dark matter measurements offers hope that this will be possible. The nongravitational interac-

tions of DM are being searched for at particle colliders, in direct detection experiments, and in so-called indirect detection experiments, where the products of DM annihilation or decay are sought.

One final state in particular that is searched for in indirect detection experiments is gamma rays which can be produced by DM annihilating, either (i) directly to photons, which would result in an unambiguous line in the case of two body decays, or (ii) into other SM particles that then decay and produce photons in the cascade. The Fermi collaboration has published limits on DM annihilation [35–37] into final states containing photons.

Recently, evidence for such a signal has been mounting, with several groups [38–45] analyzing data from the Fermi Gamma Ray Space Telescope and finding an excess of gamma rays of energy ∼1-3 GeV in the region of the Galactic Center. This excess has a spectrum and spatial morphology compatible with DM annihilation. The potential for astrophysical backgrounds, in particular millisecond pulsars in this case, to fake a signal is always a worry in indirect detection experiments. However, the observation that this gamma ray excess extends quite far beyond the Galactic Center lessens the possibility of astrophysical fakes [39], with recent studies finding the excess to extend to at least 10° from the Galactic Center [38, 46, 47].

The excess's spectrum has been fit by DM annihilating to a number of final states, depending on its mass, notably 10 GeV DM annihilating to $\tau^+\tau^-$ (and possibly other leptons) [40, 43–45, 48–53] and 30 GeV DM to $b\bar{b}$ [41–45, 48–50, 54, 55]. The size of the excess is compatible with an annihilation cross section roughly equal to that expected for a thermal relic, $\langle\sigma v_{\rm rel}\rangle = 3 \times 10^{-26}$ cm$^3$/s, suggesting that it is actually the result of DM annihilation.

30 GeV DM that annihilates to $b$ quarks is particularly interesting, primarily because direct detection experiments have their maximal sensitivity to spin-independent interactions between nuclei and DM at that mass. Reconciling the extremely strong limit from direct detection in this mass range, presently $8 \times 10^{-46}$ cm$^2$ [56], with a potential indirect detection signal poses a challenge, possibly offering a clue about the structure of the SM-DM interactions. We will focus on this DM mass and final state in this paper.

In the case of DM annihilation to SM fermions through an $s$-channel mediator, we can

roughly distinguish the distribution of final states by the spin of the mediator. Spin-0 mediators tend to couple with strength proportional to mass—either due to inheriting their couplings from the Higgs or because of general considerations of minimal flavor violation—which results in decays primarily to the heaviest fermion pair kinematically allowed. On the other hand, spin-1 mediators generally couple more democratically, leading to a more uniform mixture of final states. For this reason, the fact that the excess is well fit by 30 GeV DM annihilating dominantly to $b\bar{b}$ suggests annihilation through a scalar. However, this is problematic: to get an appreciable indirect detection signal today requires scalar DM (fermionic DM annihilating through a scalar is $p$-wave suppressed) but this leads to a spin-independent direct detection cross section that is in conflict with experimental bounds, as mentioned above. Therefore, we are led to consider a pseudoscalar mediator, instead of a scalar, between the (fermionic) DM and the SM, leading to an effective dimension-six operator of the form

$$\mathcal{L}_{\text{eff}} = \frac{m_b}{\Lambda^3}\bar{\chi}i\gamma^5\chi\bar{b}i\gamma^5 b, \tag{2.1}$$

where $\chi$ is the DM. This operator has been singled out previously as a good candidate to describe the effective interaction between the SM and the dark sector [57, 58]. It implies $s$-wave DM annihilation, which allows the gamma ray excess to be fit while having a large enough suppression scale $\Lambda$ that it is not immediately ruled out by collider measurements of monojets/photons. The direct detection signal from this operator is spin-dependent and velocity-suppressed, rendering it safe from current constraints.

To move beyond the effective, higher dimensional operator in Eq. (2.1) requires confronting electroweak symmetry breaking because the SM portion of $\mathcal{L}_{\text{eff}}$ is not an electroweak singlet:

$$\bar{b}i\gamma^5 b = i\left(\bar{b}_L b_R - \bar{b}_R b_L\right). \tag{2.2}$$

Therefore, $\mathcal{L}_{\text{eff}}$ has to include the Higgs field (which would make it a singlet) which then gets a vacuum expectation value (VEV), implying a mediator which can couple to the Higgs.

It is easy to construct a scalar-scalar interaction between DM and the SM using the "Higgs portal" operator $H^\dagger H$, where $H$ is the SM Higgs doublet, since it is a SM gauge

singlet. This portal has been well explored in the literature, particularly in its connection to DM [59–65]. In this paper, however, we expand the Higgs sector of the SM to include a second doublet, which has enough degrees of freedom to allow for a pseudoscalar to mix with the dark matter mediator. In the presence of CP violation one could also induce a pseudoscalar-scalar coupling via this portal, however it is puzzling why a new boson with CP violating couplings would not also have a scalar coupling to the dark fermion. Including two Higgs doublets allows CP to be an approximate symmetry of the theory, broken by the SM fermion Yukawa coupling matrices. Tiny CP violating couplings will need to be included in order to renormalize the theory at high orders in perturbation theory, but we simply assume that all flavor and CP violation is derived from spurions proportional to the Yukawa coupling matrices, and so has minimal effect on the Higgs potential and dark sector.

This Chapter is organized as follows. In Sec. 2.2 we introduce the two Higgs doublet model (2HDM) and the pseudoscalar mediator which mixes with the Higgs sector. We also discuss CP violation in the dark sector and in interactions between DM and SM fermions. We briefly discuss the annihilation cross section for our DM model in Sec. 2.3. In Sec. 2.4, we catalog constraints on this model, such as direct detection, Higgs and $B$ meson decays, and monojets. Section 2.5 contains our conclusions.

## *2.2 The Model*

### *2.2.1 CP-Conserving Extended Higgs Sector*

As mentioned above, a straightforward way to couple dark matter to the SM through pseudoscalar exchange is by mixing the mediator with the pseudoscalar Higgs in a 2HDM.

For concreteness, we take the DM to be a Dirac fermion, $\chi$, with mass $m_\chi$, coupled to a real, gauge singlet, pseudoscalar mediator, $a_0$, through

$$\mathcal{L}_{\rm dark} = y_\chi a_0 \bar{\chi} i\gamma^5 \chi. \tag{2.3}$$

The mediator couples to the SM via the Higgs portal in the scalar potential which is

$$V = V_{\rm 2HDM} + \frac{1}{2} m_{a_0}^2 a_0^2 + \frac{\lambda_a}{4} a_0^4 + V_{\rm port}, \tag{2.4}$$

$$V_{\rm port} = i B a_0 H_1^\dagger H_2 + \text{h.c.} \tag{2.5}$$

with $H_{1,2}$ the two Higgs doublets. $B$ is a parameter with dimensions of mass. We assume that $\mathcal{L}_{\rm dark}$ and $V$ are CP-conserving (i.e. $B$ and $y_\chi$ are both real, and there is no CP violation in $V_{\rm 2HDM}$) and we will comment on relaxing this assumption in Sec **??**. In this case, $a_0$ does not develop a VEV. We write the most general CP-conserving 2HDM potential as

$$\begin{aligned} V_{\rm 2HDM} = &\lambda_1 \left(H_1^\dagger H_1 - \frac{v_1^2}{2}\right)^2 + \lambda_2 \left(H_2^\dagger H_2 - \frac{v_2^2}{2}\right)^2 + \lambda_3 \left[\left(H_1^\dagger H_1 - \frac{v_1^2}{2}\right) + \left(H_2^\dagger H_2 - \frac{v_2^2}{2}\right)\right]^2 \\ &+ \lambda_4 \left[\left(H_1^\dagger H_1\right)\left(H_2^\dagger H_2\right) - \left(H_1^\dagger H_2\right)\left(H_2^\dagger H_1\right)\right] \\ &+ \lambda_5 \left[{\rm Re}\left(H_1^\dagger H_2\right) - \frac{v_1 v_2}{2}\right]^2 + \lambda_6 \left[{\rm Im}\left(H_1^\dagger H_2\right)\right]^2, \end{aligned} \tag{2.6}$$

with all $\lambda_i$ real. We have also imposed a $\mathbb{Z}_2$ symmetry under which $H_1 \to H_1$ and $H_2 \to -H_2$ to suppress flavor-changing neutral currents, which is only softly broken by $V_{\rm 2HDM}$ and $V_{\rm port}$. The potential is minimized at $\langle H_i \rangle = v_i/\sqrt{2}$, $i = 1, 2$, and the $W$ and $Z$ masses fix $v_1^2 + v_2^2 = v^2 = (246\ {\rm GeV})^2$. The angle $\beta$ is defined by $\tan\beta = v_2/v_1$. In unitary gauge we can decompose the doublets as

$$H_i = \frac{1}{\sqrt{2}} \begin{pmatrix} \sqrt{2}\phi_i^+ \\ v_i + \rho_i + i\eta_i \end{pmatrix}. \tag{2.7}$$

The spectrum contains a charged Higgs,

$$H^\pm = \sin\beta\, \phi_1^\pm - \cos\beta\, \phi_2^\pm, \tag{2.8}$$

with mass $m_{H^\pm}^2 = \lambda_4 v^2/2$.

The CP-even Higgs mass matrix in the $(\rho_1, \rho_2)$ basis is $\mathcal{M}_h^2$, with

$$\begin{aligned} \mathcal{M}_{h11}^2 &= \frac{v^2}{2}\left[\lambda_5 s_\beta^2 + 4\left(\lambda_1 + \lambda_3\right) c_\beta^2\right], \\ \mathcal{M}_{h22}^2 &= \frac{v^2}{2}\left[\lambda_5 c_\beta^2 + 4\left(\lambda_2 + \lambda_3\right) s_\beta^2\right], \\ \mathcal{M}_{h12}^2 &= \mathcal{M}_{h21}^2 = \frac{v^2}{2}\left(\lambda_5 + 4\lambda_3\right) s_\beta c_\beta. \end{aligned} \tag{2.9}$$

We use $s$ and $c$ to denote sine and cosine here (and will do so intermittently throughout this paper along with $t$ for tangent). The physical CP-even states are $h$ and $H$ ($m_h \le m_H$),

related to $\rho_{1,2}$ by

$$\begin{pmatrix} \rho_1 \\ \rho_2 \end{pmatrix} = \begin{pmatrix} -\sin\alpha & \cos\alpha \\ \cos\alpha & \sin\alpha \end{pmatrix} \begin{pmatrix} h \\ H \end{pmatrix}, \tag{2.10}$$
$$\tan 2\alpha = \frac{2\mathcal{M}_{h12}^2}{\mathcal{M}_{h11}^2 - \mathcal{M}_{h22}^2},$$

with masses

$$m_{h,H}^2 = \frac{1}{2}\left[\mathcal{M}_{h11}^2 + \mathcal{M}_{h22}^2 \mp \sqrt{\left(\mathcal{M}_{h11}^2 - \mathcal{M}_{h22}^2\right)^2 + 4\left(\mathcal{M}_{h12}^2\right)^2}\right].$$

We will use $\xi_\psi^\phi$ to denote the strength of the coupling of the scalar $\phi$ to $\psi$ pairs (weak gauge bosons, quarks, and leptons) in units of SM Higgs coupling to those particles. The CP-even Higgs couplings to weak gauge bosons $V = W, Z$ are rescaled by

$$\xi_V^h = \sin(\beta - \alpha), \ \xi_V^H = \cos(\beta - \alpha). \tag{2.11}$$

The neutral, imaginary components of $H_{1,2}$ combine to form a pseudoscalar,

$$A_0 = \sin\beta\,\eta_1 - \cos\beta\,\eta_2. \tag{2.12}$$

that mixes with $a_0$ due to the portal coupling,

$$V_{\text{port}} = B a_0 A_0 \left[v + \sin(\beta - \alpha)\, h + \cos(\beta - \alpha)\, H\right]. \tag{2.13}$$

The CP-odd mass matrix in the $(A_0, a_0)$ basis is

$$\mathcal{M}_A^2 = \begin{pmatrix} m_{A_0}^2 & Bv \\ Bv & m_{a_0}^2 \end{pmatrix}, \quad m_{A_0}^2 = \frac{\lambda_6 v^2}{2}. \tag{2.14}$$

Thus, the mass eigenstates, $A$ and $a$ are

$$\begin{pmatrix} A_0 \\ a_0 \end{pmatrix} = \begin{pmatrix} \cos\theta & -\sin\theta \\ \sin\theta & \cos\theta \end{pmatrix} \begin{pmatrix} A \\ a \end{pmatrix},$$
$$\tan 2\theta = \frac{2Bv}{m_{A_0}^2 - m_{a_0}^2}, \tag{2.15}$$
$$m_{a,A}^2 = \frac{1}{2}\left[m_{A_0}^2 + m_{a_0}^2 \pm \sqrt{\left(m_{A_0}^2 - m_{a_0}^2\right)^2 + 4B^2v^2}\right].$$

We can express $B$ in terms of $m_{a,A}$ and the mixing angle $\theta$,

$$B = \frac{1}{2v}\left(m_A^2 - m_a^2\right)\sin 2\theta. \tag{2.16}$$

Written in terms of mass eigenstates and mixing angles, $V_{\text{port}}$ becomes

$$V_{\text{port}} = \frac{1}{2v}\left(m_A^2 - m_a^2\right)\left[s_{4\theta} aA + s_{2\theta}^2\left(A^2 - a^2\right)\right]\left[\sin\left(\beta-\alpha\right)h + \cos\left(\beta-\alpha\right)H\right]. \tag{2.17}$$

The DM coupling to the mediator in Eq. (2.3) is simply expressed in terms of CP-odd mass eigenstates,

$$\mathcal{L}_{\text{dark}} = y_\chi\left(\cos\theta\, a + \sin\theta\, A\right)\bar{\chi} i\gamma^5\chi. \tag{2.18}$$

We will work in a Type II 2HDM, where the Yukawa couplings of the SM fermions are

$$\mathcal{L}_{\text{Yuk}} = -\bar{L}Y_e H_1 e_R - \bar{Q}Y_d H_1 d_R - \bar{Q}Y_d \tilde{H}_2 u_R + \text{h.c.}.$$

$Y_{e,d,u}$ are Yukawa matrices acting on the three generations (we employ first generation notation). $L$ and $Q$ are the left-handed lepton and quark doublets and $e_R$, $d_R$, and $u_R$ are the right-handed singlets. These couplings respect the $\mathbb{Z}_2$ symmetry $H_2 \to -H_2$ provided $u_R \to -u_R$. We can forbid the operator

$$\mathcal{L}_{\text{Yuk}} = -\bar{L}Y_\chi \tilde{H}_1 \chi_R + \text{h.c.}.$$

by taking $\chi \to -\chi$ under a separate $\mathbb{Z}_2$. Note $\tilde{H}_i$ stands for $i\sigma_2 H_i^*$. Given these Yukawa interactions the couplings of the neutral scalar mass eigenstates are then rescaled from the SM Higgs values by

$$\xi_e^h = \xi_d^h = -\frac{\sin\alpha}{\cos\beta},\ \xi_u^h = \frac{\cos\alpha}{\sin\beta}, \tag{2.19}$$

$$\xi_e^H = \xi_d^H = \frac{\cos\alpha}{\cos\beta},\ \xi_u^H = \frac{\sin\alpha}{\sin\beta}, \tag{2.20}$$

$$\xi_e^A = \xi_d^A = \tan\beta\cos\theta,\ \xi_u^A = \cot\beta\cos\theta, \tag{2.21}$$

$$\xi_e^a = \xi_d^a = -\tan\beta\sin\theta,\ \xi_u^a = -\cot\beta\sin\theta. \tag{2.22}$$

To simplify the analysis, we work close to the decoupling limit of the 2HDM where

$$\lambda_1 \simeq \lambda_2 \simeq -\lambda_3 \simeq \frac{\lambda_4}{2} \simeq \frac{\lambda_5}{2} \simeq \frac{\lambda_6}{2} \equiv \lambda \gg 1. \tag{2.23}$$

Then, $\alpha \simeq \beta - \pi/2$ and $m_h \ll m_H \simeq m_{H^\pm} \simeq m_{A_0}$. Since $h$ has SM-like couplings in this limit, we identify it with the boson with mass 125 GeV recently discovered at the LHC. The degeneracy of $H$ and $H^\pm$ (and possibly $A$, given that we expect $B$ to be somewhat small compared to $m_{A_0}$) allows for precision electroweak constraints to be satisfied.

### *2.2.2 Dark Matter CP Problem*

We now briefly discuss relaxing the assumption of CP conservation in the DM Yukawa interaction or in the scalar potential. If we write a general, possibly CP-violating, 4-Fermi interaction between quarks and DM that results after integrating out a spin-0 mediator as

$$\mathcal{L}_{\text{eff}} = \frac{1}{\Lambda^2}\frac{m_q}{v}\bar{\chi}\left(a_\chi + ib_\chi\gamma^5\right)\chi\bar{q}\left(a_q + ib_q\gamma^5\right)q, \tag{2.24}$$

we find an annihilation cross section for $\chi\bar{\chi} \to b\bar{b}$ in the nonrelativistic limit, relevant for thermal freeze-out and indirect detection, of

$$\begin{aligned}\sigma v_{\text{rel}} &= \frac{1}{2\pi}\left(\frac{m_\chi m_b}{\Lambda^2 v}\right)^2\left(b_\chi^2 + a_\chi^2 v_{\text{rel}}^2\right)\left(b_b^2 + a_b^2\right) \\ &\simeq 3\times 10^{-26}\ \frac{\text{cm}^3}{\text{s}}\left(\frac{m_\chi}{30\ \text{GeV}}\right)^2\left(\frac{54\ \text{GeV}}{\Lambda}\right)^4\left(b_\chi^2 + a_\chi^2 v_{\text{rel}}^2\right)\left(b_b^2 + a_b^2\right),\end{aligned} \tag{2.25}$$

with $v_{\text{rel}}$ the relative velocity between $\chi$ and $\bar{\chi}$. We have taken $m_b \ll m_\chi$ and normalized on parameters that give the appropriate annihilation cross section for a thermal relic as well as the gamma ray excess. This operator also leads to a spin-independent cross section for DM scattering on a nucleon of

$$\begin{aligned}\sigma_{\text{SI}} &= \frac{\mu^2}{\pi}\left(\frac{\langle N|\sum_q a_q m_q \bar{q}q|N\rangle}{\Lambda^2 v}\right)^2 a_\chi^2 \\ &\simeq 2.6\times 10^{-41}\ \text{cm}^2\left(\frac{54\ \text{GeV}}{\Lambda}\right)^4\left(\frac{\langle N|\sum_q a_q m_q \bar{q}q|N\rangle}{330\ \text{MeV}}\right)^2 a_\chi^2,\end{aligned} \tag{2.26}$$

where $\mu$ is the reduced mass of the nucleon-DM system. The LUX experiment has set a limit of $\sigma_{\text{SI}} < 8\times 10^{-46}$ cm$^2$ [56] at a dark matter mass of 30 GeV, which highlights a problem for the general dimension-six operator in Eq. (2.24). The scalar-scalar coupling needs to be suppressed by about five orders of magnitude relative to the pseudoscalar-pseudoscalar coupling (which is why the latter has been focused on in the literature) without any good reason. If not, the stringent limits from direct detection preclude the possibility of an

annihilation cross section large enough for an observable indirect detection signal or even to obtain the observed relic density and not overclose the Universe.

A scalar coupling of $a$ to $\chi$ is obtained if $y_\chi$ in Eq. (2.3) has a nonzero imaginary component. $a$ will also develop a scalar coupling to quarks if $B$ in Eq. (2.5) is not real or if there is CP violation in the rest of the scalar potential. As highlighted above in the discussion of a general dimension-six interaction, (the product of) these CP-violating phases in $y_\chi$ and $V$ must be limited to less than about $10^{-4}$ to $10^{-5}$ (ignoring possible suppressions or enhancements at large $\tan\beta$). That is, in addition to the usual EDM constraints on CP-violating phases in the scalar potential (see, e.g. [66**?** ]), these models face tests from direct detection experiments (which become probes of CP violation).

CP is not an exact symmetry of the SM; indeed, we expect to see even larger violations of CP in physics beyond the SM because of baryogenesis. In this light, simply asserting that these new interactions respect CP seems a little peculiar. It is however technically natural to assume that spurions proportional to the SM Yukawa coupling matrices are the only source of CP and flavor violation, with the consequence that CP-violating couplings outside of the CKM are tiny.

Should the evidence for this gamma ray signal remain or increase, understanding the smallness of these CP-violating couplings will pose a model-building challenge and hint about the structure of the new physics, much like the CP problems encountered in other models of physics beyond the SM.

### *2.3 Dark Matter Annihilation*

For $m_a \ll m_A$, the dark matter annihilates to SM particles primarily through $s$-channel $a$ exchange. The velocity averaged annihilation cross section for $\chi\bar{\chi} \to$ SM in the nonrelativistic limit is

$$\langle \sigma v_{\rm rel} \rangle = \frac{y_\chi^2}{8\pi} \frac{m_\chi^2}{m_a^4} s_{2\theta}^2 \tan^2\beta \left[ \left(1 - \frac{4m_\chi^2}{m_a^2}\right)^2 + \frac{\Gamma_a^2}{m_a^2} \right]^{-1} \sum_{f=b,\tau,\ldots} N_C \frac{m_f^2}{v^2} \sqrt{1 - \frac{m_f^2}{m_a^2}}. \qquad (2.27)$$

The sum is over down-type quarks ($N_C = 3$) and charged leptons ($N_C = 1$) since $a$'s coupling to up-type quarks is suppressed by $1/\tan\beta$. Evaluating this at the experimentally

favored DM mass of 30 GeV, taking $m_a = 100$ GeV (and ignoring $\Gamma_a$) gives

$$\langle \sigma v_{\rm rel} \rangle = 3 \times 10^{-26} \, \frac{\rm cm^3}{\rm s} \left( \frac{y_\chi \sin 2\theta \tan \beta}{2.4} \right)^2 . \tag{2.28}$$

We see that it is possible to achieve values of the annihilation cross section compatible with the gamma ray excess and relic density constraints with modest values of the mixing angle $\theta$, provided $\tan\beta$ is somewhat large. At this value of $m_\chi$ and for $\tan\beta$ larger than a few, the $b\bar{b}$ final state accounts for about 90% of the annihilation cross section with $\tau^+\tau^-$ making up nearly all the rest. This is in line with what is suggested by fits to the gamma ray excess.

The general requirement that $\tan\beta$ is large will help focus the mass scale of the heavy Higgs bosons. CMS's search for heavy neutral minimal supersymmetric standard model (MSSM) Higgses decaying to $\tau^+\tau^-$ [67] applies straightforwardly in this case, since the Higgs sector is the same as in the MSSM. The production cross section for $pp \to (H/A) + X$ is enhanced at large $\tan\beta$ so the lack of a signal sets an upper limit on $\tan\beta$ as a function of $m_{A,H}$. This limit is roughly $\tan\beta < 10$ at $m_{A,H} = 300$ GeV, and weakens to $\tan\beta < 60$ at $m_{A,H} = 900$ GeV.

### *2.4 Constraints on the Dark Sector*

In this section we investigate the limits on the mediator mass and the mixing angle between the mediator and the pseudoscalar of the 2HDM. Taking the heavy Higgs search described above into account, we fix the other parameters to the benchmark values $m_H = m_{H^\pm} \simeq m_A = 800$ GeV, $\tan\beta = 40$, $\alpha = \beta - \pi/2$, and $y_\chi = 0.5$ and comment on changing these later. We first consider the spin-independent direct detection cross section induced at one-loop. Current limits from direct detection experiments do not constrain this model, but future searches can possibly probe interesting regions of parameter space. We next consider Higgs decays to the pseudoscalar mediator. Searches for $h \to b\bar{b}$ can be used to put bounds to $h \to aa \to 4b$ decays for $m_h > 2m_a$ and future $h \to 2b2\mu$ searches could probe much more of the $m_a$-$\theta$ parameter space. Indirect limits on the branching for $h \to aa$ from global Higgs property fits are also quite constraining. We then consider changes to the $B_s \to \mu^+\mu^-$ branching ratio. Since this has been measured to be very close to its SM value, it is particularly constraining for a light mediator. Finally, we consider monojet searches.

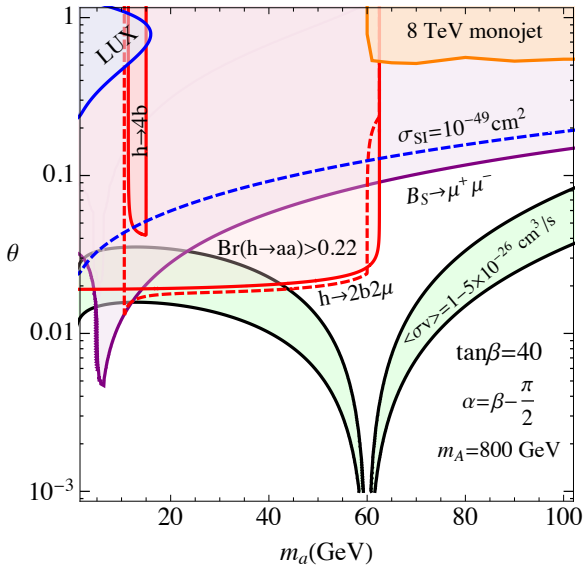


Figure 2.1: Regions of mixing angle $\theta$ vs. $m_a$ that are ruled out or suggested by various measurements. We have fixed $m_{H,H^\pm} \simeq m_A = 800$ GeV, $\tan\beta = 40$, $\alpha = \beta - \pi/2$, and $y_\chi = 0.5$. The area that gives an annihilation cross section of $\langle\sigma v_{\rm rel}\rangle = 1 - 5 \times 10^{-26}$ cm$^3$/s as indicated by fits to the gamma ray excess is between the solid black lines (shaded in green). The shaded purple region above the solid purple line is in $2\sigma$ conflict with the LHCb measurement of $B_s \to \mu^+\mu^-$. The darker red region with the solid outline is ruled out by $h \to b\bar{b}$ constraints on the $h \to 4b$ signal. The larger, lighter red region with a solid outline is ruled out from the indirect limit $\mathrm{Br}\,(h \to aa) < 0.22$ coming from fits to Higgs properties, assuming SM Higgs production. The dashed red line shows the area that could be probed by limiting $\mathrm{Br}\,(h \to aa \to 2b2\mu) \lesssim 10^{-4}$. The blue region labeled LUX is in conflict with the limit $\sigma_{\rm SI} < 8 \times 10^{-46}$ cm$^2$ while the area above the blue dashed line leads to $\sigma_{\rm SI} > 10^{-49}$ cm$^2$, potentially accessible at the next generation of direct detection experiments. The orange region shows the area ruled out by a mono-$b$-jet search at 8 TeV with 20 fb$^{-1}$ of data. See text for details.

Our main results are summarized in Fig. 2.1.

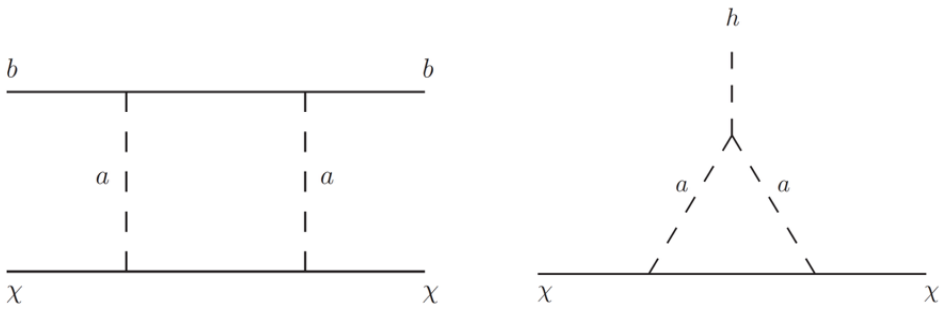


Figure 2.2: Diagrams that (with the crossed top diagram) lead to spin-independent DM-nucleon scattering. The $b$ quarks in the left diagram can also be replaced by $d$ and $s$ quarks.

### *2.4.1 Direct Detection*

One of the virtues of this model is that single pseudoscalar exchange between $\chi$ and quarks leads to (highly suppressed) spin-dependent scattering of the DM on nuclei [57, 58]. At one-loop, however, spin-independent interactions are generated through the diagrams shown in Fig. 2.2. The top diagram (plus its crossed version) leads to an effective interaction between $\chi$ and $b$ quarks at zero momentum transfer given by

$$\mathcal{L}_{\rm box} = \sum_{q=d,s,b} \frac{m_q^2 y_\chi^2 \tan^2\beta \sin^2 2\theta}{128\pi^2 m_a^2 \left(m_\chi^2 - m_q^2\right)} \left[F\left(\frac{m_\chi^2}{m_a^2}\right) - F\left(\frac{m_q^2}{m_a^2}\right)\right] \frac{m_\chi m_q}{v^2} \bar{\chi}\chi\bar{q}q. \tag{2.29}$$

The function $F$ is given in the Appendix in Eq. **??**.

The bottom diagram of Fig. 2.2 leads to a DM-Higgs coupling of

$$\mathcal{L}_{h\chi\chi} = -\frac{\left(m_A^2 - m_a^2\right)\sin^2 2\theta y_\chi^2}{64\pi^2 m_a^2} G\left(x_\chi, x_q\right) \frac{m_\chi}{v} h\bar{\chi}\chi, \tag{2.30}$$

where $x_\chi = m_\chi^2/m_a^2$, $x_q = q^2/m_a^2$, and $q$ is the momentum transfer between $\chi$ and $\bar{\chi}$. $G$ is given in Eq. **??**. This leads to an effective 4-fermion interaction relevant for spin-independent nucleon scattering,

$$\mathcal{L}_h = \frac{\left(m_A^2 - m_a^2\right) s_{2\theta}^2 y_\chi^2}{64\pi^2 m_h^2 m_a^2} G\left(x_\chi, 0\right) \frac{m_\chi m_q}{v^2} \bar{\chi}\chi\bar{q}q. \tag{2.31}$$

We have assumed $\alpha = \beta - \pi/2$ which results in SM-like couplings of $h$ to quarks, $-s_\alpha/c_\beta = c_\alpha/s_\beta = 1$. For

$$\tan\beta \lesssim 100 \left(\frac{m_A}{800\ \text{GeV}}\right), \tag{2.32}$$

the Higgs exchange contribution to direct detection dominates over the box diagram, leading to a spin-independent cross section for scattering on a nucleon of

$$\begin{aligned}\sigma_{\text{SI}} \simeq 2.2 \times 10^{-49}\ \text{cm}^2 \left(\frac{m_A}{800\ \text{GeV}}\right)^4 \left(\frac{50\ \text{GeV}}{m_a}\right)^4 \\ \times \left(\frac{m_\chi}{30\ \text{GeV}}\right)^2 \left(\frac{\theta}{0.1}\right)^4 \left(\frac{y_\chi}{0.5}\right)^4 \left(\frac{\langle N|\sum_q m_q \bar{q}q|N\rangle}{330\ \text{MeV}}\right)^2,\end{aligned} \tag{2.33}$$

using a value of the $\bar{q}q$ matrix element from Ref. [68]. Cross sections at the $10^{-48}$ to $10^{-49}$ cm$^2$ level are potentially observable at the next generation of direct detection experiments [69]. The loop suppression of the spin-independent cross section, however, is sufficient for this model to remain safe from direct detection experiments for the near future.

In Fig. 2.1, we show the area of parameter space ruled out by the LUX limit of $8 \times 10^{-46}$ cm$^2$ on a spin-independent cross section that arises from the loop diagrams above. Only areas of very large mixing angle $\theta$ and small $m_a$ are impacted. We also show the area that can be probed by a future cross section limit of $10^{-49}$ cm$^2$ which covers a much larger region.

### *2.4.2 Higgs Decays*

If $m_a < m_h$, the Higgs can decay into final states involving $a$ and, in particular, when $m_a < m_h/2$, the two body mode $h \to aa$ opens up. Using Eq. (2.17) with $\sin(\beta - \alpha) = 1$, the rate is

$$\begin{aligned}\Gamma(h \to aa) &= \frac{\left(m_A^2 - m_a^2\right)^2 \sin^4 2\theta}{32\pi m_h v^2} \sqrt{1 - \frac{4m_a^2}{m_h^2}} \\ &\simeq 840\ \text{MeV} \left(\frac{m_A}{800\ \text{GeV}}\right)^4 \left(\frac{\theta}{0.1}\right)^4,\end{aligned} \tag{2.34}$$

having taken $m_a \ll m_h$, $m_A$ in the second line. Since the width of the SM Higgs is 4 MeV, this can impact LHC measurements that broadly indicate that $h$ is SM-like to ∼10-20% if $\theta \gtrsim \text{few} \times 10^{-2}(800\ \text{GeV}/m_A)$.

This mode requires $m_a < m_h/2 \simeq 2m_\chi$, so the pseudoscalars will primarily go to $b$ quarks with a small branching to $\tau$ and $\mu$ pairs. The $h \to aa \to 4b$ signal will contribute to $h \to b\bar{b}$ searches [70]. A CMS search in $W/Z$-associated production at 7 and 8 TeV, $pp \to (W/Z) + (h \to b\bar{b})$ [71], sets a limit $\mathrm{Br}\,(h \to aa \to 4b) < 0.7$ for $2m_b < m_a < 15$ GeV. This can potentially be improved to 0.2 with 100 fb$^{-1}$ data at the 14 TeV LHC. For larger $m_a$, there are no current limits. Additionally, the $h \to 2b2\mu$ final state can offer a probe comparable to $4b$, with its relative cleanliness compensating for its rarity. Current 7 and 8 TeV data can limit this to $\mathrm{Br}\,(h \to aa \to 2b2\mu) \lesssim 10^{-3}$ for $m_a > 25$ GeV. The 14 TeV run with 100 fb$^{-1}$ data can improve this limit to $10^{-4}$ [70].

Taking the branching ratios of $a$ into account, the limits above translate into a limit $\mathrm{Br}\,(h \to aa) \lesssim 0.9$ for $2m_b < m_a < 15$ GeV currently, with the possibility of improving this to $\mathrm{Br}\,(h \to aa) \lesssim 0.1 - 0.2$ in the future.

Since we are in the decoupling limit, the production cross section of the Higgs is unchanged from its SM value in this model (unless we add further states). Therefore there are strong limits on unobserved final states, such as $aa$, that would dilute the signal strength in the observed channels. Given current data, this limits $\mathrm{Br}\,(h \to aa) < 0.22$ [72].

The decay $h \to \chi\bar{\chi}$ through the bottom diagram in Fig. 2.2 is loop-suppressed and offers no meaningful constraints. For larger $m_a$, the three-body decays $h \to aa^*$, $aA^*$ become the dominant exotic Higgs decay modes, but are suppressed by the extra particle in the final state and are also not constraining.

We show the limits on the mixing angle as a function of $m_a$ coming from the determination $\mathrm{Br}\,(h \to aa \to 4b) < 0.7$ as well as the indirect constraint $\mathrm{Br}\,(h \to aa) < 0.22$ in Fig. 2.1. We also show the limit that can be set by a future measurement of $\mathrm{Br}\,(h \to aa \to 2b2\mu) < 10^{-4}$. $h \to aa$ decays provide strong constraints when kinematically allowed, i.e. $m_a \lesssim 60$ GeV.

### *2.4.3 B Physics Constraints*

A light $a$ can also potentially be constrained by its contributions to the decay $B_s \to \mu^+\mu^-$. For $m_a \ll m_Z$, the correction due to s-channel $a$ exchange can be simply written as [73]

$$\mathrm{Br}\left(B_s \to \mu^+\mu^-\right) \simeq \mathrm{Br}\left(B_s \to \mu^+\mu^-\right)_{\mathrm{SM}} \left| 1 + \frac{m_b m_{B_s} t_\beta^2 s_\theta^2}{m_{B_s}^2 - m_a^2} \frac{f\left(x_t, y_t, r\right)}{Y\left(x_t\right)} \right|^2 , \tag{2.35}$$

with $x_t = m_t^2/m_W^2$, $y_t = m_t^2/m_{H^\pm}^2$, $r = m_{H^\pm}^2/m_W^2$,

$$f\left(x, y, r\right) = \frac{x}{8}\left[ -\frac{r\left(x-1\right) - x}{\left(r-1\right)\left(x-1\right)} \log r + \frac{x \log x}{\left(x-1\right)} - \frac{y \log y}{\left(y-1\right)} + \frac{x \log y}{\left(r-x\right)\left(x-1\right)} \right], \tag{2.36}$$

and $Y(x)$ the usual Inami-Lim function,

$$Y\left(x\right) = \frac{x}{8}\left[ \frac{x-4}{x-1} \log x + \frac{3x \log x}{\left(x-1\right)^2} \right]. \tag{2.37}$$

The average of the LHCb and CMS measurements of this mode is $\mathrm{Br}\left(B_s \to \mu^+\mu^-\right) = \left(2.9 \pm 0.7\right) \times 10^{-9}$ [74–76]. This should be compared against the SM prediction, which we take to be $\left(3.65 \pm 0.23\right) \times 10^{-9}$ [77, 78]. This offers a strong test of the model, especially for a light $a$, which we show in Fig. 2.1.

### *2.4.4 Collider Probes*

Monojet and monophoton searches have become standard techniques to look for dark matter at hadron colliders in recent years (see, e.g., [79–86]).

To estimate the reach that such searches might have in this model, we make use of a recent analysis [87] designed to probe dark matter that couples preferentially to heavy quarks, taking advantage of $b$-tagging a jet recoiling against missing energy to cut down substantially on backgrounds.

For our signal, we use MadGraph 5 [88] to generate matched samples of $\chi\bar{\chi} + (0, 1, 2)j$ (with $j$ representing both $b$- and light flavor/gluon-jets), shower and hadronize with Pythia 6 [89], and use Delphes 2 [90] for detector simulation. We take a 50% $b$-tag efficiency for $p_T > 80$ GeV, which measurements from CMS [**?** ] and ATLAS [**?** ] show is conservative (a larger efficiency would lead to stronger limits).

The most useful signal region defined in Ref. [87] for this model has the following requirements: (i) missing transverse energy greater than 350 GeV, (ii) no more than two jets with $p_T > 50$ GeV, (iii) the leading jet has $p_T > 100$ GeV and is $b$-tagged, (iv) no isolated leptons, and (v) if there is a second jet, its separation in azimuthal angle with respect to the missing energy is $\Delta\phi > 0.4$. Using backgrounds estimated in [87] at the 8 TeV LHC (mainly $Z$+jets and $t\bar{t}$+jets), we can identify regions of parameter space that can be expected to be probed by this search with 20 fb$^{-1}$ of data. Monojet searches of this type are most sensitive when $m_a > 2m_\chi$ since then $a$ can be produced on-shell and decay to $\chi\bar{\chi}$. If $m_a < 2m_\chi$ the reach substantially weakens due to the additional particle in the final state and the softness of the missing energy since the $\chi\bar{\chi}$ pair tends to be created close to threshold.

This model is relatively less well constrained by monojet searches than the EFTs studied in Refs. [57] and [87] because of the suppressed coupling to top at large $\tan\beta$. The values of $\theta$ as a function of $m_a$ that would be ruled out by the search described above are shown in Fig. 2.1. Extending this search to 100 fb$^{-1}$ of 14 TeV data could improve the reach in $\theta$ by a factor of $\sim 3$ [87].

### *2.5 Conclusions and Outlook*

An excess in gamma rays from the Galactic Center as measured by the Fermi Gamma Ray Space Telescope can be explained by 30 GeV DM annihilating dominantly into $b\bar{b}$ pairs. To do so while eluding bounds on spin-independent scattering of DM on nuclei suggests that the mediator between the dark sector and the SM is a pseudoscalar. We have studied a 2HDM where the pseudoscalar mediator mixes with the CP-odd Higgs, giving rise to interactions between DM and the SM.

At one-loop, scalar-scalar interactions between DM and SM quarks arise. This leads to a spin-independent cross section for direct detection well below the current bound of $8 \times 10^{-46}$cm$^2$ at a dark matter mass of 30 GeV. Future limits at better than $10^{-49}$cm$^2$ could impact this model. We also consider decays of the 125 GeV SM-like Higgs boson involving the mediator. If the mediator is light $h \to aa \to 4b$, $2b2\mu$ can be constraining with data from the 14 TeV LHC. Additional contributions to $B_s \to \mu^+\mu^-$ in this model eliminate some of the favored parameter space for $m_a < 10$ GeV. This scenario is not well tested by

monojet searches, including ones that rely on $b$-tagging to increase the sensitivity to DM coupled to heavy quarks, due to a suppressed coupling of the mediator to $t$ quarks.

Changing the benchmark parameters that we used above does not greatly change the general results. For example, if we lower lower $m_A$ to decrease the $h \to aa$ signal coming from Eq. (2.17), we have to decrease $\tan\beta$ because of the CMS heavy Higgs search [67]. Then, to obtain the correct annihilation cross section in Eq. (2.27), we have to increase the mixing angle (or, equivalently, $B$) which in turn increases the $h \to aa$ rate.

One obvious piece of evidence in favor of this scenario would be finding heavy Higgses at the LHC. However, conclusively determining whether these heavy Higgses are connected to 30 GeV DM annihilating at the center of the galaxy will be a formidable challenge. Among the possible signatures to probe this scenario is $A \to ha \to 2b + \text{inv}$. We leave a detailed study of this search and others for future work.

Chapter 3

# DARK MATTER: NEUTRINO CONNECTION

Cold dark matter explains a wide range of data on cosmological scales. However, there has been a steady accumulation of evidence for discrepancies between simulations and observations at scales smaller than galaxy clusters. One promising way to affect structure formation on small scales is a relatively strong coupling of dark matter to neutrinos. We construct an experimentally viable, simple, renormalizable model with new interactions between neutrinos and dark matter and provide the first discussion of how these new dark matter-neutrino interactions affect neutrino phenomenology. We show that addressing the small scale structure problems requires asymmetric dark matter with a mass that is tens of MeV. Generating a sufficiently large dark matter-neutrino coupling requires a new heavy neutrino with a mass around 100 MeV. The heavy neutrino is mostly sterile but has a substantial $\tau$ neutrino component, while the three nearly massless neutrinos are partly sterile. This model can be tested by future astrophysical, particle physics, and neutrino oscillation data. Promising signatures of this model include alterations to the neutrino energy spectrum and flavor content observered from a future nearby supernova, anomalous matter effects in neutrino oscillations, and a component of the $\tau$ neutrino with mass around 100 MeV.

## *3.1 Introduction*

The existence of dark matter (DM) is required by a number of experimental results, from galactic rotation curves, to gravitational lensing observations, to the cosmic microwave background (CMB). Because of its success in accounting for data at cosmological scales, the cold DM (CDM) paradigm has become the baseline scenario for studying DM-related physics. Despite these successes, evidence for puzzles at galactic or smaller scales that CDM cannot account for have been accumulating in recent years [91–97]. These puzzles go by

several names: the "missing satellites," "too big to fail," and "core vs. cusp" problems. For general, recent reviews of these small scale structure discrepancies see [98, 99].

Simulations based on CDM predict that there should be many thousands of DM subhalos in a Milky Way size galaxy, in contrast to the few dozen known Milky Way satellite galaxies (for a review see [100]). This discrepancy is termed the "missing satellites" problem. The apparent deficit in the number of satellite galaxies could be due to conventional astrophysics, such as the inability of low mass DM subhalos to form stars (for example, due to supernova feedback or reionization blowing regular matter out of subhalos), making them hard to detect (see [101] and references therein), or it could be due to the properties of the DM particle. Several ways to change the vanilla CDM paradigm have been suggested in order to affect structure on small scales and suppress the formation of small DM subhalos, including: (i) the DM could be warmer [102, 103], (ii) the DM could self-interact [104–107], or (iii) the DM could stay in thermal equilibrium with radiation to lower temperatures than typically expected. To realize option (iii), the DM must interact strongly with the components of the relativistic plasma, either photons, neutrinos, or dark radiation. The use of stronger-than-expected interactions of DM with neutrinos to solve the missing satellites problem has long been recognized [108–113]. In this paper we consider a DM candidate that couples to a heavy sterile neutrino through a dark sector mediator. DM-neutrino interactions are induced by neutrino mixing. We focus on the particle physics and astrophysical constraints on these interactions, and also describe the effects of strong DM-neutrino interactions on structure formation.

Structure formation involves a competition between gravity, which causes density inhomogeneities to grow, and pressure, which resists the gravitational collapse. In general, in the early Universe when the temperature was extremely high, the DM was in thermal equilibrium with the relativistic plasma composed of photons, neutrinos, and possibly other Standard Model (SM) states, via nongravitational interactions that are typically assumed to be present. After the temperature drops below the DM mass, the DM abundance eventually falls out of chemical equilibrium, fixing its (comoving) number density. However, in the case of neutrino-interacting DM, the DM remains in kinetic equilibrium with the plasma via elastic scattering off neutrinos for a longer period of time. These interactions with the

relativistic plasma allow the DM to feel an additional pressure that resists gravitational collapse and therefore suppresses the formation of structure.

As the temperature continues to drop, the DM goes out of kinetic equilibrium. This happens at a decoupling temperature $T_{\rm d}$ which can be roughly estimated by determining when the rate for the DM momentum to appreciably change via scattering falls below the expansion rate of the Universe. Since it is nonrelativistic, while in kinetic equilibrium the DM has momentum of order $\sqrt{m_\chi T}$ where $m_\chi$ is its mass and $T$ is the temperature. After $N$ scatterings on the components of the relativistic plasma (which carry momentum $T$), the change in DM momentum is typically about $\sqrt{N}T$. For this change to be comparable to the DM momentum itself implies that $N \sim m_\chi/T$. The rate for $N$ scatterings is $\Gamma = n_r\sigma/N \sim (T\, n_r\sigma)/m_\chi$ where $n_r \propto T^3$ is the plasma (radiation) number density and $\sigma$ is the cross section for scattering. The cross section for scattering on relativistic plasma scales as $\sigma = T^2/\Lambda^4$ where $\Lambda$ is the scale of the operator mediating the interaction. The decoupling temperature is found when $\Gamma = H \sim T^2/M_{\rm Pl}$ where $H$ is the Hubble rate and $M_{\rm Pl}$ is the Planck mass. Solving for the decoupling temperature gives the scaling $T_{\rm d} \sim \Lambda(m_\chi/M_{\rm Pl})^{1/4}$. This expression captures the intuitive expectation that as the interaction strength increases ($\Lambda$ decreases) $T_{\rm d}$ decreases.

Because the Universe is expanding after an initial period of inflation, density perturbations on smaller scales enter the horizon before those of larger size. Since only density perturbations with a size smaller than the horizon can grow, perturbations on smaller scales begin to grow before perturbations on larger scales, so that the decoupling temperature sets a minimum size for DM structures that can form. The growth of DM perturbations on scales smaller than the horizon at $T > T_{\rm d}$ is suppressed by the finite pressure of the coupled DM-plasma gas. For $T < T_{\rm d}$, the DM pressure drops to zero and density perturbations on scales of order the horizon size at $T = T_{\rm d}$ and smaller can grow. Because the (comoving) DM number density remains a constant, and since we know the present DM mass density, the lower bound on the size of unsuppressed DM structures can be expressed as a lower bound on the mass of gravitationally bound DM objects, $M_{\rm cutoff}$. As we will see in Section 3.3, this cutoff can be related to the decoupling temperature via $M_{\rm cutoff} \sim 10^8 M_\odot (\mathrm{keV}/T_{\rm d})^3$, where $M_\odot \simeq 2 \times 10^{30}$ kg is the mass of the Sun. The standard weakly interacting massive

particle (WIMP) CDM scenario with $\Lambda \sim m_\chi \sim 100$ GeV leads to a decoupling temperature around 10 MeV and hence $M_{\rm cutoff} \ll M_\odot$, which is too small to be relevant for the small scale structure puzzles [114–116].

Strong neutrino-DM interactions lower $T_{\rm d}$ which increases $M_{\rm cutoff}$, offering a solution to the missing satellites problem by suppressing the formation of smaller halos. Of course, $M_{\rm cutoff}$ must be chosen to be consistent with observations of halo masses. An analysis of satellite galaxies indicates that the mass of their surrounding DM halos before accretion onto the Milky Way was around $M_{\rm halo} \sim 10^9 M_\odot$ [117]. Measurements of the Lyman-$\alpha$ absorption lines in the spectra of distant quasars due to the presence of clumps of intergalactic neutral hydrogen (the "Lyman-$\alpha$ forest") indicate that the halos with $M_{\rm halo} \sim 3\times 10^8 M_\odot$ exist [118]. Similarly, DM substructure can be observed using gravitational lensing, with the smallest structures observed having $M_{\rm halo} \sim 1 \times 10^8 M_\odot$ [119, 120]. Since tidal disruption could cause these observed halo masses to be smaller than the original halo, and since a value for $M_{\rm cutoff} < M_{\rm halo}$ is certainly allowed, in this work we consider models with $M_{\rm cutoff}$ in the range $10^7 M_\odot - 10^9 M_\odot$. This range requires a decoupling temperature $T_{\rm d} \sim$ keV. The scaling of $T_{\rm d}$ implies $(\Lambda^4 m_\chi)^{1/5} \sim 50$ MeV. Therefore, in this scenario the DM mass is indicated to be of order tens of MeV.

There are two other small scale structure problems in the CDM paradigm, the "core vs. cusp" and "too big to fail" problems. Simulations of standard CDM predict that the DM density profile $\rho$ in a galaxy should form a cusp at the center, $\rho \propto r^{-1}$ [121]. Observations in some dwarf galaxies indicate that actual DM density profiles appear to be more cored, with a constant DM density in the center [122]. This is the "core vs. cusp" problem. The "too big to fail problem" is that simulations predict that the most massive Milky Way satellite galaxies should be more massive than they are observed to be. In this paper we will spend most of our time detailing the impact of strong neutrino-DM interactions on the missing satellites problem, but we address the other two problems briefly.

This Chapter is organized as follows. In Section 3.2, we build a model of DM that interacts strongly enough with neutrinos to obtain a cutoff mass in the range $10^7 M_\odot - 10^9 M_\odot$ and examine the constraints on it. Section 3.3 contains a detailed calculation of the cutoff mass in the model. Effects on supernovae are especially interesting and we examine them

in this model in Section 3.4. In Section 3.5 we discuss some possible tests of the model and we conclude in Section 3.6.

## *3.2 The Model*

### *3.2.1 Ingredients and basics*

Interactions between neutrinos and SM gauge singlets, such as DM, can be safely generated through the "neutrino portal." In this scenario, couplings of the SM to DM occur through the operator $H\ell$, where $H$ is the Higgs doublet and $\ell$ is a lepton doublet containing a neutrino and a charged lepton. An effective 4-fermi interaction between neutrinos and DM can be generated that looks schematically like $(H\ell)^2\,(\mathrm{DM})^2$. At the renormalizable level, this higher dimensional operator arises due to the exchange of a mediator that is either neutral or charged under the symmetry that is typically invoked to keep the DM stable. If the mediator is neutral, then exchange of this mediator also leads to neutrino and DM self-interactions. To focus primarily on DM-neutrino interactions, we study the case where the mediator is also charged under the DM stabilization symmetry.

In light of the discussion above, we introduce a complex scalar, $\phi$, and a Dirac fermion, $\chi$, which are oppositely charged under a global, conserved $\mathrm{U}(1)_\mathrm{d}$ that acts as the DM stabilization symmetry. The SM fields are all neutral with respect to this $\mathrm{U}(1)_\mathrm{d}$. The lighter of $\phi$ and $\chi$ is therefore stable and is our DM candidate. For definiteness, and because the opposite situation gives qualitatively the same results, we focus on the situation where the DM is fermionic with $\chi$ lighter than $\phi$.

Additionally, we give $\phi$ lepton number $-1$ so that we can generate an effective DM-neutrino coupling through the operator $\phi\bar{\chi}\nu$ without breaking lepton number. The other ingredients in the model are a pair of left-handed Weyl fermions, $N_{1,2}$, with lepton number $-1$ and $+1$ respectively, that are SM gauge singlets, i.e. sterile neutrinos.

We assume that lepton number is conserved in interactions involving $N_{1,2}$. The observed masses of the light neutrinos could be of the lepton-number violating Majorana type, arising from other lepton-number–violating interactions at a high scale, or Dirac. Although Dirac neutrino masses can easily be made consistent with our model, for definiteness we will

assume the tiny observed masses are Majorana, arising e.g. through a standard seesaw scenario. Below the seesaw scale, the terms in the Lagrangian relevant for the neutrino masses are given by

$$-\mathcal{L}_{\rm m} = \frac{m_{ij}}{\langle H\rangle^2} H\ell_i H\ell_j + M N_1 N_2 + \lambda_i N_1 H \ell_i + \text{h.c.}, \tag{3.1}$$

where $i, j = e, \mu, \tau$ are lepton flavor indices and $H$ is the Higgs doublet. Electroweak and Lorentz indices have been suppressed. $m_{ij}$ is the effective Majorana mass matrix for the active neutrinos which can be generated at a very high scale by interactions that violate lepton number, the details of which are irrelevant for us. We assume that each of the entries in $m$ is much smaller than $M$.

The interaction of the sterile neutrinos with the DM and mediator is given by

$$-\mathcal{L}_{\rm int} = \left(y_1 \phi^* N_1 + y_2 \phi N_2\right) \chi_L + \text{h.c.}, \tag{3.2}$$

We have assumed that the couplings of the right-handed component of $\chi$ can be ignored compared to those of the left-handed component—reversing or relaxing this assumption does not change any of the physics we are interested in.

After electroweak symmetry is broken, the Higgs field gets a vacuum expectation value, $\langle H\rangle \equiv v = 174$ GeV, which leads, in the basis $(\nu_i, N_1^*, N_2)$, to the neutrino mass matrix,

$$\begin{pmatrix} m_{ij} & \lambda_j v & 0 \\ \lambda_i v & 0 & M \\ 0 & M & 0 \end{pmatrix}. \tag{3.3}$$

$N_1^*$ pairs up with

$$\hat{\nu}_4 = \frac{M N_2 + \sum_i \lambda_i v \nu_i}{\sqrt{M^2 + \sum_i \lambda_i^2 v^2}} \tag{3.4}$$

to form a Dirac fermion $\hat{N} = (\hat{\nu}_4, N_1^*)^{\rm T}$ with mass $m_4 = \sqrt{M^2 + \sum_i \lambda_i^2 v^2}$. To avoid limits on the number of neutrino species present during the time of neutrino decoupling from measurements of the CMB [123] as well as from big bang nucleosynthesis (BBN) [124], we take $m_4 > 10$ MeV. The orthogonal linear combinations of $\nu_i$ and $N_2$ furnish three Majorana neutrinos with masses $m_{1,2,3}$ which are extremely small compared to $m_4$, at most $\mathcal{O}\left(0.5 \text{ eV}\right)$.

We write the relationship between the mass eigenstates and the flavor eigenstates explicitly using the unitary matrix $U$ that diagonalizes the mass matrix,

$$\nu_i = U_{ij}\hat{\nu}_j, \tag{3.5}$$

with $i = e, \mu, \tau, N$ (defining $\nu_N \equiv N_2$) and $j = 1, \ldots, 4$.

The mediator $\phi$ decays to $\bar{\chi}$ and antineutrinos through Eq. (3.2). The rate for this is

$$\Gamma_{\phi \to \bar{\nu}\bar{\chi}} = \sum_i |U_{Ni}|^2 \frac{y_2^2 m_\phi}{16\pi}, \tag{3.6}$$

where the sum runs over kinematically allowed neutrinos, and we neglect the light neutrino masses and $m_\chi$. We will be most interested in the case where the heavy neutrino can decay invisibly to $\chi\bar{\chi}$ plus a light neutrino through an intermediate $\phi$ with a rate,

$$\Gamma_{\hat{N} \to \nu\chi\bar{\chi}} = \frac{\left(y_1^2 + |U_{N4}|^2 y_2^2\right) m_4}{32\pi} \times \begin{cases} 1 & \text{if } m_\phi \ll m_4 \\ \left(1 - |U_{N4}|^2\right) \frac{y_2^2}{192\pi^2} \left(\frac{m_4}{m_\phi}\right)^4 & \text{if } m_\phi \gg m_4, \end{cases} \tag{3.7}$$

where we have ignored $m_\chi$. As long as this is kinematically allowed ($m_4 > 2m_\chi$, since the light neutrino masses are negligible) it is the dominant decay channel for the heavy neutrino. The heavy neutrino can also decay visibly through the weak neutral current. The rate for the decay to $\nu e^+ e^-$, for example, is

$$\Gamma_{\hat{N} \to \nu e^+ e^-} = \left(1 - |U_{N4}|^2\right) \frac{G_F^2 m_4^5}{192\pi^3}. \tag{3.8}$$

In the phenomenologically interesting region $G_F m_4^2, G_F m_\phi^2 \ll 1$, so the visible decays of the heavy neutrino are highly suppressed.

We will be particularly interested in the cross section for the light neutrinos to scatter on DM at rest, through diagrams like that shown in Figure 3.1. Defining $\sigma_{\hat{\nu}_i\chi}$ as the cross section for the $i$th neutrino mass eigenstate to scatter, $\hat{\nu}_i\chi \to \sum_{j=1}^3 \hat{\nu}_j\chi$, we have

$$\sigma_{\hat{\nu}_i\chi} = \frac{|U_{Ni}|^2}{|U_{e4}|^2 + |U_{\mu 4}|^2 + |U_{\tau 4}|^2} \sigma_{\nu\chi}, \quad \sigma_{\nu\chi} = \sum_{i=1}^3 \sigma_{\hat{\nu}_i\chi}, \tag{3.9}$$

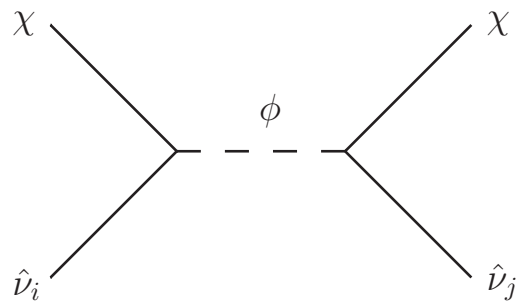


Figure 3.1: Diagram relevant for neutrino scattering on DM and for DM annihilation to neutrinos.

with

$$\frac{d\sigma_{\nu\chi}}{dE'_\nu} = \frac{g^4}{32\pi} m_\chi \left\{ \frac{1}{\left(m_\phi^2 - m_\chi^2 - 2m_\chi E_\nu\right)^2 + m_\phi^2 \Gamma_\phi^2} + \frac{{E'_\nu}^2/E_\nu^2}{\left(m_\phi^2 - m_\chi^2 + 2m_\chi E'_\nu\right)^2 + m_\phi^2 \Gamma_\phi^2} \right\}. \tag{3.10}$$

In this expression, $E_\nu$ is the initial neutrino energy and $E'_\nu$ is the final neutrino energy which is in the range $E_\nu/\left(1 + 2E_\nu/m_\chi\right) < E'_\nu < E_\nu$. We have ignored the light neutrino masses, made use of the unitarity of $U$, and defined the coupling

$$g \equiv y_2 \sqrt{|U_{e4}|^2 + |U_{\mu 4}|^2 + |U_{\tau 4}|^2}. \tag{3.11}$$

Without loss of generality, we will set $g > 0$ throughout this paper.

In the limit that the neutrino energy is small, $E_\nu \ll m_{\chi,\phi}$, the cross section becomes

$$\sigma_{\nu\chi} = \frac{g^4}{8\pi} \frac{E_\nu^2}{\left(m_\phi^2 - m_\chi^2\right)^2} = 5 \times 10^{-38} \mathrm{cm}^2 \left(\frac{g}{0.3}\right)^4 \left(\frac{E_\nu}{1\ \mathrm{keV}}\right)^2 \left(\frac{40\ \mathrm{MeV}}{m_\phi}\right)^4, \tag{3.12}$$

ignoring terms of order $m_\chi^2/m_\phi^2$ on the RHS. This form for the cross section matches on to $\sigma = T^2/\Lambda^4$ with $\Lambda \sim \sqrt{m_\phi^2 - m_\chi^2}/g$. As mentioned in the introduction, to have $10^7 M_\odot \lesssim M_{\mathrm{cutoff}} \lesssim 10^9 M_\odot$, we require that $\Lambda$ and $m_\chi$ are $\mathcal{O}\left(\text{few} \times 10\ \mathrm{MeV}\right)$. In other words, we need $m_\chi$ and $m_\phi$ to be tens of MeV and $g \gtrsim 0.1$.

When the temperature of the Universe is larger than $m_\chi$, the DM and anti-DM will exist in chemical equilibrium with the rest of the constituents of the plasma. As the Universe cools below $m_\chi$, the DM and anti-DM number densities are depleted through annihilation to light neutrinos via $\phi$ exchange (also through diagrams like the one in Figure 3.1) which occurs with a cross section

$$\sigma_{\rm ann} v = \frac{g^4 m_\chi^2}{16\pi m_\phi^4} = 3 \times 10^{-20} \frac{\rm cm^3}{\rm s} \left(\frac{g}{0.3}\right)^4 \left(\frac{m_\chi}{20\ \rm MeV}\right)^2 \left(\frac{40\ \rm MeV}{m_\phi}\right)^4 . \tag{3.13}$$

This process sets a lower limit on the DM mass to avoid the production of neutrinos during BBN. The requirement is that $m_\chi \gtrsim 10$ MeV [124, 125]. Additionally, for parameter values motivated by small scale structure considerations, this annihilation cross section is too large for the DM to be a thermal relic. We assume that its relic density is set by a primordial DM–anti-DM asymmetry. Whether this asymmetry is connected to the baryon asymmetry is beyond the scope of this work.

There are also constraints on the strength of the DM-neutrino interaction from measurements of the Lyman-$\alpha$ forest [126] as well as the CMB [127, 128], which again imply that the DM has a mass greater than about 10 MeV.

To determine whether $g \gtrsim 0.1$ and $m_{\chi,\phi} \sim$ few $\times$ 10 MeV are feasible requires examining the constraints on $|U_{e4}|$, $|U_{\mu 4}|$, and $|U_{\tau 4}|$. We do this in the next section. We assume that $m_4 > 2m_\chi$, so that the heavy neutrino decays invisibly.

### *3.2.2 Neutrino mixing matrix elements*

Below, we determine what values of the elements of the neutrino mixing matrix, $U$, are allowed by data from lepton and meson decays and neutrino oscillation experiments. We pay particular attention to $|U_{e4}|$, $|U_{\mu 4}|$, and $|U_{\tau 4}|$ since they directly enter the cross section relevant for keeping DM in thermal equilibrium with the neutrinos. The constraints on these matrix elements for the case of an additional, heavy, invisibly decaying neutrino are not well organized and not always correctly treated in the literature. We collect these constraints and show the limits on these matrix elements from our analysis in Figure 3.2. We defer discussion of constraints from supernovae to Section 3.4.

*Limits on $|U_{e4}|$, $|U_{\mu 4}|$, and $|U_{\tau 4}|$ from particle decays*

We now examine the existing limits on $|U_{e4}|$, $|U_{\mu 4}|$, and $|U_{\tau 4}|$ in the case of an invisibly decaying heavy neutrino with mass above around 10 MeV that can be derived from meson and lepton decays.

We first focus on decays of a meson $M$ to a lepton $\ell$ and neutrino mass eigenstate $\hat{\nu}_i$, $M^+ \to \ell^+ \hat{\nu}_i$. Since the heavy neutrino decays invisibly, all final state neutrino mass eigenstates result in the same signal, $\ell^+$ and missing energy, up to a difference in the energy of the $\ell^+$. The light neutrino masses can all be neglected, while the heavy neutrino mass must be retained. The decay rate to light neutrinos is

$$\Gamma_{M^+ \to \ell^+ \hat{\nu}_{1,2,3}} = \sum_{i=1}^{3} |U_{\ell i}|^2 \, \Gamma^{\rm SM}_{M^+ \to \ell^+} = \left(1 - |U_{\ell 4}|^2\right) \Gamma^{\rm SM}_{M^+ \to \ell^+} \tag{3.14}$$

and the rate to the heavy neutrino is

$$\Gamma_{M^+ \to \ell^+ \hat{\nu}_4} = |U_{\ell 4}|^2 \, \rho_{M\ell}\left(m_4\right) \Gamma^{\rm SM}_{M^+ \to \ell^+}. \tag{3.15}$$

$\Gamma^{\rm SM}_{M^+ \to \ell^+}$ is the rate for this process as calculated in the SM for a massless neutrino. $\rho_{M\ell}\left(m_4\right)$ is a factor that reflects the reduced phase space available as well as possible enhancement to helicity-suppressed decays with $\rho_{M\ell}\left(m_4 = 0\right) = 1$ and $\rho_{M\ell}\left(m_4 \geq m_M - m_\ell\right) = 0$. There are therefore two signatures of a heavy neutrino in this decay: (i) a change in the total rate for $M \to \ell$ from the SM expectation and (ii) if kinematically allowed, a peak in the $\ell$ energy spectrum at $(m_M^2 + m_\ell^2 - m_4^2)/2m_M$ in the $M$ rest frame.

Decays with more than two particles in the final state, such as muon decay, leptonic $\tau$ decays, and semileptonic kaon decays, are modified analogously, with a straightforward adjustment of the phase space and the possible inclusion of a second $|U_{\ell 4}|$ if two neutrinos are in the final state. We now discuss the available data.

Peak searches in $\pi \to e\nu$ [129, 130] strongly constrain $|U_{e4}|$ while searches for peaks in $\pi \to \mu\nu$ [135], and $K \to \mu\nu$ [136, 137] similarly limit $|U_{\mu 4}|$. We show these limits in Figure 3.2.

Limits on $|U_{e4}|$ and $|U_{\mu 4}|$ can be obtained by comparing $\Gamma_{\pi \to e\nu}$ to $\Gamma_{\pi \to \mu\nu}$. Defining

$$R = \left(\frac{\Gamma_{\pi \to e\nu}}{\Gamma_{\pi \to \mu\nu}}\right)_{\rm exp} \Bigg/ \left(\frac{\Gamma_{\pi \to e\nu}}{\Gamma_{\pi \to \mu\nu}}\right)_{\rm SM} = \frac{1 + |U_{e4}|^2 \left[\rho_{\pi e}\left(m_4\right) - 1\right]}{1 + |U_{\mu 4}|^2 \left[\rho_{\pi \mu}\left(m_4\right) - 1\right]}, \tag{3.16}$$

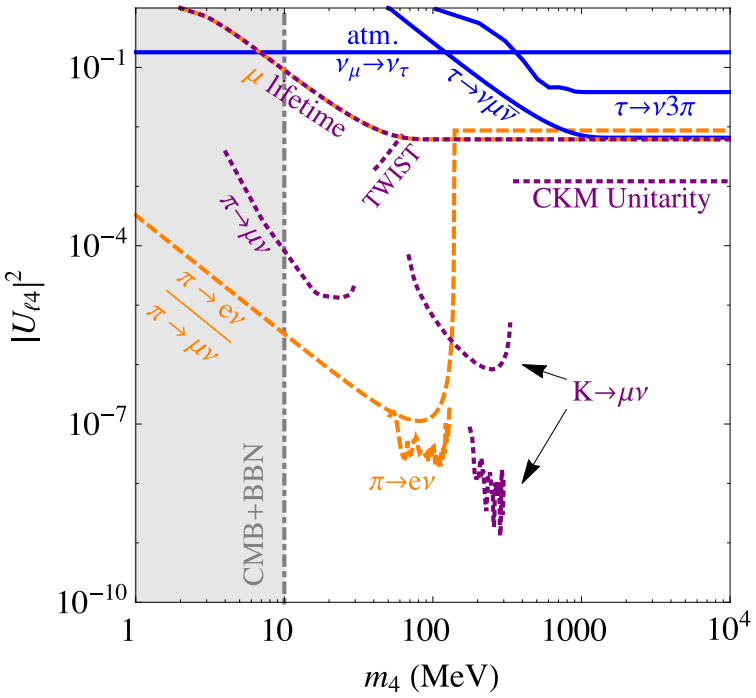


Figure 3.2: 90% C. L. upper limits on $|U_{\ell 4}|^2$, $\ell = e, \mu, \tau$, as functions of the heavy neutrino mass $m_4$ from meson and lepton decays. Limits on $|U_{e4}|^2$ (dashed, orange) come from searches in $\pi \to e\nu$ [129, 130], the ratio of $\Gamma(\pi \to e\nu)/\Gamma(\pi \to \mu\nu)$ [131–133] and the measurement of the muon lifetime [134]. $|U_{\mu 4}|^2$ limits (dotted, purple) are derived from peak searches in $\pi \to \mu\nu$ [135] and $K \to \mu\nu$ [136, 137], the muon lifetime measurement [134], the energy spectrum in muon decay (labeled "TWIST") [138, 139], and the unitarity of the measurements of the CKM matrix [10]. We have derived limits on $|U_{\tau 4}|^2$ (blue, solid) from the rate for $\tau \to \mu\nu\bar{\nu}$ and data from Ref. [140] on $\tau \to \nu 3\pi$. We also show the limit on $|U_{\tau 4}|$ from atmospheric neutrino oscillations described in Section 3.2.2 and the lower bound on $m_4$ from BBN and CMB measurements. Where rates depend on more than one $|U_{\ell 4}|$, we assume only one is dominant to produce each limit. See text for details.

current data [131, 132] and SM prediction [133] gives $R = 0.996 \pm 0.003$. This is particularly constraining on $|U_{e4}|$ since $\pi \to e\hat{\nu}_4$ is not as helicity-suppressed as the decay to light neutrinos. In Figure 3.2 we show the limit that $R$ implies on $|U_{e4}|$ if we assume that $|U_{\mu 4}| = 0$ which gives a conservative limit for $m_4 < m_\pi$.

Nonzero values of $|U_{e4}|$ and $|U_{\mu 4}|$ can also affect the relationship between the Fermi constant extracted from measurements of the muon lifetime, $G_\mu$, and determinations using high energy data. In the on-shell renormalization scheme, for example, the Fermi constant can be expressed in terms of the $W$ and $Z$ boson masses and the fine structure constant through

$$G_F = \frac{\pi\alpha}{\sqrt{2}\left(1 - m_W^2/m_Z^2\right) m_W^2 \left(1 - \Delta r\right)}, \tag{3.17}$$

where $1 - \Delta r = 0.9636 \pm 0.0004$ encodes radiative corrections. The presence of a heavy neutrino with $m_4 > m_\mu - m_e$ changes the relationship between $G_F$ measured in this way and $G_\mu$ via

$$G_\mu^2 = \left(1 - |U_{e4}|^2\right)\left(1 - |U_{\mu 4}|^2\right) G_F^2. \tag{3.18}$$

The expression when $m_4 < m_\mu - m_e$ is more complicated but straightforward. The very precise measurement of the muon lifetime [134] gives $G_\mu = (1.1663787 \pm 0.0000006) \times 10^{-5}$ GeV$^{-2}$. Using $m_W = 80.385 \pm 0.015$ GeV and $m_Z = 91.1876 \pm 0.0021$ GeV results in $G_F = (1.168 \pm 0.001) \times 10^{-5}$ GeV$^{-2}$. We use these values to set an upper limit on the larger of $|U_{e4}|$ or $|U_{\mu 4}|$, conservatively assuming that the smaller of the two can be neglected, in Figure 3.2. For $m_4 > m_\mu - m_e$, the limit is $|U_{e4}|$, $|U_{\mu 4}| < 7.9 \times 10^{-2}$ at 90% C. L.

For $m_4 < m_\mu - m_e$, the shape of the $e^+$ energy spectrum in $\mu^+$ decay is modified. This spectrum was most accurately measured in [138] which was used to set a limit on $|U_{\mu 4}|$ in [139] for $m_4 > 40$ MeV which we also show in Figure 3.2, labeled as "TWIST."[1]

There is also a constraint on $|U_{\mu 4}|$ that can be derived using the unitarity of the quark mixing (CKM) matrix, $V$. $V_{ud}$ is most accurately measured using superallowed nuclear beta

[1]The reason we only show the limit for $m_4 > 40$ MeV is that there is a gap in the limit on $|U_{\mu 4}|$ between the regions probed by $\pi \to \mu\nu$ and $K \to \mu\nu$, i.e. for 40 MeV $< m_4 <$ 80 MeV [139].

decays. For $m_4$ larger than several MeV, the rates for these are proportional to

$$\left(1-|U_{e4}|^2\right)|V_{ud}|^2\,G_F^2. \tag{3.19}$$

$V_{ud}$ is extracted by dividing this by $G_\mu^2$. Doing so gives [10]

$$\frac{|V_{ud}|}{\sqrt{1-|U_{\mu 4}|^2}} = 0.97425 \pm 0.00022. \tag{3.20}$$

A value of $V_{us}$ can be extracted from $K_L \to \pi^- e^+ \nu$ decay. For $m_4 > m_{K^0} - m_{\pi^\pm} - m_e$, the rate for this is proportional to

$$\left(1-|U_{e4}|^2\right)|V_{us}|^2\,G_F^2 \tag{3.21}$$

and again dividing by $G_\mu^2$ results in [10]

$$\frac{|V_{us}|}{\sqrt{1-|U_{\mu 4}|^2}} = 0.2253^{+0.0015}_{-0.0013}. \tag{3.22}$$

Squaring then adding (3.21) and (3.22) and using the unitarity of the CKM matrix implies that

$$\frac{1-|V_{ub}|^2}{1-|U_{\mu 4}|^2} = 0.9999^{+0.0008}_{-0.0007}. \tag{3.23}$$

At this level $|V_{ub}|$ is negligible and can be ignored. Doing so, this translates into the constraint $|U_{\mu 4}| < 3.5 \times 10^{-2}$ at 90% C. L.

To find limits on $|U_{\tau 4}|$, we look at processes involving the $\tau$ neutrino such as $\tau$ decays or decays of $D_s$ mesons. Existing searches using $D_s$ decays for heavy neutrinos all look for visible decays of the heavy neutrino, so they are not sensitive to this scenario. Consequently, we focus on $\tau$ decays. In deriving our limits on $|U_{\tau 4}|$ below, we assume that $|U_{e4}|$, $|U_{\mu 4}| \ll |U_{\tau 4}|$. In this case, the total rate for $\tau$ to decay to a generic final state $X$ plus missing energy is

$$\Gamma_{\tau \to X\nu} = \left[1+|U_{\tau 4}|^2\left(\rho_{\tau X}\left(m_4\right)-1\right)\right]\Gamma^{\mathrm{SM}}_{\tau \to X}, \tag{3.24}$$

where, as before, $\rho_{\tau X}\left(m_4\right)$ is a kinematic factor that depends on the heavy neutrino mass.

Because leptonic $\tau$ decay rates are well-predicted and well-measured, they can offer meaningful constraints on $|U_{\tau 4}|$. We can use the measurements of the branching ratios for

$\tau \to e\bar{\nu}\nu$ and $\tau \to \mu\bar{\nu}\nu$ of $17.83 \pm 0.04\%$ and $17.41 \pm 0.04\%$ respectively [10] along with the independently measured $\tau$ lifetime, $(290.17 \pm 0.62) \times 10^{-15}$ s [141], to determine the experimental rates,

$$\begin{aligned} \Gamma^{\rm exp}_{\tau\to e\bar{\nu}\nu} &= (4.04 \pm 0.09) \times 10^{-13}\ \text{GeV}, \\ \Gamma^{\rm exp}_{\tau\to \mu\bar{\nu}\nu} &= (3.95 \pm 0.09) \times 10^{-13}\ \text{GeV}. \end{aligned} \tag{3.25}$$

Using these with the SM expectations for these rates which take into account the error on $m_\tau$ [142],

$$\begin{aligned} \Gamma^{\rm SM}_{\tau\to e\bar{\nu}\nu} &= (4.031 \pm 0.001) \times 10^{-13}\ \text{GeV}, \\ \Gamma^{\rm SM}_{\tau\to \mu\bar{\nu}\nu} &= (3.920 \pm 0.001) \times 10^{-13}\ \text{GeV}, \end{aligned} \tag{3.26}$$

and the expression in (3.24) can limit $|U_{\tau 4}|$. The constraint from $\tau \to \mu$ decay, shown in Figure 3.2,[2] is stronger since the central value of the measured rate is further from the SM expectation than the $\tau \to e$ mode, although still in agreement. For $m_4 > m_\tau - m_\mu$ the 90% C. L. limit is $|U_{\tau 4}| < 8 \times 10^{-2}$ and weakens to $|U_{\tau 4}| < 0.4$ at $m_4 = 130$ MeV.

We can also set a limit on $|U_{\tau 4}|$ by looking for changes in the differential rates for $\tau$ decays to multiparticle final states. This procedure was undertaken by the ALEPH collaboration [140] to place an upper limit of 18.2 MeV at 95% C. L. on the mass of the $\tau$ neutrino using $\tau \to \nu 3\pi$ and $\tau \to \nu 5\pi$ decays. We use the data for the $\tau \to \nu 3\pi$ rate as a function of the three pion invariant mass from [140], modeling the $\tau \to \nu 3\pi$ decay as occurring through the chain $\tau \to \nu a_1 \to \nu\pi\rho \to \nu 3\pi$ to set a limit on $|U_{\tau 4}|$ varying $m_4$, also shown in Figure 3.2. This limit is less strong than what we derived from $\tau \to \mu$ decays, partially due to the fact that properly modeling the $3\pi$ rate is nontrivial. Properly modeling the $5\pi$ decay mode is even more difficult but could offer an improvement in the limit due to the reduced phase space available which enhances the effects of a massive neutrino.

---

[2] Our limits on $|U_{\tau 4}|$ for a heavy neutrino that decays invisibly differ substantially from those in [143] which also considered shifts in leptonic $\tau$ decays. The main reason for this is that we consider a unitary neutrino mixing matrix whereas [143] does not [effectively making the replacement $\rho_{\tau X}(m_4) \to \rho_{\tau X}(m_4) + 1$ in (3.24)] with the consequence that our limits weaken as the heavy neutrino mass is decreased. This is to be expected for a unitary mixing matrix since the heavy neutrino becomes indistinguishable from the light neutrinos as it is made lighter. Additionally, since the presence of a heavy neutrino in the final state also affects the other decay modes, we limit the change in the leptonic *rate* itself using the branching ratio and the independent determination of the $\tau$ lifetime. In contrast [143] limited shifts of the branching ratio effectively assuming the total width was unchanged.

As mentioned above, solutions to small scale structure problems imply that

$$g = y_2 \sqrt{\sum_\ell |U_{\ell 4}|^2} \sim 0.3.$$

Given the constraints outlined above, and without increasing $y_2$ to nonpertubative values, this is only possible to achieve with $|U_{\tau 4}| \gtrsim 0.1$. In this case $m_4 \lesssim 300$ MeV and $|U_{e4}|$, $|U_{\mu 4}| \ll |U_{\tau 4}|$. In the rest of the paper, we therefore simplify our analysis by making the approximation that $\lambda_{e,\mu} = 0$ in Eq. (3.1). In that case, $|U_{e4}| = |U_{\mu 4}| = 0$ and $U_{\tau 4} \equiv \sin\theta_\tau$ with $\theta_\tau = \tan^{-1}(-\lambda_\tau v/M)$. The light Majorana neutrinos are linear combinations of $\nu_e$, $\nu_\mu$ and $\nu_{\tau N} \equiv \cos\theta_\tau \nu_\tau - \sin\theta_\tau N_2$ while the heavy Dirac neutrino has mass $m_4 = M/\cos\theta_\tau$ and contains $\hat{\nu}_4 = \cos\theta_\tau N_2 + \sin\theta_\tau \nu_\tau$ and $N_1^*$.[3]

*Constraints from neutrino oscillation experiments*

In the limit that $U_{e4}$ and $U_{\mu 4}$ are zero, we can parameterize the $4 \times 4$ matrix $U$ using only four angles, $\theta_\tau$ as defined above, $\theta_{12}$, $\theta_{13}$, and $\theta_{23}$,

$$\begin{aligned} U &= \begin{pmatrix} 1 & 0 & 0 & 0 \\ 0 & 1 & 0 & 0 \\ 0 & 0 & c_\theta & s_\theta \\ 0 & 0 & -s_\theta & c_\theta \end{pmatrix} \begin{pmatrix} 1 & 0 & 0 & 0 \\ 0 & c_{23} & s_{23} & 0 \\ 0 & -s_{23} & c_{23} & 0 \\ 0 & 0 & 0 & 1 \end{pmatrix} \begin{pmatrix} c_{13} & 0 & s_{13} & 0 \\ 0 & 1 & 0 & 0 \\ -s_{13} & 0 & c_{13} & 0 \\ 0 & 0 & 0 & 1 \end{pmatrix} \begin{pmatrix} c_{12} & s_{12} & 0 & 0 \\ -s_{12} & c_{12} & 0 & 0 \\ 0 & 0 & 1 & 0 \\ 0 & 0 & 0 & 1 \end{pmatrix} \\ &= \begin{pmatrix} c_{12}c_{13} & c_{13}s_{12} & s_{13} & 0 \\ -c_{23}s_{12} - c_{12}s_{13}s_{23} & c_{12}c_{23} - s_{12}s_{13}s_{23} & c_{13}s_{23} & 0 \\ -c_\theta(c_{12}c_{23}s_{13} - s_{12}s_{23}) & -c_\theta(c_{23}s_{12}s_{13} + c_{12}s_{23}) & c_\theta c_{13}c_{23} & s_\theta \\ s_\theta(c_{12}c_{23}s_{13} - s_{12}s_{23}) & s_\theta(c_{23}s_{12}s_{13} + c_{12}s_{23}) & -s_\theta c_{13}c_{23} & c_\theta \end{pmatrix}, \end{aligned} \tag{3.27}$$

with $c_\theta \equiv \cos\theta_\tau$, $s_\theta \equiv \sin\theta_\tau$ and $c_{ij} \equiv \cos\theta_{ij}$, $s_{ij} \equiv \sin\theta_{ij}$. For simplicity, we have ignored possible $CP$-violating phases in the mixing matrix.

[3]The reason that we did not choose to add just a single Weyl sterile neutrino earlier is that in such a scenario, after integrating the sterile neutrino out, the light neutrino mass matrix element $m_{ij}$ receives contributions proportional to the product of mixing angles $\theta_i\theta_j M$, where $M$ is the sterile neutrino mass and the mixing angle between active neutrino $i$ and the sterile neutrino is again $\theta_i \sim \lambda_i v/M$. Obtaining a mixing angle large enough to be interesting in this case requires a sterile neutrino that is too light to avoid cosmological difficulties.

Although we have four flavors of neutrino, our analysis of existing constraints differs from existing sterile neutrino analyses because the fourth mass eigenstate is assumed to be heavier than several MeV, in order to avoid cosmological constraints from the CMB [123] and BBN [124]. As discussed above, the heavy fourth mass eigenstate is mostly comprised of sterile and tau flavors, in order to satisfy laboratory and precision electroweak constraints on electron and muon neutrino mixing with a neutral heavy lepton. Current terrestrial experiments produce either $\mu$ or $e$ flavor neutrinos at the source, and so can only produce a linear combination of the three light mass eigenstates. Since the light mass eigenstates are comprised of all four flavors, $e$, $\mu$, $\tau$, and sterile $N_2$, the presence of the sterile component could affect neutrino oscillation experiments. Oscillations via the heavy neutrino are independent of the particular value of its mass since they correspond to a length

$$L = \frac{4\pi p}{\Delta m^2} \simeq \frac{4\pi p}{m_4^2} \lesssim 2.5 \times 10^{-12}\ \text{cm} \left(\frac{p}{\text{MeV}}\right), \tag{3.28}$$

where $p$ is the momentum of the neutrinos in question, using the lower bound on the heavy neutrino mass of about 10 MeV. Therefore, the light mass differences must be given by the solar and atmospheric mass splittings as usual [144],

$$\Delta m^2_{12} = \Delta m^2_{\odot} \simeq 7.5 \times 10^{-5}\ \text{eV}^2, \ \ \left|\Delta m^2_{13}\right| = \Delta m^2_{\text{atm}} \simeq 2.5 \times 10^{-3}\ \text{eV}^2, \tag{3.29}$$

where $\Delta m^2_{ij} \equiv m_i^2 - m_j^2$.

We begin by noting that our assumption that $U_{e4}$ and $U_{\mu 4}$ are negligible allows us to determine $\theta_{12}$, $\theta_{13}$, and $\theta_{23}$ using terrestrial neutrino experiments which are insensitive to $\theta_\tau$. Combining these measurements with solar neutrino experiments allows for possible sensitivity to $\theta_\tau$. We describe this procedure below.

In principle, one needs to account for the effect of the different interaction with matter of the sterile neutrinos [145, 146], which can be included via a potential $V_{\text{nc}}$ in the flavor basis for the active neutrino flavors of

$$V_{\text{nc}} = -\frac{G_F}{\sqrt{2}} n_n \tag{3.30}$$

where $n_n$ is the neutron density, with the opposite sign for antineutrinos. In matter with equal numbers of protons and neutrons and density of 2.7 g/cm$^3$, a length scale of 4000

km can be derived from $1/V_{\rm nc}$, which gives an estimate of the distance scale required for matter interactions to have an important effect in the analysis of neutrino oscillations [147] in the Earth's crust. Currently, the strongest constraints on the active neutrino mixing parameters derive from experiments which are not at long enough baseline to be highly sensitive to the matter effects. However, as we point out below, a strong limit on $\theta_\tau$ may be extracted from the IceCube and Super-Kamionkande experiments, due the difference in matter effects between sterile and active neutrinos as they travel through the Earth.

The best determination of $U_{e3}$ is by the reactor experiment Daya Bay [148], which measures electron antineutrino disappearance over a distance of 1.6 km. The value of $U_{\mu 3}$ may be determined by measurements of muon neutrino and antineutrino disappearance by the K2K [149] and MINOS experiments [150], with baselines of 250 km and 730 km, respectively. Because matter effects are not highly significant at these baselines, extraction of this parameter is little affected by the possible presence of a sterile component in the third mass eigenstate. $U_{e2}$ can be determined by the long baseline reactor experiment KamLAND [151] which has a baseline average of 180 km. These measurements of $U_{e3}$, $U_{\mu 3}$, and $U_{e2}$ can be combined to give determinations of $\theta_{12}$, $\theta_{13}$, and $\theta_{23}$ that are independent of $\theta_\tau$, and these angles must be close to the values given by the usual three neutrino fits to data [144],

$$\theta_{12} \sim 32^\circ,\ \theta_{13} \sim 8^\circ,\ \theta_{23} \sim 40^\circ. \tag{3.31}$$

Turning now to solar neutrinos, we note that electron neutrino disappearance is mainly governed by the flavor composition of the second mass eigenstate, since we may neglect the small angle $\theta_{13}$. High energy solar electron neutrinos are produced in the core of the sun, primarily via $^8$B decays, and have a large effective mass from the matter interactions, larger than $\sqrt{\Delta m^2_{12}}$ but smaller than $\sqrt{|\Delta m^2_{23}|}$. These electron neutrinos are approximately an energy eigenstate of the effective Hamiltonian which includes matter interactions. Adiabatic evolution of the electron neutrinos as they exit the core causes them to exit the sun primarily as the second mass eigenstate in vacuum. Neglecting $\theta_{13}$, the fraction of this mass eigenstate which is detected as electron neutrino is $|s_{12}|^2$, while the fraction $|c_{12}s_{23}\sin\theta_\tau|^2$ is undetectable sterile. Hence, high energy charged current electron neutrino detection from

solar neutrino experiments and the solar neutral current flux [152] can be used to constrain $\theta_\tau$ when combined with either the KamLAND determination of $\theta_{12}$ or with the theoretical calculation of the $^8$B flux. Because the KamLAND experiment, while very constraining of $\sqrt{\Delta m^2_{12}}$, is not as sensitive to $U_{e2}$, the theoretical calculation of the $^8$B flux currently gives the best precision on this determination. Experimentally, a combination of electron scattering and neutral current measurements are used to calibrate the flux [153, 154] and the sterile neutrino component could affect this. Since the $^8$B flux is theoretically known to about the 15% level currently [155], we obtain a limit of $|\sin\theta_\tau| \lesssim 0.6$. This agrees with analyses of the combined solar data and KamLAND that has shown that the probability of electron neutrino disappearance into sterile neutrinos could be substantial [156, 157].

Strong limits on $\theta_\tau$ come from the change in matter effects due to mixing with the sterile neutrino. As mentioned above, the light eigenstates are made up of $\nu_e$, $\nu_\mu$, and $\nu_{\tau N}$. In the presence of nonzero $\theta_\tau$, $\nu_{\tau N}$ has diminished weak interactions compared to $\nu_\mu$, with a potential given by $V_{\tau N} = V_{\rm nc}\cos^2\theta_\tau$. A recent search by Super-Kamiokande [158] used atmospheric neutrinos to look for $\mu \to$ sterile transitions. Because of the lack of matter effects for the sterile neutrinos, this can manifest as a change in the distribution of muon neutrino zenith angle in the detector from the standard $\mu \to \tau$ transition scenario. At 90% C. L., the limit is $|U_{\tau 4}| = |\sin\theta_\tau| < 0.42$. Similar effects were searched for in data from IceCube and DeepCore, using the language of neutrino nonstandard interactions (NSI) [159]. In NSI studies, the difference in weak interaction strength between the light flavor eigenstate $\nu_{\tau N}$ and that of $\nu_\tau$ is parameterized by $\epsilon_{\tau\tau}$ with

$$\epsilon_{\tau\tau} = \frac{1}{6}\left(\frac{V_{\tau N}}{V_{\rm nc}} - 1\right) = \frac{\sin^2\theta_\tau}{6}. \tag{3.32}$$

In Ref. [159], a 90% C. L. of $\epsilon_{\tau\tau} < 0.03$ from azimuthal distributions of neutrinos was found. This also translates into $|U_{\tau 4}| < 0.42$. We show this limit along with those from $\tau$ decays in Figure 3.2.

### *3.2.3 New couplings to the Z and Higgs*

At one loop, through the diagram shown on the left in Figure 3.3, an effective coupling of DM to the $Z$ boson is generated. In the limit that $m_4 \gg m_\phi$, this effective interaction is

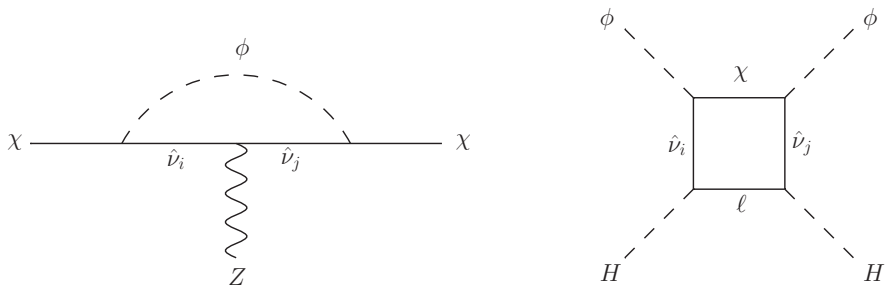


Figure 3.3: Left: one loop diagram which gives rise to an effective $\chi$-$\bar{\chi}$-$Z$ coupling. Right: diagram that contributes to the $|\phi|^2 |H|^2$ operator.

$$\mathcal{L}_{Z\bar{\chi}\chi} = -\frac{g_{\rm w}}{\cos\theta_{\rm w}} \left( \frac{y_2 \sin 2\theta_\tau}{8\pi} \right)^2 Z_\mu \bar{\chi}_L \gamma^\mu \chi_L, \tag{3.33}$$

where $g_{\rm w}$ is the weak coupling strength and $\theta_{\rm w}$ is the weak mixing angle. This operator contributes to the invisible decay width of the $Z$ (the rate for $Z \to$ neutrinos is unchanged due to the unitarity of $U$ for $m_4 \ll m_Z/2$[4]). The good agreement between the SM expectation for this rate and experiment offers a potential constraint on the model. The rate for $Z \to \chi\bar{\chi}$ through this operator is

$$\Gamma_{Z\to\chi\bar{\chi}} = 4.2 \times 10^{-4} \, (y_2 \sin 2\theta_\tau)^4 \ \text{MeV}. \tag{3.34}$$

The 95% C. L. upper limit on extra contributions to the $Z$ invisible width is 2.0 MeV [161]. This translates to a weak limit of $|y_2 \sin 2\theta_\tau| < 8.3$.

This effective $Z_\mu \bar{\chi}_L \gamma^\mu \chi_L$ interaction can lead to the scattering of DM on normal matter. For phenomenologically interesting values of the parameters, however, this scattering is highly suppressed: taking $y_2 = 1$ and $\theta_\tau = 0.3$, the cross section is about $10^{-7} - 10^{-6}$ times that of neutrino scattering. Because this cross section is so small, using proton beam dumps to produce the heavy neutrino, though production of $D_s \to \tau\nu_\tau$ (as used in searches for visibly decaying heavy neutrinos [162–164]), which decays to DM that scatters in a detector (see, e.g. [165–168]) is not promising.

[4] A global fit of electroweak precision data shows a slight preference for nonzero values of $U_{\tau 4}$ if $m_4 \gtrsim 45$ GeV due to a decrease in the invisible $Z$ width [160].

We now consider interactions involving the Higgs. The operators proportional to $\lambda_i$ in (3.1) will lead to contributions to the invisible width of the Higgs boson after electroweak symmetry breaking, through $h \to N_1 \nu_i$. Since we ignore $\lambda_{e,\mu}$ and take $m_4 \ll m_h = 125$ GeV, the rate for this decay is

$$\Gamma_{h\to\text{inv.}} = \frac{\lambda_\tau^2}{16\pi} m_h. \tag{3.35}$$

The invisible branching ratio of the Higgs is presently limited to about 25% [72], which translates into $|\lambda_\tau| \lesssim 2 \times 10^{-2}$. This is not constraining on the model since $|\lambda_\tau| = (m_4/v)|\sin\theta_\tau|$ is less than $2 \times 10^{-3}$ if $m_4 < 300$ MeV.

At one loop, as seen on the right in Figure 3.3, a logarithmically-divergent dimension-4 operator involving the scalar $\phi$ and the Higgs doublet is generated,

$$\mathcal{L}_{\phi H} = \lambda_{\phi H} |\phi|^2 |H|^2, \tag{3.36}$$

with

$$\lambda_{\phi H} \sim \left(\frac{y_1 \lambda_\tau}{2\pi}\right)^2 \log\left(\frac{\Lambda^2}{M^2}\right) = \frac{g^2}{4\pi^2}\left(\frac{y_1}{y_2}\right)^2 \left(\frac{m_4}{v}\right)^2 \log\left(\frac{\Lambda^2}{M^2}\right), \tag{3.37}$$

where $\Lambda$ is the scale of the physics that enters to cut this contribution off. After electroweak symmetry breaking, this gives a contribution to the mass of $\phi$ given by $\delta m_\phi^2 = \lambda_{\phi H} v^2$. This contribution defines a lower bound on $m_\phi$; obtaining a mass below this value requires some fine-tuning of this contribution against the bare value of the mass. Noting that $M \simeq m_4$ and choosing $\Lambda = 1$ TeV,

$$\delta m_\phi^2 \sim (10 \text{ MeV})^2 \left(\frac{g}{0.3}\right)^2 \left(\frac{y_1/y_2}{0.5}\right)^2 \left(\frac{m_4}{100 \text{ MeV}}\right)^2 \left[\log\left(\frac{1 \text{ TeV}}{m_4}\right) \Big/ 10\right]. \tag{3.38}$$

Therefore, $\phi$ can have a mass in the tens of MeV range for a heavy neutrino with mass of $\mathcal{O}(100 \text{ MeV})$ without running into any fine-tuning problems, even for a cutoff at the TeV scale.

### *3.3 Solving The Missing Satellites Problem*

As was mentioned in the introduction, DM-neutrino interactions will suppress the growth of small scale DM density perturbations in the early Universe, helping to alleviate the missing

satellites problem. This suppression of small scale structure occurs below the maximum of two different length scales for washing out structure. These two length scales have different physical origins and will be discussed in detail in this section. Since the DM density is known, this maximum length scale corresponds to a mass cutoff scale, $M_{\rm cutoff}$, below which the formation of less massive structures is suppressed. These cutoff scales have been examined previously in the literature [108–110, 113–115, 169], but we reproduce them here for completeness. We also explicitly show the role of $g_{\rm eff}$ (the effective number of relativistic, bosonic degrees of freedom) in the following equations, in order to clarify discrepancies in the literature.

The first scale for washing out small scale structure is set at early times when the DM is in thermal equilibrium with the relativistic plasma. Once $T \lesssim m_\chi$ the expansion of the Universe will cause the plasma density to decrease enough such that the annihilation and production scattering processes keeping DM in chemical equilibrium with the plasma will freeze out, ending DM number-changing processes. (Note that DM-neutrino interactions that are strong enough to solve the missing satellites problem force DM to be asymmetric and not a thermal relic–see the discussion following Eq. (3.13).) However, DM-neutrino elastic scattering can keep the DM in thermal equilibrium even after chemical decoupling. The DM eventually will fall out of thermal equilibrium once the DM-neutrino elastic scattering rate drops below the Hubble expansion rate of the Universe. This time when elastic scattering ceases is called kinetic decoupling. After this, the DM simply free-streams and washes out small scale structure, setting another scale below which structure formation is suppressed.

In the following we discuss how DM-neutrino interactions can lead to a value of $M_{\rm cutoff}$ in the range of $10^7 M_\odot - 10^9 M_\odot$ which is large enough to solve the missing satellites problem. We will find the range of interesting DM-neutrino coupling, $g$, and DM and mediator masses, $m_\chi$ and $m_\phi$, which can achieve these cutoff mass scales.

### *3.3.1 Kinetic decoupling condition*

Kinetic decoupling occurs when the rate for DM-neutrino collisions to change the DM momentum, $\gamma(T)$, becomes small compared to the Hubble parameter, $H(T)$. Hence the

decoupling temperature, $T_{\rm d}$, can be estimated by solving

$$\gamma(T_d) = H(T_d), \tag{3.39}$$

where

$$\gamma(T) = \frac{1}{3m_\chi T}\int_0^\infty \frac{d^3p}{(2\pi)^3} f(p/T)(1-f(p/T))\int_{-4p^2}^0 dt(-t)\frac{d\sigma_{\nu\chi}}{dt}. \tag{3.40}$$

Here $f(p/T) = (e^{p/T}+1)^{-1}$ is the Fermi-Dirac distribution function describing the neutrinos in the massless limit and $t$ is the usual Mandelstam variable. This kinetic decoupling equation comes from an approximate solution to the Boltzmann equation, see [170]. An exact, though more complicated, analytical form is also available [171]. As we will soon show, DM and the neutrinos must remain in kinetic equilibrium until $T \simeq 1$ keV, which occurs after the neutrinos decouple from the photons at $T \simeq 1$ MeV, in order for DM to solve the missing satellites problem. This means that the terms on the LHS of Eq. (3.39) which have to do with the neutrino-DM fluid should be evaluated at the neutrino temperature, which differs from the photon temperature via $T_\nu = (4/11)^{1/3}T_\gamma$. In what follows all temperatures are photon temperatures and the factor of $(4/11)^{1/3}$ has been included when necessary.

We solve for $T_{\rm d}$ using the approximate form of the total DM-neutrino cross section for $E_\nu \ll m_\chi,\ m_\phi$. This is a good approximation near decoupling since at this point $E_\nu \sim T \ll m_\chi,\ m_\phi$. Hence

$$\frac{d\sigma_{\nu\chi}}{dt} = \frac{g^4}{32\pi\left(m_\phi^2 - m_\chi^2\right)^2}. \tag{3.41}$$

Using this in Eq. (3.39), the remaining integrals can be done analytically and the decoupling temperature is given by

$$\begin{aligned} T_{\rm d} &= \left(\frac{5082}{31\pi\sqrt{5\pi}}\right)^{1/4}\left(\frac{g_{\rm eff}(T_d)^{1/8}}{M_{\rm Pl}^{1/4}}\right)\left(\frac{m_\chi^{1/4}\sqrt{m_\phi^2-m_\chi^2}}{g}\right) \\ &= 1.6\text{ keV}\ \left(\frac{g_{\rm eff}(T_{\rm d})}{3.36}\right)^{1/8}\left(\frac{m_\chi}{20\text{ MeV}}\right)^{1/4}\left(\frac{\sqrt{m_\phi^2-m_\chi^2}}{35\text{ MeV}}\right)\left(\frac{g}{0.3}\right)^{-1}, \end{aligned} \tag{3.42}$$

where $g_{\rm eff}(T)$ is the effective number of relativistic, bosonic degrees of freedom at temperature $T$. This expression for the decoupling temperature contains the correct parametric dependence derived using simple arguments in the introduction. Note that we used the

expression for the Hubble parameter during the radiation dominated period (valid down to $T \simeq 1$ eV) given by

$$H = \sqrt{\frac{4\pi^3 g_{\rm eff}(T)}{45 M_{\rm Pl}^2}} T^2. \tag{3.43}$$

### *3.3.2 The cutoff mass scale*

There are two main processes that erase primordial density fluctuations in the DM fluid on small scales: (i) acoustic oscillations in the coupled, relativistic plasma of the early universe up until the time of kinetic decoupling, and (ii) free streaming of DM after kinetic decoupling. The larger of the two scales set by these processes determines $M_{\rm cutoff}$.

While DM remains in thermal equilibrium with the relativistic plasma, it is involved in the acoustic oscillations of the plasma since it couples to the neutrinos. This results in damped oscillations in the DM power spectrum that appear on the scale of the horizon at kinetic decoupling, $H_{\rm d}^{-1} = a_{\rm d}\eta_{\rm d}$, where $\eta_{\rm d} = \int_0^{t_{\rm d}} dt/a(t)$ is the comoving distance a photon can travel from the beginning of the Universe until the time of kinetic decoupling [115]. Here $a(t)$ denotes the scale factor in a Friedmann-Robertson-Walker metric and $a_{\rm d}$ is the scale factor at the time of kinetic decoupling. This smallest distance scale corresponds to a DM halo mass cutoff given by

$$M_{\rm ao} = \rho_\chi(T_{\rm d}) \frac{4\pi}{3} (a_{\rm d}\eta_{\rm d})^3, \tag{3.44}$$

where $\rho_\chi(T)$ is the DM energy density (equal to its mass density for $T < T_{\rm d} \ll m_\chi$) at temperature $T$. Since the mass enclosed in a given volume remains the same even as that volume expands, $M_{\rm ao}$ can also be expressed in terms of the DM density and scale factor today as

$$M_{\rm ao} = \rho_\chi(T_0) \frac{4\pi}{3} (a_0\eta_{\rm d})^3. \tag{3.45}$$

Using typical values and assuming entropy in a comoving volume is conserved from $T_{\rm d}$ until today, this becomes

$$M_{\rm ao} = 2 \times 10^8 M_\odot \left(\frac{g_{\rm eff}(T_{\rm d})}{3.36}\right)^{-1/2} \left(\frac{T_{\rm d}}{\rm keV}\right)^{-3}, \tag{3.46}$$

where we used $H_0 = 67$ km/s/Mpc, $\Omega_\chi = 0.27$, $g_{\rm eff}(T_0) = 3.36$ and $T_0 = 2.7$ K.

After kinetic decoupling, DM free-streams, washing out structure on scales smaller than $\ell_{\rm eq} = \pi a_{\rm eq} \int_{t_{\rm d}}^{t_{\rm eq}} dt (v_{\rm phys}/a(t))$ at the time of matter-radiation equality [114, 115]. Here $a_{\rm eq}$ is the scale factor at matter-radiation equality, $v_{\rm phys} = v/a(t)$ is the velocity of the DM particles, and $v$ is their constant comoving velocity. This scale describes the distance that DM free-streams from $T_{\rm d}$ to $T_{\rm eq} \simeq 1$ eV. Up until $T_{\rm eq}$ this scale grows as $\ln T$ and the growth after $T_{\rm eq}$, proportional to $T^{-1/3}$, has been neglected. Evaluating $\ell$ today we find

$$\ell_0 = \left(\frac{a_0}{a_{\rm d}}\right)\left(\frac{v}{a_{\rm d}}\right)\frac{\pi}{H_{\rm d}} \ln\left[\frac{g_{\rm eff}(T_{\rm d})^{1/3} T_{\rm d}}{g_{\rm eff}(T_{\rm eq})^{1/3} T_{\rm eq}}\right]. \tag{3.47}$$

Approximating the DM velocity at the time of decoupling as $v/a_{\rm d} = \sqrt{(4/11)^{1/3} T_{\rm d}/m_\chi}$, the cutoff mass scale due to DM free-streaming is given by

$$\begin{aligned} M_{\rm fs} &= \rho_\chi(T_0)\frac{4\pi}{3}\ell_0^3 \\ &= 3\times 10^5 M_\odot \left(\frac{g_{\rm eff}(T_{\rm d})}{3.36}\right)^{-1/2}\left(\frac{m_\chi}{20\ {\rm MeV}}\right)^{-3/2}\left(\frac{T_{\rm d}}{\rm keV}\right)^{-3/2} \\ &\qquad \times\left\{1+\ln\left[\left(\frac{g_{\rm eff}(T_{\rm d})}{3.36}\right)\left(\frac{T_{\rm d}}{\rm keV}\right)\right]/6.0\right\}^3. \end{aligned} \tag{3.48}$$

The smallest mass object formed by DM is the largest of $M_{\rm ao}$ and $M_{\rm fs}$. Comparing Eq. (3.46) and Eq. (3.48), we see that in order to obtain values of $M_{\rm cutoff}$ in the range $10^7 - 10^9 M_\odot$ with $m_{\chi,\phi} \sim$ few $\times$ 10 MeV, $T_{\rm d} \sim$ keV is needed and acoustic oscillations set the cutoff scale. Hence, combining Eq. (3.42) and Eq. (3.46), we have that

$$M_{\rm cutoff} = 4\times 10^7\ M_\odot \left(\frac{g_{\rm eff}(T_{\rm d})}{3.36}\right)^{-7/8}\left(\frac{g}{0.3}\right)^3\left(\frac{m_\chi}{20\ {\rm MeV}}\right)^{-3/4}\left(\frac{\sqrt{m_\phi^2 - m_\chi^2}}{35\ {\rm MeV}}\right)^{-3}. \tag{3.49}$$

The left panel of Figure 3.4 shows the cutoff scale varying $m_\chi$ and $m_\phi$. We take $g = 0.42$ to be as large as allowed by limits on $|U_{\tau 4}|$ from $\tau$ decays and neutrino oscillation experiments with $y_2 = 1$. On the right panel we display the coupling $g$ required to obtain $M_{\rm cutoff} = 10^7$, $10^8$, and $10^9 M_\odot$ as a function of $m_\chi$ for $m_\phi = 20$ and 40 MeV. We set $y_2 = 1$ and show the resulting upper limit on $g = y_2\,|U_{\tau 4}|$ from the limit $|U_{\tau 4}| < 0.42$ as found in Section 3.2.2.

Finally, we note that the effect of DM-photon interactions on the nonlinear structure formation of satellite galaxies in a Milky Way sized galaxy has been simulated in [172]. The effects of DM-photon interactions on structure formation should be very similar to the

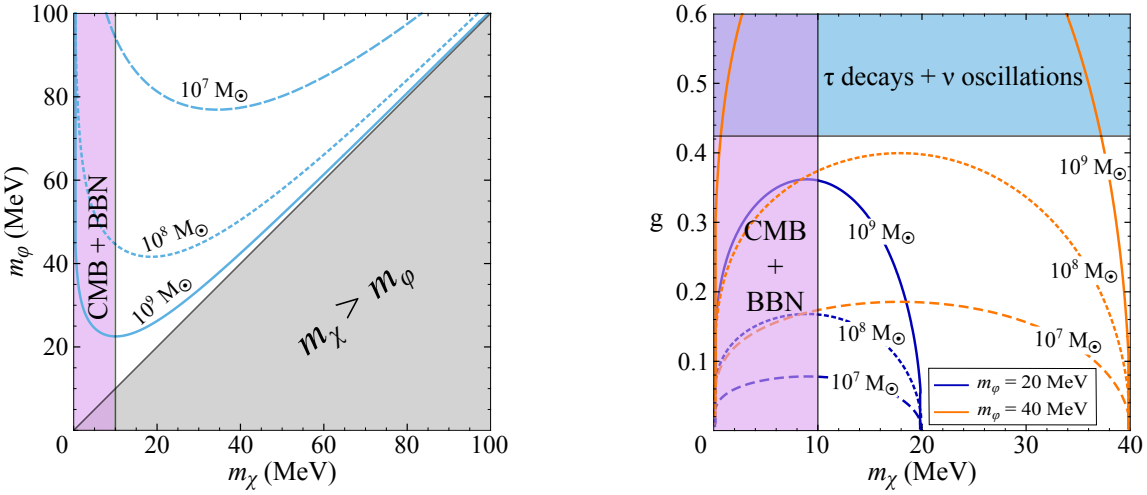


Figure 3.4: Left: Values of $m_\phi$ required for $M_{\text{cutoff}} = 10^7$ (dashed), $10^8$ (dotted), and $10^9 M_\odot$ (solid) as functions of $m_\chi$. To fix $g = y_2 \, |U_{\tau 4}|$, we set $y_2 = 1$ and take the largest value of $|U_{\tau 4}|$ allowed by $\tau$ decays and neutrino oscillation experiments, 0.42, as shown in Figure 3.2. The gray shaded region on the bottom-right corresponds to the unphysical situation where the mediator is lighter than the DM. Right: the coupling $g$ required for $M_{\text{cutoff}} = 10^7$, $10^8$, and $10^9 M_\odot$ varying the DM mass for $m_\phi = 20$ and 40 MeV. The upper limit on $g = y_2 \, |U_{\tau 4}|$ of 0.42 (c.f. Section 3.2.2) assuming $y_2 = 1$ is also shown. In both plots we show the lower limit on the DM mass from observations of the CMB and BBN.

effects of DM-neutrino interactions since they both suppress structure formation on small scale due to acoustic oscillations. They find that for a constant DM-neutrino cross section, $\sigma_{\mathrm{DM}-\gamma} \gtrsim 7 \times 10^{-35}$ cm$^2$ for $m_\chi = 20$ MeV, is ruled out at the 2 sigma level since then DM-photon interactions would wash out too much structure to be consistent with the number of satellite galaxies that we observe in the Milky Way. In our scenario, the DM-neutrino cross section is not a constant, but at the time of kinetic decoupling when the value of the DM-neutrino cross section is most important for affecting small scale structure, we have that for typical parameters, $\sigma \simeq g^4(3T_{\mathrm{d}})^2/(8\pi(m_\phi^2 - m_\chi^2)^2) \simeq 2 \times 10^{-36}$ cm$^2$, which is within the bounds of Ref. [172], but still large enough to significantly decrease structure formation on small scales. Similarly, in simulations of a model in which dark matter interacts with dark radiation [173], small galaxies form later and have lower central densities than in standard CDM.

## *3.4 Implications for supernovae*

Supernovae (SNe), being abundant sources of neutrinos, can offer interesting information about strong DM-neutrino interactions. In this section we examine the effects of such interactions on the properties of SNe neutrinos. We also comment on how the addition of strong DM-neutrino interactions to SNe feedback affects, but does not alleviate, the "core vs. cusp" and "too big to fail" problems.

### *3.4.1 Neutrino emission and cooling*

In the standard picture of core collapse SNe, the three flavors of neutrinos and antineutrinos are produced in the supernova (SN) at temperatures around 30 MeV, mainly via nucleon bremsstrahlung and electron neutrino-antineutrino annihilation. Outside of the first neutronization burst of electron neutrinos, the neutrinos remain trapped in the dense core of the collapsing star for $\sim 0.2$ s at which point they free-stream out of the star over a time period of $\sim 10$ s, carrying away the binding energy of the remaining proto-neutron star $\sim 3 \times 10^{53}$ erg. For recent reviews see e.g., [174, 175].

DM candidates with $m_\chi \lesssim 100$ MeV are light enough to be thermally produced in SNe. If these DM candidates are weakly interacting, then they can be constrained since the

presence of this DM could help cool the proto-neutron star, producing a neutrino signal that is in conflict with the observations from SN 1987A. In our scenario, DM (with a mass $\gtrsim 10$ MeV) will also be produced in the SN. However, due to the strong DM-neutrino interactions, this DM will thermalize with the neutrino gas and maintain a thermal distribution out to large radii until the temperature of the neutrinos falls below the DM mass, suppressing DM production.

Neutrinos begin to free-stream away from the SN when the density of the stellar material drops, which occurs where the matter temperature is $\sim 5$ MeV $< m_\chi$. At this point, DM production is suppressed, but the coupled DM-neutrino gas from the core will still diffuse out of the star, cooling the star on timescales set by the speed of sound in the DM-neutrino fluid. In this sense, strong DM-neutrino interactions are similar to strong neutrino self-interactions in SNe since they both involve the emission of a strongly-coupled gas, and hence strong DM-neutrino interactions do not significantly affect the cooling time for SNe [127, 176]. Thus it is likely that this neutrino-interacting DM will not come into conflict with the observation of neutrino cooling from SN 1987A.

In [177] a similar scenario of relatively strong DM-nucleon and DM-neutrino interactions inside SNe was considered. In this case, the DM thermalized with the stellar material and bound the neutrinos to the star out to larger radii and lower temperatures (a result similar to what would be expected from simply increasing the strength of neutrino interactions with regular matter). This would lead to an overall decrease in the energies of the emitted neutrinos and an increase in the cooling time, resulting in a rough bound of $m_\chi \gtrsim 10$ MeV in order to be consistent with the neutrino observations from SN 1987A. However, for the case of DM that only interacts with neutrinos, it is natural to expect that the constraint on $m_\chi$ will be weakened since the DM does not have strong interactions with the stellar material and is not trapped in the core of the star. A precise study of the emission of neutrinos is beyond the scope of this work and will be explored in a future paper [178].

Finally, Refs. [127, 179] find that the constraints on neutrino-interacting DM from SNe come not from cooling, but from SN neutrinos scattering off the DM and out of the line of sight of our detectors. They place a bound on the DM-neutrino cross section of $\sigma_{\hat{\nu}_i\chi} \lesssim 10^{-25}$ cm$^2$ $(m_\chi/\text{MeV})$ by requiring that the neutrino mean free path be larger than the Earth-

SN distance for a nearby SN. In the next section, we will find that our neutrino-DM cross section abides by this constraint except near resonance, producing a feature in the neutrino spectra which should be observable in the next galactic SN.

### *3.4.2 Observation of a nearby supernova*

An interesting consequence of strong DM-neutrino interactions is the scattering of SN neutrinos off DM on their way to Earth. The parameters implied by the missing satellite problem make this particularly intriguing because the resonant neutrino energy for scattering, $E_{\rm res} = (m_\phi^2 - m_\chi^2)/2m_\chi$, is in the range of energies produced in SNe since both $\chi$ and $\phi$ have masses that are tens of MeV.

We consider a light neutrino mass eigenstate $i$ that was emitted from a SN. As it travels from the SN to Earth, scattering on DM can deflect it, decreasing the flux that is observed,

$$\text{Flux}\,(\hat{\nu}_i)_{\rm Earth} = \text{Flux}\,(\hat{\nu}_i)_{\rm SN}\, e^{-\Gamma_i d}, \tag{3.50}$$

where

$$\Gamma_i = \sigma_{\hat{\nu}_i\chi} \times \frac{1}{d}\int_0^d dx\, n_\chi. \tag{3.51}$$

As defined in (3.9), $\sigma_{\hat{\nu}_i\chi}$ is the cross section for $\hat{\nu}_i$ to scatter on DM at rest, $d$ is the distance between the SN and Earth, and $n_\chi$ is the DM number density along the line of sight. Using (3.9), we can isolate the mass eigenstate dependence,

$$\Gamma_i = \frac{|U_{Ni}|^2}{|U_{e4}|^2 + |U_{\mu 4}|^2 + |U_{\tau 4}|^2}\Gamma, \tag{3.52}$$

with

$$\Gamma = \sigma_{\nu\chi} \times \frac{1}{d}\int_0^d dx\, n_\chi\,(x)\,. \tag{3.53}$$

To get a rough idea of what distance scale this attenuation occurs on, we set $n_\chi(x)$ to a constant value, with a magnitude equal to the local DM density, which is typical on galactic scales. That is, we take $n_\chi(x) = \bar{n}_\chi = (0.3\ \text{GeV}/m_\chi)\ \text{cm}^{-3}$. Then, $1/\Gamma = 1/\sigma_{\nu\chi}\bar{n}_\chi$ defines a length scale over which the scattering of DM is important. This length scale can be

comparable to galaxy sizes for neutrinos with energy close to the resonance energy, $E_{\rm res}$. At this energy the cross section is, for $m_\phi \gg m_\chi$,

$$\sigma_{\nu\chi} \simeq \frac{4\pi}{m_\phi^2} = 3 \times 10^{-24}\ {\rm cm}^2 \left(\frac{40\ {\rm MeV}}{m_\phi}\right)^2, \tag{3.54}$$

where we have also assumed that $m_\phi < m_4$ so that $\Gamma_\phi = g^2 m_\phi/16\pi$. This cross section leads to an attenuation length

$$\frac{1}{\Gamma} \simeq 7\ {\rm kpc} \left(\frac{m_\phi}{40\ {\rm MeV}}\right)^2 \left(\frac{m_\chi}{20\ {\rm MeV}}\right). \tag{3.55}$$

The cross section is this large only in a region of width $\mathcal{O}({\rm MeV})$ around $E_{\rm res}$. Off resonance, the cross section drops quite rapidly below the bound found in [127, 179]. Therefore, the DM-neutrino interactions show up as a feature in the spectrum of neutrinos from a SN at an energy given by $E_{\rm res} = (m_\phi^2 - m_\chi^2)/2m_\chi$.

The mixing matrix $U$ determines the relative attenuation of each eigenstate. For simplicity, in the tribimaximal approximation which is a good rough description of the neutrino mixing pattern, $\sin\theta_{12} = 1/\sqrt{3}$, $\sin\theta_{23} = 1/\sqrt{2}$, and $\theta_{13} = 0$, the attenuation scales for the three light eigenstates are

$$\frac{1}{\Gamma_1} \simeq \frac{6}{\Gamma}, \quad \frac{1}{\Gamma_2} \simeq \frac{3}{\Gamma}, \quad \frac{1}{\Gamma_3} \simeq \frac{2}{\Gamma}. \tag{3.56}$$

Because of this hierarchy, the fraction of $\hat{\nu}_1$ neutrinos is increased due to scattering on DM. As for the flavor composition of the neutrinos, because $\hat{\nu}_1$ has a larger component of $\nu_e$ than $\hat{\nu}_2$ or $\hat{\nu}_3$, the fraction of electron neutrinos detected from a SN is likewise increased. Thus, an increase in the electron neutrino fraction at $E_{\rm res}$ is a telltale sign of strong DM-neutrino interactions.

Beyond affecting the signals from nearby SNe, neutrino-DM interactions can leave an imprint in the diffuse SN background (DSNB). This was studied in detail in [180] in the context of an effective interaction between (scalar) DM and neutrinos. For parameters relevant for our scenario, the spectral distortion at $E_{\rm res}$ could be observable at proposed next generation experiments like Hyper-Kamiokande.[5]

[5]In a similar vein (although unconnected to SNe), neutrinos with energies of $10^2 - 10^3$ TeV have been explored as probes of new neutrino interactions due to scattering [181]. Because of the suppression of the scattering cross section at high energies, $\sigma_{\nu\chi} \propto 1/E_\nu$, and the small DM density relevant for neutrinos traveling cosmological distances, $\rho_\chi \sim 1.5\ {\rm keV/cm}^3$, this is unimportant in our scenario.

### *3.4.3 The "core vs. cusp" and "too big to fail problems"*

SNe can also figure prominently in potential solutions to the "core vs. cusp" problem. This problem arises from the discrepancy in the DM density profile near the centers of galaxies between standard CDM simulations, which predict cusps, and observations, which favor cores. Some simulations [182–186] and analytic models [187, 188] that include feedback from SNe on the DM indicate that such a coupling can modify the shape of DM profiles near the centers of galaxies, hence solving the core vs. cusp problem. The energy transferred from SNe to the interstellar medium modifies the gravitational potential felt by the DM, allowing the DM to move away from the center of the galaxy, creating a more cored profile. In some simulations, taking reasonable values for the SN rate, transferring on the order of $10^{50} - 10^{51}$ ergs per SN to the DM is sufficient to turn a cusped halo into a cored one [182, 186].

Additionally, SN feedback can address the "too big to fail problem," in which simulations predict that the Milky Way satellite galaxies should be more massive than they are observed to be. SN feedback has been shown to reduce the DM density in the center of galaxies, and this helps allieviate the too big to fail problem [189]. In [186], N-body simulations including SN feedback showed that indeed the too big to fail problem could be solved by SN feedback moving DM from the center region of galaxies out to larger radii.

It has also been suggested that SN feedback may not be sufficient to address these small scale structure problems [190, 191]. Maximally, around 1% of the supernova energy can be transferred to DM gravitationally, causing the DM to move away from the center of galaxies, via the method described above. The other 99% of the SN energy is released in the form of neutrinos. In the case of strong DM-neutrino interactions, the neutrinos released by a SN can transfer energy to DM by elastic scattering. This increases the transfer of energy from SNe to DM and potentially makes SN feedback more effective at solving the core vs. cusp and too big to fail problems.

Simple estimates show that the energy transfer from SNe to DM through this mechanism is of the right order of magnitude to solve the core vs. cusp problem. However, since the scattering length of the neutrinos is a kpc or larger, as seen in Section 3.4.2, each neutrino

emitted by a SN in the inner region of a galaxy scatters at most an $\mathcal{O}(1)$ number of times as it leaves the galaxy. In, for example, a bright dwarf galaxy like Fornax, it is estimated that about $10^5$ SNe have occurred [191], each of which emitted about $10^{58}$ neutrinos so that maximally around $10^{63}$ DM particles will gain energy from SNe neutrinos through scattering. This should be compared to the roughly $10^{68}$ DM particles in Fornax, given a galactic mass of $10^9 M_\odot$ and a 20 MeV DM mass. Therefore, the energy from SNe is only distributed to a small fraction of the DM and cannot turn a core into a cusp. Accounting for neutrinos from stars that do not become SNe could have an effect on the core vs. cusp problem and will be studied in future work [178].

### *3.5 Future Tests*

As we have described, to achieve a cutoff on DM structures of $M_{\rm cutoff} \sim 10^8 M_\odot$ requires $|U_{\tau 4}| \gtrsim 0.1$. One promising test of strong DM-neutrino interactions is to improve the searches that are sensitive to $|U_{\tau 4}|$. We discuss prospects for this improvement below.

#### *3.5.1 $\tau$ decays*

For $m_4 > 100$ MeV the strongest constraint on $|U_{\tau 4}|$ comes from $\tau$ decays, in particular our estimate using changes to $\Gamma_{\tau \to \mu \nu \bar{\nu}}$. However, the measurements of the branching ratio for $\tau \to \mu$ were not searches for heavy neutrinos and could be subject to systematic biases in acceptance estimates that assume a vanishing neutrino mass. The best dedicated experimental search for a heavy component to $\nu_\tau$ used LEP data, based on about $10^5$ $\tau^+\tau^-$ pairs, looking at hadronic three- and five-prong decays [140]. We strongly suggest that new experimental searches be undertaken to search for a massive (greater than 10 MeV) neutrino component of $\nu_\tau$. The B-factories have each collected about $10^4$ times more $\tau$ pairs and Belle II will improve on that by an order of magnitude. Therefore the statistical errors in such a search could conceivably improve by $\sim 100$. Using several decay channels is a good strategy since multi-prong hadronic final states are more sensitive to the reduced phase space available but leptonic decays are subject to less theoretical uncertainty. Although the search in Ref. [140] was systematics limited, if the systematic errors for new dedicated searches can be controlled to the level of the statistical ones, an improvement

of the sensitivity to $|U_{\tau 4}|$ by a factor of 10 would be possible, exploring a large amount of parameter space favored by solutions to small scale structure problems. Improving these searches would be a highly desirable test of DM-neutrino interactions.

We also briefly mention here that the value of $|V_{us}|$ extracted using $\tau$ decays to strange mesons is smaller than that obtained by other methods [192]. In particular, the central value obtained using the ratio $\Gamma_{\tau\to K\nu}/\Gamma_{\tau\to\pi\nu}$ is about 1% below the value from $|V_{ud}|$ and CKM unitarity (assuming $U_{\mu 4} = 0$). The value using the inclusive strange rate is even smaller, about 4% smaller than the CKM unitarity value. While not statistically significant, these are intriguing and could be signs of a heavy neutrino component to $\nu_\tau$ since final states involving kaons have less phase space available (which is suggested by the inclusive, multibody final states leading to a smaller $|V_{us}|$). The value of $|U_{\tau 4}|$ required to align the central values of $|V_{us}|$ from $\Gamma_{\tau\to K\nu}/\Gamma_{\tau\to\pi\nu}$ and CKM unitarity is in tension with the estimate of the limit from $\tau \to \mu$ decay derived in Section 3.2.2 but, as mentioned above, there could be an unaccounted for systematic bias in this estimate. If the discrepancy in $|V_{us}|$ measurements becomes significant, it could be another hint of the existence of an $\mathcal{O}(100$ MeV) component to the $\tau$ neutrino.

### *3.5.2 Matter effects on neutrino oscillations*

For $m_4$ below 100 MeV, the strongest limit on $|U_{\tau 4}|$ is due to matter effects in atmospheric neutrino oscillations. The lack of weak interactions of the sterile neutrino leads to a difference in the matter effects between $\nu_\mu$ and the linear combination of $\nu_\tau$ and sterile that makes up the light neutrinos. Limits on $|U_{\tau 4}|$ have been derived from analyzing the zenith angle distribution of muon neutrinos at Super-K [158] and in IceCube and (low energy) DeepCore data in the language of neutrino NSI [159]. The Super-K limit on $|U_{\tau 4}|$ is statistics limited and will be improved with more data. An analysis of the PINGU upgrade of IceCube indicates that it will be able to place a 90% C. L. upper limit on the NSI parameter $\epsilon_{\tau\tau}$ of $1.7 \times 10^{-2}$ [193]. This will improve the reach on $|U_{\tau 4}|$ to about 0.3. Furthermore, a year of full DeepCore data will allow $\epsilon_{\tau\tau}$ to be probed at 90% C. L. to $6 \times 10^{-3}$ [159] which will allow values of $|U_{\tau 4}| > 0.2$ to be tested. This is a very promising test of the model.

### *3.5.3 $U_{e4}$ and $U_{\mu 4}$*

In addition to a nonzero $U_{\tau 4}$ we might expect, at some level, that $U_{e4}$ and $U_{\mu 4}$ are also not vanishing in this model. While it is technically natural for $U_{e4}$ and $U_{\mu 4}$ to be extremely suppressed compared to $U_{\tau 4}$ (radiative contributions to $U_{e4}, U_{\mu 4}$ are necessarily generated but are proportional to the light neutrino masses and are therefore tiny), it is not a requirement that the sterile-active neutrino coupling only violate $L_\tau$. (We use $L_\ell$ to label the global U(1) associated with lepton flavor $\ell$.) In most of this paper, for simplicity and in light of the phenomenological requirement that $U_{\tau 4} \gg U_{e4}, U_{\mu 4}$, we have ignored $U_{e4}$ and $U_{\mu 4}$ but it is possible that they are nonzero. In fact, it is easy to contemplate a model in which the hierarchy $U_{\tau 4} \gg U_{e4}, U_{\mu 4}$ is enforced with $U_{e4}, U_{\mu 4} \neq 0$ by imposing a symmetry that satisfies minimal flavor violation (MFV). In an MFV scenario, we would expect that $\lambda_i$ in Eq. (3.1) are proportional to the lepton Yukawas so that, in addition, $U_{\mu 4} \gg U_{e4}$.

If we take the reasonable view that in this model $U_{e4}$ and $U_{\mu 4}$ are not strictly zero, we could potentially expect to see a signal in the observables that we used to constrain $U_{e4}$ and $U_{\mu 4}$ in Section 3.2.2. Furthermore, we might also expect signals in lepton-flavor–violating (LFV) processes such as $\tau \to \mu\gamma$, $\tau \to e\gamma$, $\mu \to e\gamma$, or $\mu \to e$ conversion. The fact that this model includes a neutrino with a mass above 10 MeV adds additional motivation to search for LFV–a relatively large $m_4$ reduces the GIM-suppression of such processes. The decay $\tau \to \mu\gamma$ could be particularly interesting in an MFV context, while the effort to greatly improve the reach in sensitivity to $\mu \to e\gamma$ and $\mu \to e$ conversion makes these processes interesting as well.

Lastly, a nonzero value of $U_{\mu 4}$ would also open up the possibility of observing this model in $\nu_\mu \to \nu_\tau$ oscillations at the proposed short baseline experiment MINSIS [194]. MINSIS proposes to use the NUMI beamline at Fermilab with a kton-scale emulsion cloud chamber detector, capable of observing $\tau$ neutrinos, situated 1 km away. Early studies indicate that, for $|U_{\tau 4}|^2 = 0.1$, sensitivity to $|U_{\mu 4}|^2$ above roughly $10^{-6}$ is possible [194].

### *3.6 Conclusions*

The paradigm of CDM does an excellent job of describing a wide range of data on the scales of galaxy clusters or larger. However, there appear to be persistent discrepancies between predictions in the CDM paradigm and observations at smaller scales.

We have focused on one of these problems, that of missing satellites. This problem can be solved by introducing strong interactions between neutrinos and DM which keep the DM in thermal equilibrium with the relativistic matter in the early Universe to lower temperatures than typically expected. This washes out structures with masses below a particular scale $M_{\rm cutoff}$. If $M_{\rm cutoff}$ is chosen to be in the range $10^7 - 10^9 M_\odot$, then the expectation for the number of satellite galaxies of a Milky Way sized galaxy can be brought into agreement with observations, solving the missing satellites problem. A cutoff of this size requires a large DM-neutrino scattering cross section. This can be realized in a renormalizable theory if the DM has a mass that is tens of MeV and is coupled to a sterile neutrino that mixes with the active neutrinos. The strength of the mixing that is required combined with both cosmological and particle physics data implies that the sterile neutrino mixes most with $\nu_\tau$ and leads to a heavy neutrino that is mostly sterile but with a sizable $\nu_\tau$ component. There are a number of signatures of this scenario, both for astrophysical and particle physics experiments.

Strong DM-neutrino interactions are particularly interesting for supernovae. The mass scale implied by a solution to the missing satellites problem indicates that a future observation of neutrinos from a nearby supernova could show an imprint of DM-neutrino scattering. This scenario can also be tested at neutrino oscillation experiments, due to the the change of matter effects due to the sterile neutrino. There will be progress on these measurements, probing regions of parameter space that are able to solve small scale structure problems. $\tau$ decays are also a promising area to search for the signs of neutrino-DM interactions. Improvements of the searches for a massive component of $\nu_\tau$ would be a useful way of probing this model. Lastly, lepton-flavor–violating processes are well motivated by this scenario. The reach of searches for these processes will be greatly improved in the near future, opening up the opportunity for discovery.

Chapter 4

# BARYON ASYMMETRY: $CP$ VIOLATION AND BARYOGENESIS IN TWO HIGGS DOUBLET MODELS

We consider a general two-Higgs-doublet model with $CP$ violation. W give a perturbative expansion for the mass eigenstates in terms of the small $CP$ violating phase. These analytical expressions are used to show that $\mathcal{O}(10^{-2})$ $CP$ violation is allowed by the experimental bounds on the electron electric dipole momnent in some regions of the parameter space. These regions also include parameters that are expected to give a strongly first order electroweak phase transition required for electroweak baryogenesis. We also comment on how to incorporate the $CP$ violation into the searches for a strongly first order electroweak phase transition which could explain the matter–antimatter asymmetry in the Universe.

## *4.1 Introduction*

Measurements of the CMB [17] and abundances of light nuclei [23] show that there is more matter than antimatter in the Universe. This asymmetry is often quantified as the net baryon-to-entropy ratio

$$\eta \equiv \frac{n_B - n_{\bar{B}}}{s} \simeq 10^{-10}, \tag{4.1}$$

where $s$ is the entropy density of the Universe.

In order to explain this asymmetry, three conditions must be met [24]: **(1)** Baryon number ($B$) must be violated. **(2)** Charge ($C$) and charge-parity ($CP$) symmetries must be violated. **(3)** $B$-, $C$-, and $CP$-violating processes should happen out of thermal equilibrium. (These are called Sakharov conditions.)

It was first suggested by Kuzmin, Rubakov and Shaposhnikov [29] that baryogenesis could occur during the electroweak (EW) phase transition. This process is then called *electroweak baryogenesis* (EWBG). **(1)** Baryon number in the SM is anomalously violated. **(2)** Quark mixing matrix in the SM has a $CP$-violating phase. **(3)** EW phase transition could

provide out-of-equilibrium conditions if it is a first-order phase transition. In Section 1.2.2 it was described in detail why EWBG does not work in the SM. Here we summarize these problems.

1. While the rate of $B$ violation is exponentially small ($e^{-4\pi/\alpha_w} \sim 0$) at zero temperature (since it happens via a tunneling process between vacua with different baryon numbers), it is very rapid at high temperatures, $T \gg 100$ GeV (happening via sphaleron processes). Hence a baryon number that is produced, for example, at a GUT scale would be washed out. However, there is a conserved quantum number, baryon $-$ lepton number ($B - L$) in the SM that can be the source of a net baryon number production[1].

2. $CP$ violation in the SM comes from the CKM matrix. One can use the Jarlskog invariant [196] to give a parametrization invariant measure of CP violation. The Jarlskog invariant is defined as

$$J = \mathrm{Im}(V_{ij}V_{kl}V_{kj}^{*}V_{il}^{*}) \tag{4.2}$$

$$= c_{12}c_{23}c_{13}^{2}s_{12}s_{23}s_{13}\sin\delta \qquad \text{(in Kobayashi - Maskawa parametrization)} \tag{4.3}$$

   where $c_{ij} \equiv \cos\theta_{ij}$ is the mixing angle between $i$ and $j$ quark, and $\delta$ is the phase in the CKM matrix. Notice that even if the $CP$ violating phase is large, it gets multiplied by small mixing angles, making $J$ ($\sim 10^{-5}$) small. Furthermore, since $CP$ violating processes involve all three generations of quarks, they are suppressed by small Yukawa couplings. It has been shown that the $CP$ violation in the SM results in a $B$ asymmetry of $10^{-20}$ [26, 27]. Hence, we need to extend the SM to allow more $CP$ violation.

3. If the EW phase transition is first order, the transition causes bubble nucleation. A first-order phase transition needs the order parameter, in this case the expectation value of the Higgs filed, $v(T)$, to change abruptly at the critical temperature ($T_c \sim 100$

[1]This works even if neutrinos are Majorana particles (and hence $L$ is not conserved). In the case of Majorana neutrinos, the baryogenesis scale puts an upper bound on the neutrino masses [195].

GeV). Inside the bubbles is the broken phase, with a non-zero $v$ of the Higgs field. The rate of $B$ violation inside the bubble is proportional to $e^{-4\pi v(T)/g_2 T}$, where $g_2$ is the $SU(2)$ coupling constant and $T$ is the temperature immediately after the phase transition [29]. This phase transition can only produce the required non-equilibrium conditions if the rate of $B$ violation is slower than the expansion rate of the universe. This puts an upper limit on the Higgs expectation value ($v(T)/T \gtrsim 1$) and consequently on the Higgs mass. A strongly first order EW phase transition requires a Higgs of mass less than 60 GeV in the SM. Alternately, with a Higgs mass of 125 GeV, the transition is a crossover. Rapid $B$ violation would then let the baryon number equilibrate to zero if $B - L$ is zero. One solution to this problem is to extend the scalar sector of the SM to have two Higgs doublets.

It was shown that in a two-Higgs-doublet model (2HDM), EW phase transition can be first order [197, 198]. In addition, there can be $CP$ violation in this extended Higgs sector to generate enough $CP$ violation for baryogenesis. A numerical analysis of the 2HDM phase space was done in Ref [198] and was shown that $CP$ conserving 2HDMs with a Higgs boson of mass 125 GeV can indeed accommodate a strongly first-order phase transition.

The literature for 2HDMs is mostly based on $CP$ conserving models because the analysis is simpler. This is because in the case of $CP$ violation, $CP$-even and $CP$-odd fields mix, making the definition of mass eigenstates more complicated. This complexity limited the studies of 2HDMs to either $CP$ conserving models or to small portions of the parameter space of $CP$ violating models, such as those with large mass splittings between the Higgs bosons or specific ordering of the masses (*e.g.* [199]). A more general study of $CP$-violating 2HDMs is required especially for baryogenesis purposes. In [32], I use the fact that we expect the new $CP$ violating phase to be of $\mathcal{O}(0.1)$ or less, and give a perturbative expansion of the Higgs states in terms of a small $CP$ violating phase. I focus on the portion of the parameter space that gives a first-order phase transition (e.g. $\tan\beta < 4, \mu_3 > 100$ GeV, $m_{\tilde{A}} > 300$ GeV), and I find the allowed $CP$ violation that is consistent with experimental limits on electron electric dipole moment (EDM). I also comment on how to include $CP$ violation in searches for a first-order phase transition in an easy way.

This Chapter is organized as follows. In Section 4.2 I give the general form of the 2HDM potential and calculate the approximate mass eigenstates for the $CP$ violating case. In Section 4.3 I discuss how to include $CP$ violation in phase transition analyses of the EWBG. In Section 4.4 I use the recent electron EDM to constrain the $CP$-violating phase in 2HDMs. In Section 4.6 I give my concluding remarks.

## *4.2 The Two Higgs Doublet Model*

In this section I briefly introduce the 2HDM, an extension of the SM. 2HDMs are motivated to accommodate EWBG[2]. The model has two complex scalar $SU(2)$ doublets, $\Phi_1$ and $\Phi_2$. Together, they have eight degrees of freedom, three of which are fictitious Nambu-Goldstone bosons that are *eaten* by the gauge bosons $W^{\pm}$ and $Z$. Hence there are five physical Higgs bosons left: two charged, and three neutral. If there is no $CP$ violation, two of the three neutral Higgs bosons are $CP$-even, and the third one is $CP$-odd. In the case of $CP$ violation, the mass eigenstates are not the $CP$ eigenstates, as we will discuss shortly.

One usually imposes a $Z_2$ symmetry on the Higgs potential, with $\Phi_1 \to \Phi_1$ and $\Phi_2 \to -\Phi_2$, so that there are no flavor changing neutral currents (FCNCs) at tree level[3]. By convention, $\Phi_2$ always couples to up-type quarks. The rest of the Higgs–fermion couplings are such that $\Phi_1$ and $\Phi_2$ do not couple to fermions of a given charge at the same time. Hence, there are four types of 2HDMs that do not induce FCNCs[4]. (See Table 4.1.) This $Z_2$ symmetry can be softly broken and be the source of $CP$ violation in the scalar sector. For a more complete treatment of 2HDMs, see the review in [201].

---

[2]Of course, apart from baryogenesis reasons, two Higgs doublets are a necessary feature of supersymmetry. In MSSM there is a fermionic superpartner for every scalar –Higgsino is the superpartner to Higgs. In order to cancel the gauge anomaly that the Higgsino would bring, one needs to introduce a second Higgs doublet, hence a second Higgsino.

[3]There are other ways to suppress FCNC in the two Higgs doublet model, see for example [200].

[4]Top-quark Yukawa coupling is by far the most important ingredient for EWBG. Therefore, phase transition analysis can be done without specifying a particular 2HDM.

| Fermion / Model | $u$ | $d$ | $e$ |
|---|---|---|---|
| Type I | $\Phi_2$ | $\Phi_2$ | $\Phi_2$ |
| Type II | $\Phi_2$ | $\Phi_1$ | $\Phi_1$ |
| Lepton-specific | $\Phi_2$ | $\Phi_2$ | $\Phi_1$ |
| Flipped | $\Phi_2$ | $\Phi_1$ | $\Phi_2$ |

Table 4.1: Two-Higgs-Doublet models categorized with respect to their couplings to the SM fermions. First generation notation is employed.

The most general potential that has a softly broken $Z_2$ symmetry is [202]

$$\begin{aligned} V = {} & \lambda_1 \left(\Phi_1^\dagger \Phi_1 - \frac{v_1^2}{2}\right)^2 + \lambda_2 \left(\Phi_2^\dagger \Phi_2 - \frac{v_2^2}{2}\right)^2 + \lambda_3 \left[\left(\Phi_1^\dagger \Phi_1 - \frac{v_1^2}{2}\right) + \left(\Phi_2^\dagger \Phi_2 - \frac{v_2^2}{2}\right)\right]^2 \\ & + \lambda_4 \left[(\Phi_1^\dagger \Phi_1)(\Phi_2^\dagger \Phi_2) - (\Phi_1^\dagger \Phi_2)(\Phi_2^\dagger \Phi_1)\right] \\ & + \lambda_5 \left(\mathrm{Re}(\Phi_1^\dagger \Phi_2) - \frac{v_1 v_2}{2}\cos\xi\right)^2 + \lambda_6 \left(\mathrm{Im}(\Phi_1^\dagger \Phi_2) - \frac{v_1 v_2}{2}\sin\xi\right)^2 , \end{aligned} \tag{4.4}$$

where $\lambda_i$ are real. The minimum of this potential is at

$$\langle \Phi_1 \rangle = \frac{1}{\sqrt{2}} \begin{pmatrix} 0 \\ v_1 \end{pmatrix}, \quad \langle \Phi_2 \rangle = \frac{1}{\sqrt{2}} \begin{pmatrix} 0 \\ v_2\, e^{i\xi} \end{pmatrix} . \tag{4.5}$$

The angle $\xi$ is the $CP$ violating phase. If $\lambda_5 = \lambda_6$, the last two terms in Eq. 4.4 can be combined into $\lambda_5 |\Phi_1^\dagger \Phi_2|^2$ and the 2HDM potential does not depend on $\xi$.

### *4.2.1 CP-Conserving 2HDM*

Before investigating the $CP$ violation, let us start with the less complicated case of $CP$-conserving 2HDM ($\xi = 0$) to get an idea of the new Higgs sector. Two Higgs fields are

$$\Phi_1 = \frac{1}{\sqrt{2}} \begin{pmatrix} \phi_1^+ \\ v_1 + \rho_1 + i\eta_1 \end{pmatrix}, \quad \Phi_2 = \frac{1}{\sqrt{2}} \begin{pmatrix} \phi_2^+ \\ v_2 + \rho_2 + i\eta_2 \end{pmatrix} . \tag{4.6}$$

The mass eigenstates are found by inserting $\Phi_1$ and $\Phi_2$ into Eq.4.4. There are two charged Higgs bosons

$$H^{\pm} = \frac{1}{\sqrt{2}}(-\sin\beta\,\phi_1^{\pm} + \cos\beta\,\phi_2^{\pm}) \ , \tag{4.7}$$

with mass $m_{H^{\pm}}^2 = \frac{\lambda_4}{2}\,v^2$, where $\tan\beta = \frac{v_2}{v_1}$ and $v^2 = v_1^2 + v_2^2$. Here $v = 246$ GeV is set by the $W^{\pm}/Z$ mass. The two fields that are orthogonal to $H^{\pm}$ are the the two fictitious Nambu-Goldstone bosons,

$$G^{\pm} = \frac{1}{\sqrt{2}}(\cos\beta\,\phi_1^{\pm} + \sin\beta\,\phi_2^{\pm}) \ . \tag{4.8}$$

There is a $CP$-odd Higgs boson

$$A = -\sin\beta\,\eta_1 + \cos\beta\,\eta_2 \ , \tag{4.9}$$

with mass $m_A^2 = \frac{\lambda_6}{2}\,v^2$. The field that is orthogonal to $A$ is the third fictitious Nambu-Goldstone boson,

$$G^0 = \cos\beta\,\eta_1 + \sin\beta\,\eta_2 \ . \tag{4.10}$$

The two $CP$-even states are the eigenstates of the mass matrix (written in $(\rho_1,\ \rho_2)^{\mathrm{T}}$ basis)

$$M^2 = \frac{v^2}{2}\begin{pmatrix} 4(\lambda_1+\lambda_3)\,c_\beta^2 + \lambda_5\,s_\beta^2 & \frac{1}{2}\,(4\lambda_3+\lambda_5)\ s_{2\beta} \\ \frac{1}{2}\,(4\lambda_3+\lambda_5)\ s_{2\beta} & 4(\lambda_2+\lambda_3)\,s_\beta^2 + \lambda_5\,c_\beta^2 \end{pmatrix} \ . \tag{4.11}$$

Eigenvectors of this matrix are the two $CP$-even Higgs bosons

$$H = \cos\alpha\,\rho_1 + \sin\alpha\,\rho_2 \ , \tag{4.12}$$

$$h = -\sin\alpha\,\rho_1 + \cos\alpha\,\rho_2 \ , \tag{4.13}$$

with eigenvalues

$$m_H^2 = \frac{v^2}{4}\left(4\lambda_3 + \lambda_5 + 4(\lambda_2\,s_\beta^2 + \lambda_1\,c_\beta^2) + \Delta\right) \ , \tag{4.14a}$$

$$m_h^2 = \frac{v^2}{4}\left(4\lambda_3 + \lambda_5 + 4(\lambda_2\,s_\beta^2 + \lambda_1\,c_\beta^2) - \Delta\right) \ , \tag{4.14b}$$

where $s_\beta \equiv \sin\beta$ and

$$\Delta = \sqrt{(4\lambda_3+\lambda_5)s_{2\beta}^2 + [(-4\lambda_3+\lambda_5)c_{2\beta} + 4(\lambda_2\, s_\beta^2 - \lambda_1\, c_\beta^2)]^2}\ ,$$
$$\tan 2\alpha = \frac{(4\lambda_3+\lambda_5)s_{2\beta}}{4(\lambda_1+\lambda_3)c_\beta^2 - 4(\lambda_2+\lambda_3)s_\beta^2 - \lambda_5 c_{2\beta}}\ .$$

Note that $h$ is the lighter Higgs. We take $h$ to be the observed Higgs with $m_h = 125$ GeV. The case where $H$ is lighter, although interesting, will not be discussed here.

Higgs–fermion and Higgs–vector boson couplings in the 2HDM are modified from their SM values. Furthermore, with the addition of four new Higgs bosons, there are a lot more new interactions[5]. For brevity, only the new neutral Higgs couplings in Type II 2HDM is presented below[6].

$$\begin{aligned} -\mathcal{L}_{\text{Type II}} &\supset y_u\, \bar{Q}U(i\sigma_2)\Phi_2^* + y_d\, \bar{Q}D\Phi_1 + y_\ell\, \bar{L}E\Phi_1 + |D_\mu\Phi_1|^2 + |D_\mu\Phi_2|^2 + \text{h.c.}, \qquad (4.15)\\ &\supset \sum_{h_i=h,H,A}\left[\frac{m_f}{v}\, h_i\left(c_{h_i}^f\, \bar{f}f - \tilde{c}_{h_i}^f\, \bar{f}i\gamma_5 f\right) + a_{h_i}\, h_i\left(\frac{2M_W^2}{v}W^+W^- + \frac{M_Z^2}{v}ZZ\right)\right]. \end{aligned}$$

The coefficients $c, \tilde{c}$ and $a$ are given in Table 4.2. Even though the fermion couplings are given only for Type II, gauge boson couplings are the same in all of the models. If $CP$ is conserved, the pseudoscalar $A$ does not couple to the gauge bosons and has only pseudoscalar couplings with the fermions. We will see in the next section how this changes in $CP$-violating 2HDMs. The SM Higgs ($h$) couplings to gauge bosons are modified by $\sin(\beta-\alpha)$. Note that if $\beta-\alpha = \frac{\pi}{2}$, $h$ couplings are exactly the same as the SM Higgs couplings. This limit ($\beta-\alpha \to \frac{\pi}{2}$) is called the *alignment limit*. LHC measurements of the 125 GeV-Higgs couplings shows that if we have a Type II 2HDM, we should be close to the alignment limit [203]. In this limit, $H$ couplings to up-type quarks are suppressed by $\tan\beta$ while couplings to down-type quarks and leptons are proportional to $\tan\beta$.

---

[5]The reader is encouraged to go through the calculations of these new interactions.

[6]Type II 2HDM is by far the most studied model since MSSM Higgs sector is Type II.

| | $h$ | $H$ | $A$ |
|---|---|---|---|
| $c_u$ | $\frac{\cos\alpha}{\sin\beta}$ | $\frac{\sin\alpha}{\sin\beta}$ | $-$ |
| $\tilde{c}_u$ | $-$ | $-$ | $\cot\beta$ |
| $c_{d,\ell}$ | $-\frac{\sin\alpha}{\cos\beta}$ | $\frac{\cos\alpha}{\cos\beta}$ | $-$ |
| $\tilde{c}_{d,\ell}$ | $-$ | $-$ | $\tan\beta$ |
| $a$ | $\sin(\beta-\alpha)$ | $\cos(\beta-\alpha)$ | $-$ |

Table 4.2: Neutral Higgs couplings to fermions and gauge bosons in Type II 2HDM (in units of the SM Higgs couplings). See Eq. 4.15 and the following paragraph for details.

### *4.2.2 CP-Violating 2HDM*

If $\lambda_5 \neq \lambda_6$ in Eq. 4.4 and the phase $\xi$ does not vanish, there is $CP$ violation in the Higgs sector. As before one inserts the two Higgs fields

$$\Phi_1 = \frac{1}{\sqrt{2}} \begin{pmatrix} \phi_1^+ \\ v_1 + \rho_1 + i\eta_1 \end{pmatrix}, \quad \Phi_2 = \frac{1}{\sqrt{2}} \begin{pmatrix} \phi_2^+ \\ v_2\, e^{i\xi} + \rho_2 + i\eta_2 \end{pmatrix} . \tag{4.16}$$

into Eq. 4.4 to find the mass eigenstates. The two charged Higgs bosons are the same as before,

$$H^\pm = \frac{1}{\sqrt{2}}(-\sin\beta\,\phi_1^\pm + \cos\beta\,(e^{-i\xi}\phi_2)^\pm), \tag{4.17}$$

with mass $m^2_{H^\pm} = \frac{\lambda_4}{2}\,v^2$.

The neutral mass eigenstates are more complicated. Since now the Higgs potential violates $CP$ explicitly, there is no mass eigenstates with definite $CP$ assignment. The $CP$-odd ($\eta$) and $CP$-even ($\rho$) components of the two Higgs fields mix. The mass matrix for the neutral Higgs bosons, in the $(\rho_1,\ \rho_2,\ A)^{\mathrm{T}}$ basis, is

$$M^2 = \frac{v^2}{2} \begin{pmatrix} 4(\lambda_1+\lambda_3)c_\beta^2 + (\lambda_5 c_\xi^2 + \lambda_6 s_\xi^2)s_\beta^2 & \left[4\lambda_3 + (\lambda_5 c_\xi^2 + \lambda_6 s_\xi^2)\right] s_\beta\, c_\beta & (\lambda_6-\lambda_5)s_\beta\, c_\xi\, s_\xi \\ \left[4\lambda_3 + (\lambda_5 c_\xi^2 + \lambda_6 s_\xi^2)\right] s_\beta\, c_\beta & 4(\lambda_2+\lambda_3)s_\beta^2 + (\lambda_5 c_\xi^2 + \lambda_6 s_\xi^2)c_\beta^2 & (\lambda_6-\lambda_5)c_\beta\, c_\xi\, s_\xi \\ (\lambda_6-\lambda_5)s_\beta\, c_\xi\, s_\xi & (\lambda_6-\lambda_5)c_\beta\, c_\xi\, s_\xi & \frac{1}{2}(\lambda_5+\lambda_6+(\lambda_6-\lambda_5)c_{2\xi}) \end{pmatrix}. \tag{4.18}$$

It is clear that this matrix mixes the $CP$-even fields, $\rho_{1,2}$ and the $CP$-odd state, $A$. (The combination of $\eta_{1,2}$ that is orthogonal to $A$ is the fictitious Nambu-Goldstone boson $G^0$ as

in the previous section.) Eigenvectors of $M$ are the neutral Higgs bosons. In order to find the eigensystem of $M$, we will use non-degenerate perturbation theory, expanding the mass matrix in $\xi$ for $(\lambda_6 - \lambda_5)\xi \ll 1$. As we will see later, $\xi$ should be $O(10^{-2})$ so as not to produce a large electron EDM. $\lambda_{5,6}$ are dimensionless coefficients in the Higgs potential and they are expected to be $O(1)$ (or at least smaller than $4\pi$ if one wishes to treat the system perturbatively). Hence, the condition $(\lambda_6 - \lambda_5)\xi \ll 1$ is justified. A stronger constraint on the parameter space where the expansion is valid will come from the non-degeneracy condition, as will become clear shortly.

Expanding $M^2$ in Eq. 4.18 up to $O(\xi^2)$ gives

$$M^2 \simeq \frac{v^2}{2}\begin{pmatrix} 4(\lambda_1+\lambda_3)\,c_\beta^2 + \lambda_5\, s_\beta^2 & \frac{1}{2}(4\lambda_3+\lambda_5)\,s_{2\beta} & 0 \\ \frac{1}{2}(4\lambda_3+\lambda_5)\,s_{2\beta} & 4(\lambda_2+\lambda_3)\,c_\beta^2 + \lambda_5\, s_\beta^2 & 0 \\ 0 & 0 & \lambda_6 \end{pmatrix} + \frac{v^2}{2}\Lambda\, M_\xi^2 \ , \tag{4.19}$$

where $\Lambda = \frac{\lambda_6 - \lambda_5}{2}$ and

$$M_\xi^2 = \begin{pmatrix} 2\,\xi^2 s_\beta^2 & \xi^2 s_{2\beta} & 2\,\xi s_\beta \\ \xi^2 s_{2\beta} & 2\,\xi^2 c_\beta^2 & 2\,\xi c_\beta \\ 2\,\xi s_\beta & 2\,\xi c_\beta & -2\,\xi^2 \end{pmatrix} \ . \tag{4.20}$$

Note that the $\xi$-independent part of $M^2$ in Eq. 4.19 is exactly the same as the $CP$-conserving 2HDM mass matrix (together with the pseudoscalar $A$ state) in Eq. 4.11. The mass matrix can be *approximately* diagonalized using the rotation matrix

$$\begin{aligned} R &= \begin{pmatrix} -\cos\alpha_b \sin\alpha & \cos\alpha\cos\alpha_b & -\sin\alpha_b \\ \cos\alpha\cos\alpha_c + \sin\alpha\sin\alpha_b\sin\alpha_c & \cos\alpha_c\sin\alpha - \cos\alpha\sin\alpha_b\sin\alpha_c & -\cos\alpha_b\sin\alpha_c \\ \cos\alpha\sin\alpha_c - \cos\alpha_c\sin\alpha\sin\alpha_b & \cos\alpha\cos\alpha_c\sin\alpha_b + \sin\alpha\sin\alpha_c & \cos\alpha_b\cos\alpha_c \end{pmatrix} \\ &\simeq \begin{pmatrix} -\sin\alpha - \frac{\Lambda v^2(1-a)}{2(m_H^2-m_h^2)}\xi^2 \sin 2\gamma\cos\alpha & \cos\alpha - \frac{\Lambda v^2(1-a)}{2(m_H^2-m_h^2)}\xi^2\sin 2\gamma\sin\alpha & -a\,\xi\cos\gamma \\ \cos\alpha - \frac{\Lambda v^2(1-b)}{2(m_H^2-m_h^2)}\xi^2\sin 2\gamma\sin\alpha & \sin\alpha + \frac{\Lambda v^2(1-b)}{2(m_H^2-m_h^2)}\xi^2\sin 2\gamma\cos\alpha & -b\,\xi\sin\gamma \\ b\,\xi\sin\gamma\cos\alpha - a\,\xi\cos\gamma\sin\alpha & a\,\xi\cos\gamma\cos\alpha + b\,\xi\sin\gamma\sin\alpha & 1 \end{pmatrix} + O(\xi^3), \end{aligned} \tag{4.21}$$

where $a = \frac{\Lambda v^2}{m_A^2 - m_h^2}$, $b = \frac{\Lambda v^2}{m_A^2 - m_H^2}$, $\gamma = \alpha + \beta$ and the angles

$$\sin\alpha_b \simeq a\,\xi\cos\gamma, \ \ \sin\alpha_c \simeq b\,\xi\sin\gamma \tag{4.22}$$

mixes $\rho_1$ and $A$, and $\rho_2$ and $A$ respectively. $\sin\alpha$ is defined in Eq. 4.14.

With this rotation, mass eigenstates (and their masses) in $CP$-violating 2HDMs can be written in terms of the $CP$-conserving states as

$$\tilde{h} \simeq h - \sin\alpha_b A, \qquad m^2_{\tilde{h}} \simeq m^2_h + \xi^2\Lambda v^2(1-a)\cos^2\gamma, \tag{4.23a}$$

$$\tilde{H} \simeq H - \sin\alpha_c A, \qquad m^2_{\tilde{H}} \simeq m^2_H + \xi^2\Lambda v^2(1-b)\sin^2\gamma, \tag{4.23b}$$

$$\tilde{A} \simeq A + \sin\alpha_b h + \sin\alpha_c H, \quad m^2_{\tilde{A}} \simeq m^2_A + \xi^2\Lambda v^2(-1 + a\cos^2\gamma + b\sin^2\gamma). \tag{4.23c}$$

Importance of non-degeneracy can be seen here: The small parameter $\xi$ is multiplied with the inverse of the mass differences (of the neutral Higgs bosons) in the expansion. For $\Lambda \sim O(1)$ and $\xi \sim O(10^{-2})$, one needs $m^2_A - m^2_{h,H} \gtrsim (25\text{ GeV})^2$ for this expansion to be valid.

Higgs couplings in a $CP$-violating 2HDM are different than of a $CP$-conserving 2HDM. The new couplings can be seen in Table 4.3 (compare these couplings to the ones in Table 4.2). Due to the mixing between the $CP$-even and $CP$-odd states, all of the neutral Higgs bosons have $CP$-even and $CP$-odd couplings to fermions. For example, in a $CP$-violating 2HDM, the observed Higgs boson with mass 125 GeV is expected to have $CP$-odd couplings to fermions. Furthermore, the Higgs boson that is mostly $CP$-odd, $A$, now couples to the weak bosons $W/Z$.

| | $\tilde{h}$ | $\tilde{H}$ | $\tilde{A}$ |
|---|---|---|---|
| $c_u$ | $\frac{\cos\alpha}{\sin\beta}$ | $\frac{\sin\alpha}{\sin\beta}$ | $\sin\alpha_b\cos\alpha + \sin\alpha_c\sin\alpha$ |
| $\tilde{c}_u$ | $-\sin\alpha_b\cot\beta$ | $-\sin\alpha_c\cot\beta$ | $\cot\beta$ |
| $c_{d,\ell}$ | $-\frac{\sin\alpha}{\cos\beta}$ | $\frac{\cos\alpha}{\cos\beta}$ | $-\sin\alpha_b\sin\alpha + \sin\alpha_c\cos\alpha$ |
| $\tilde{c}_{d,\ell}$ | $-\sin\alpha_b\tan\beta$ | $-\sin\alpha_c\tan\beta$ | $\tan\beta$ |
| $a$ | $\sin(\beta-\alpha)$ | $\cos(\beta-\alpha)$ | $\sin(\beta-\alpha)\sin\alpha_b + \cos(\beta-\alpha)\sin\alpha_c$ |

Table 4.3: Neutral Higgs boson couplings to fermions and gauge bosons in a $CP$-violating Type II 2HDM (in units of the SM Higgs couplings). See Eq. 4.15 for the definitions.

### *4.3 CP Violation and The Finite Temperature Potential*

As mentioned in the Introduction, one motivation to study 2HDMs is to get a successful EWBG. In order to produce the observed matter–antimatter asymmetry, 2HDMs should both have a first-order EW phase transition and also extra $CP$ violation. It has been shown that $CP$-conserving 2HDMs can accommodate a first-order phase transition with a 125 GeV Higgs boson [198]. I will not go into the details of how to study the phase transition here, but I will comment on how to incorporate a small $CP$ violation in the finite-temperature Higgs potential.

The zero-temperature 2HDM potential that is used in phase-transition studies differs (in parametrization) from the one in Eq. 4.4,

$$\begin{aligned} V_0 = &-\mu_1^2\Phi_1^\dagger\Phi_1 - \mu_2^2\Phi_2^\dagger\Phi_2 - \mu^2\Phi_1^\dagger\Phi_2 - \mu^{2*}\Phi_2^\dagger\Phi_1 + h_1(\Phi_1^\dagger\Phi_1)^2 + h_2(\Phi_2^\dagger\Phi_2)^2 \\ &+ h_3(\Phi_1^\dagger\Phi_1)(\Phi_2^\dagger\Phi_2) + h_4|\Phi_1^\dagger\Phi_2|^2 + \frac{h_5}{2}\left[(\Phi_1^\dagger\Phi_2)^2 + (\Phi_2^\dagger\Phi_1)^2\right]. \end{aligned} \tag{4.24}$$

Note that $\mu^2$ term softly breaks the aforementioned $Z_2$ symmetry. If $\mu^2$ is either real or purely imaginary, then there is no $CP$ violation. The self-coupling constants $h_i$ $(i = 1, \ldots, 5)$ are real and satisfy

$$h_1 > 0, \quad h_2 > 0, \quad 2\sqrt{h_1\, h_2} + h_3 > 0, \quad 2\sqrt{h_1\, h_2} + h_3 + h_4 \pm h_5 > 0, \tag{4.25}$$

so that the potential is bounded from below. These are the renormalized couplings at the EW scale. The renormalization group flow would drive these couplings to different values at different scales, and one should impose that the potential is at least metastable at the EW scale. This puts constraints on the coupling constants at the weak scale, and consequently bounds on the Higgs masses. Furthermore, the vacuum of 2HDMs is richer than the SM vacuum. For example one can have charge-breaking or $CP$-violating vacua. The stability of these minima are studied in Ref.[201] and references therein. We also get two constraint equations by minimizing the potential,

$$-\mu_1^2\, v_1 - \mathrm{Re}(e^{i\xi}\mu^2)\, v_2 + h_1\, v_1^3 + \frac{h_3 + h_4 + h_5\cos(2\xi)}{2}\, v_2^2\, v_1 = 0, \tag{4.26}$$

$$-\mu_2^2\, v_2 - \mathrm{Re}(e^{i\xi}\mu^2)\, v_1 + h_2\, v_2^3 + \frac{h_3 + h_4 + h_5\cos(2\xi)}{2}\, v_1^2\, v_2 = 0. \tag{4.27}$$

The parameters in Eq.4.24 are related to the parameters in Eq. 4.4, and to the Higgs boson masses as

$$\mu_1^2 = \lambda_1\, v_1^2 + \lambda_3\, v^2 = \frac{1}{2}\left[m_h^2\, s_\alpha^2 + m_H^2\, c_\alpha^2 - \left(\bar{\mu}^2 s_{2\beta} - \frac{m_H^2 - m_h^2}{2}\, s_{2\alpha}\right)\tan\beta\right], \quad (4.28a)$$

$$\mu_2^2 = \lambda_2\, v_2^2 + \lambda_3\, v^2 = \frac{1}{2}\left[m_h^2\, c_\alpha^2 + m_H^2\, s_\alpha^2 - \left(\bar{\mu}^2 s_{2\beta} - \frac{m_H^2 - m_h^2}{2}\, s_{2\alpha}\right)\cot\beta\right], \quad (4.28b)$$

$$\mathrm{Re}(\mu^2) = \frac{v^2}{4}\lambda_5\, s_{2\beta}\cos\xi, \quad \mathrm{Im}(\mu^2) = -\frac{v^2}{4}\lambda_6\, s_{2\beta}\sin\xi, \quad (4.28c)$$

$$h_1 = \lambda_1 + \lambda_3 = \frac{1}{4\, v^2\, c_\beta^2}\left[2m_h^2\, s_\alpha^2 + 2m_H^2\, c_\alpha^2 - \bar{\mu}^2 s_{2\beta}\tan\beta\right], \quad (4.28d)$$

$$h_2 = \lambda_2 + \lambda_3 = \frac{1}{4\, v^2\, s_\beta^2}\left[2m_h^2\, c_\alpha^2 + 2m_H^2\, s_\alpha^2 - \bar{\mu}^2 s_{2\beta}\cot\beta\right], \quad (4.28e)$$

$$h_3 = 2\lambda_3 + \lambda_4 = \frac{1}{v^2}\left[2m_{H^\pm}^2 + (m_H^2 - m_h^2)\frac{s_{2\alpha}}{s_{2\beta}} - \bar{\mu}^2\right], \quad (4.28f)$$

$$h_4 = -\lambda_4 + \frac{\lambda_5 + \lambda_6}{2} = \frac{1}{v^2}\left[\bar{\mu}^2 - 2m_{H^\pm}^2 + m_A^2\right], \quad (4.28g)$$

$$h_5 = \frac{\lambda_5 - \lambda_6}{2} = \frac{1}{v^2}\left[\bar{\mu}^2 - m_A^2\right], \quad (4.28h)$$

where $\bar{\mu}^2 \equiv \frac{2\mathrm{Re}(\mu^2)}{\sin 2\beta} \simeq \frac{2\mu^2}{\sin 2\beta}$.

In the case of small $CP$ violation, one can use Eq. 4.23 to replace $m_{h,H}$ in Eq. 4.28 with the masses of the mostly $CP$-even states, $m_{\tilde{h},\tilde{H}}$

$$m_h^2 \simeq m_{\tilde{h}}^2 + \xi^2 \frac{(m_{\tilde{h}}^2 - \bar{\mu}^2)(m_A^2 - \bar{\mu}^2)}{m_A^2 - m_{\tilde{h}}^2}\cos^2\gamma, \quad (4.29)$$

$$m_H^2 \simeq m_{\tilde{H}}^2 + \xi^2 \frac{(m_{\tilde{H}}^2 - \bar{\mu}^2)(m_A^2 - \bar{\mu}^2)}{m_A^2 - m_{\tilde{H}}^2}\sin^2\gamma, \quad (4.30)$$

and the mass of the mostly $CP$-odd Higgs boson is calculated from

$$m_{\tilde{A}}^2 \simeq m_A^2 + \xi^2(m_A^2 - \bar{\mu}^2)\left(-1 + \frac{m_A^2 - \bar{\mu}^2}{m_A^2 - m_h^2}\cos^2\gamma + \frac{m_A^2 - \bar{\mu}^2}{m_A^2 - m_H^2}\sin^2\gamma\right). \quad (4.31)$$

Hence, the parameters used are $m_{\tilde{H}}, m_{\tilde{h}}, m_{H^\pm}, m_A, \beta, \alpha, \xi$, and $\mu^2$. In the next section, we will constrain the angle $\xi$ by using the bounds on the electron EDM and show that $\xi \sim O(10^{-2})$. This small $CP$ violation is not expected to change the strength of the phase transition; however, it would affect the baryon asymmetry in the Universe.

The finite-temperature potential is

$$V(\phi_1,\phi_2,T) = V_0 + \frac{T^2}{24}\left(\sum_{\text{bosons}} g_i m_i^2(\phi_1,\phi_2) + \frac{1}{2}\sum_{\text{fermions}} g_i m_i^2(\phi_1,\phi_2)\right) - \frac{T}{12\pi}\sum_{\text{bosons}} g_i m_i^3(\phi_1,\phi_2) + O\left(m\log\left(\frac{m}{T}\right)\right), \tag{4.32}$$

where $g_i$ counts the number of degrees of freedom for a particle $i$ with mass $m_i$, and $\phi_i = |\Phi_i|$, $i = 1, 2$. Some general properties of a potential of this type was discussed in Section 1.2.2. In the SM, dominant contributions to this potential come from top quark[7] and $W/Z$ bosons. In 2HDMs, there is also contributions due to the extra Higgs bosons. In order to have a first-order phase transition, one requires that $\frac{v_c}{T_c} \gtrsim 1$, where $v_c = \sqrt{v_{1c}^2 + v_{2c}^2}$ is the minimum of the Higgs fields at the critical temperature $T_c$.

With the large number of parameters in 2HDMs, finding the parameter space that accommodates a first-order phase transition is a hefty task and can only be done numerically. For example, in Ref. [198] the authors analyzed $CP$-conserving 2HDMs and determined the regions of parameter space that would give a first-order phase transition and that are compatible with various experimental constraints. Some of the results of this study can be seen in Fig. 4.1 (figures taken from [198]). A heavy $CP$-odd Higgs, and a large splitting between the $CP$-odd and the heavier $CP$-even Higgs bosons are preferred for a first-order phase transition. (The lighter $CP$-even Higgs boson is set to be the observed 125 GeV Higgs boson.) This large mass splitting is interesting because it strengthens the case for using non-degenerate perturbation theory in the analysis of $CP$-violating 2HDMs as described above. Furthermore $\tan\beta < 4$ and $\beta - \alpha \simeq \frac{\pi}{2}$ are also preferred. Even though small $CP$ violation is expected not to have a significant effect on the strength of the phase transition, it is very important for producing the observed amount of baryon asymmetry. It would be interesting to see if it can be incorporated into a full study of EWBG in 2HDMs.

[7] Since top-quark couples to $\Phi_2$ in all four types of 2HDMs, one does not need to specify the model type while studying the phase transition.

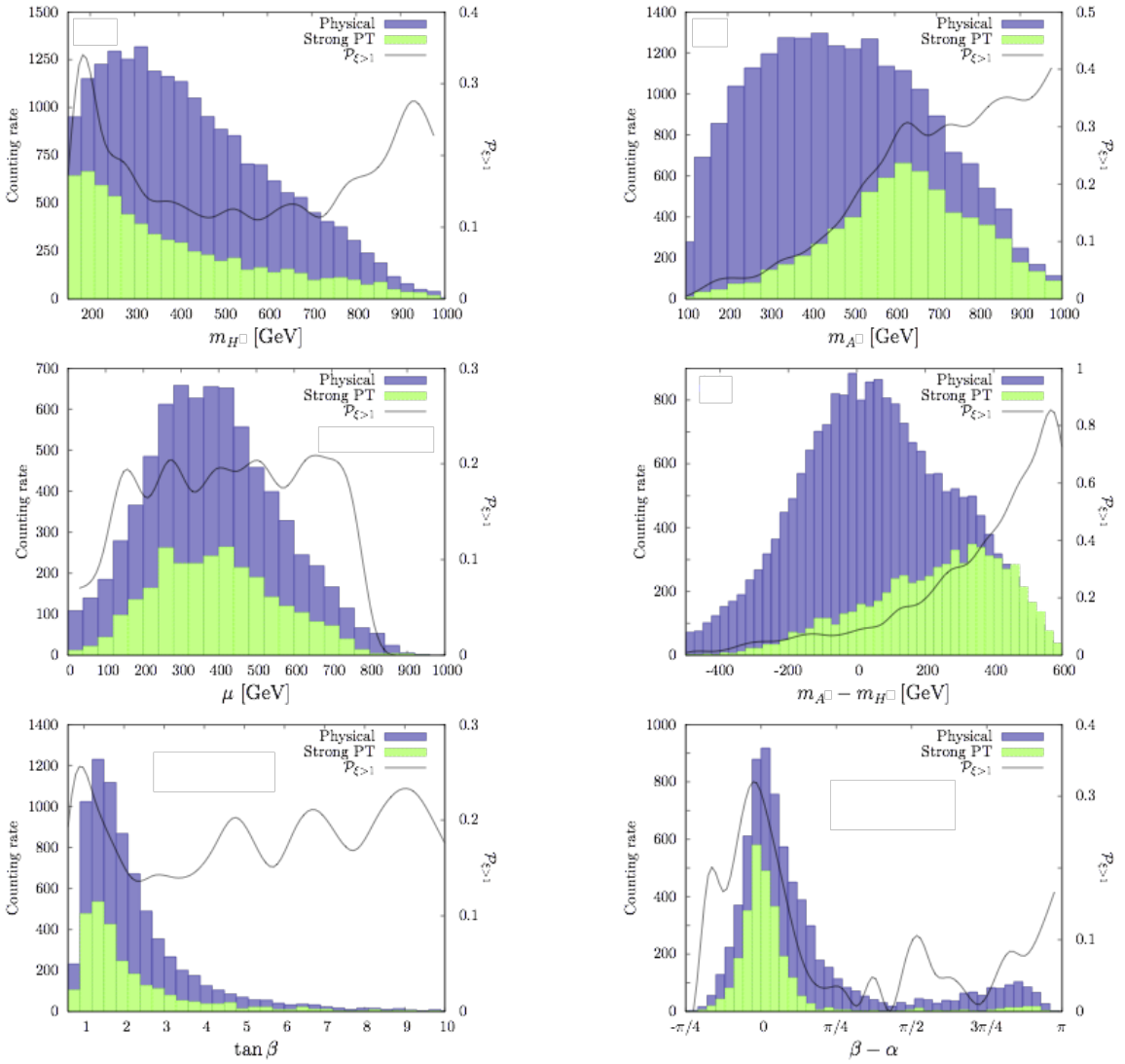


Figure 4.1: $CP$-conserving, Type II 2HDM parameter space that give a first-order phase transition [198]. Purple/dark bars indicate the number of *physical* points, which pass experimental constraints (Higgs branching ratios, EW precision tests, etc) as well as perturbativity limits and green/light bars indicate the number of points that give a first-order phase transition. The black line is the ratio of green points to purple points, and gives the probability of a first-order phase transition as a function of the parameter under investigation. The lighter $CP$-even Higgs is taken to be the observed 125 GeV Higgs boson. Note that in [198] the authors use $\alpha \to \alpha + \pi/2$.

### *4.4 Electron EDM Constraint*

EDMs violate $CP$ and $T$. Consequentially, they are a good handle on how much $CP$ violation we can expect from new physics sources. In the SM, the only source of $CP$ violation is in the quark sector via the CKM matrix[8] (see Section 1.1.1 for some details about quark mixing and the CKM matrix). The $CP$-violating phase in the CKM matrix produces a small EDM for the neutron ($d_n \simeq 10^{-32}\, e\,\text{cm}$) and an even smaller one for the electron ($d_e \leq 10^{-38}\, e\,\text{cm}$) [204]. Experimental bounds, though very stringent, are orders of magnitude higher than SM predictions: $|d_n| < 3.3 \times 10^{-26}\, e\,\text{cm}$ at 95% confidence level (CL) [205] and $|d_e| < 0.87 \times 10^{-28}\, e\,\text{cm}$ at 90% confidence level (CL) [206]. For good theoretical and experimental reviews on the EDMs, see [204, 205, 207]. Here I will only consider the electron EDM, because it gives more stringent constraints on the possible $CP$ violation in 2HDMs [199].

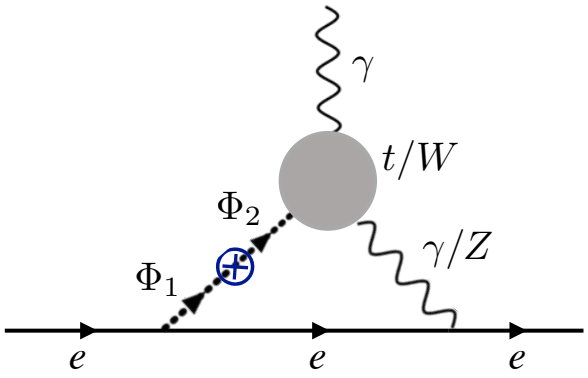


Figure 4.2: Top-loop diagram contributing to the electron EDM in a Type II 2HDM. Diagrams involving a $Z$ exchange are suppressed compared to the ones with a photon exchange.

The electron EDM in a 2HDM was calculated by Barr and Zee [208, 209]. The leading diagrams that contribute to the EDM, called the Barr-Zee diagrams, are two-loop diagrams involving either a top quark loop or a boson loop (see Figure.4.2). In the models with a softly broken $Z_2$ symmetry, the CP violation only comes from the neutral Higgs bosons.

[8]The strong $CP$ problem that is caused by the $\theta_3 G\tilde{G}$ term is assumed to be solved by the axion. There can also be $CP$ violation in the neutrino sector, but this has not been observed yet.

Therefore, we do not need to include any diagrams without a neutral Higgs in the loops. The diagrams that include a $Z$ boson come with a factor of $\frac{1}{4} - \sin^2\theta_W$, which makes their contribution much smaller than the diagrams that include a photon that couples to the electron. Hence, we will only consider the top- and $W$-loop contributions to the EDM. These contributions are [208, 209]

$$\left[\frac{d_e}{e}\right]_t = \left[\frac{16\alpha}{3(4\pi)^3}\sqrt{2}G_F m_e\right]\left([f(z_H^t)+g(z_H^t)]\mathrm{Im}Z_0 - [f(z_H^t)-g(z_H^t)]\mathrm{Im}\tilde{Z}_0\right), \quad (4.33a)$$

$$\left[\frac{d_e}{e}\right]_W = -\left[\frac{4\alpha}{(4\pi)^3}\sqrt{2}G_F m_e\right]\left(3f(z_H^W)+5g(z_H^W)\right)\sin^2\beta\,\mathrm{Im}Z_0\ , \quad (4.33b)$$

where $z_H^i = \frac{m_i^2}{m_H^2}$ $(i = t, W)$, $m_e$ is the electron mass, $\alpha$ is the fine structure constant (at scale $m_e$), $G_F$ is the Fermi constant, and

$$f(z) = \frac{z}{2}\int_0^1 \frac{1-2x(1-x)}{x(1-x)-z}\ln(\frac{x(1-x)}{z})\,dx\ , \quad g(z) = \frac{z}{2}\int_0^1 \frac{1}{x(1-x)-z}\ln(\frac{x(1-x)}{z})\,dx\ ,$$

$$\frac{\langle\phi_2^{0*}\phi_1^0\rangle}{v_1 v_2^*} \equiv \sum_n \sqrt{2}G_F\, Z_{0n}\frac{1}{q^2+m_{H_n}^2}\ , \qquad \frac{\langle\phi_2^0\phi_1^0\rangle}{v_1 v_2} \equiv \sum_n \sqrt{2}G_F\,\tilde{Z}_{0n}\frac{1}{q^2+m_{H_n}^2}\ ,$$

where $\phi_i^0 = \rho_i + i\eta_i$ is the neutral part of $\Phi_i$. In the above equations, $n$ runs through the number of Higgs particles. If there is more than one Higgs boson, Eq.4.33a and 4.33b become a sum over the different Higgs bosons. In the following analyses, we will not assume that the lightest Higgs dominates the loop contributions, so we will take all of the neutral Higgs bosons into account.

We can now employ the expansion that we used to find the mass eigenstates and the new fermion and gauge boson couplings in a $CP$-violating 2HDM in Section 4.2.2 to get the top- and $W$-loop contributions to the electron EDM as

$$\left[\frac{d_e}{e}\right]_t \simeq -\frac{\sqrt{2}G_F\, m_e\,\alpha}{6\pi^3}\xi\big(m_A^2-\mu^2\big)\left[c_\gamma c_\alpha\frac{f(z_{\tilde{A}}^t)s_\beta - f(z_{\tilde{h}}^t)}{c_\beta(m_A^2-m_{\tilde{h}}^2)} + c_\gamma s_\alpha\frac{-g(z_{\tilde{A}}^t)c_\beta + g(z_{\tilde{h}}^t)}{s_\beta(m_A^2-m_{\tilde{h}}^2)}\right.$$
$$\left. + s_\gamma s_\alpha\frac{f(z_{\tilde{A}}^t)s_\beta - f(z_{\tilde{H}}^t)}{c_\beta(m_A^2-m_{\tilde{H}}^2)} + s_\gamma c_\alpha\frac{g(z_{\tilde{A}}^t)c_\beta + g(z_{\tilde{H}}^t)}{s_\beta(m_A^2-m_{\tilde{H}}^2)}\right], \quad (4.34a)$$

$$\left[\frac{d_e}{e}\right]_W \simeq \frac{\sqrt{2}G_F\, m_e\,\alpha}{16\pi^3}\xi\big(m_A^2-\mu^2\big)\tan\beta\left[c_\gamma\frac{\sin(\beta-\alpha)}{m_A^2-m_{\tilde{h}}^2}H(z_{\tilde{A}}^W, z_{\tilde{h}}^W) + s_\gamma\frac{\cos(\beta-\alpha)}{m_A^2-m_{\tilde{H}}^2}H(z_{\tilde{A}}^W, z_{\tilde{H}}^W)\right], \quad (4.34b)$$

where

$$H(z_{\tilde{A}}^W, z_{\tilde{i}}^W) = 3\big[f(z_{\tilde{A}}^W) - f(z_{\tilde{i}}^W)\big] + 5\big[g(z_{\tilde{A}}^W) - g(z_{\tilde{i}}^W)\big]$$

for $i = \tilde{h}, \tilde{H}$.

This is a good point to remind ourselves of the parameters we have in the $CP$-violating 2HDM: the charged Higgs boson mass, $m_{H^\pm}$, the heavier mostly $CP$-even neutral Higgs boson mass, $m_{\tilde{H}}$, the lighter mostly $CP$-even neutral Higgs boson mass, $m_{\tilde{h}}(= 125\text{GeV})$, the mostly $CP$-odd Higgs boson mass $m_{\tilde{A}}$, $\tan\beta(\equiv \frac{v_2}{v_1})$, $\alpha(= \beta - \frac{\pi}{2})$ and $\mu$. We can see that the top- and the $W$-loop contributions to the electron EDM do not depend on the charged Higgs mass. This is expected since the $CP$ violation is mediated by the neutral scalars in this model. We set the charged Higgs to be degenerate with $\tilde{H}$, since this then satisfies EW precision constraints [198][9]. The dependence of the electron EDM on the rest of the parameters can be seen in Fig.4.3. There is cancellation between the top- and the $W$-loop in some portions of the parameter space which allows a large $CP$ violation. In general an $\mathcal{O}(10^{-2})$ $CP$ violation is allowed. Below are some general observations.

- It can be seen from Eq.4.34 that the electron EDM is proportional to $\Lambda\, v^2 \simeq m_{\tilde{A}}^2 - \frac{2\mu^2}{\sin 2\beta}$. A large $CP$-violating phase is allowed if there is good cancellations between $m_{\tilde{A}}$ and $\mu$. For example, for $m_{\tilde{A}} = 600$ GeV and $\mu = 400$ GeV, the phase $\xi$ is basically unsuppressed. Note that these parameters are also favored by a first-order phase transition (see Fig. 4.1).

- There is a cancellation between the top- and $W$-loop contributions to the electron EDM at $\tan\beta \sim 1$. A strong deviation from or preference of $\beta - \alpha = \frac{\pi}{2}$ is not found throughout the examined parameter space (figures not shown).

- Allowed parameter space does not change appreciably by changing $m_{\tilde{H}}$ (figures not shown).

---

[9] Actually, it is enough to have a charged Higgs degenerate with any of the neutral scalars to satisfy the EW precision constraints. However, there are other constraints on the charged Higgs mass, for example coming from $B$-meson decays, which puts a lower bound of $\sim 300$ GeV on the allowed mass [210]. Hence, the charged Higgs can not be degenerate with the 125 GeV Higgs.

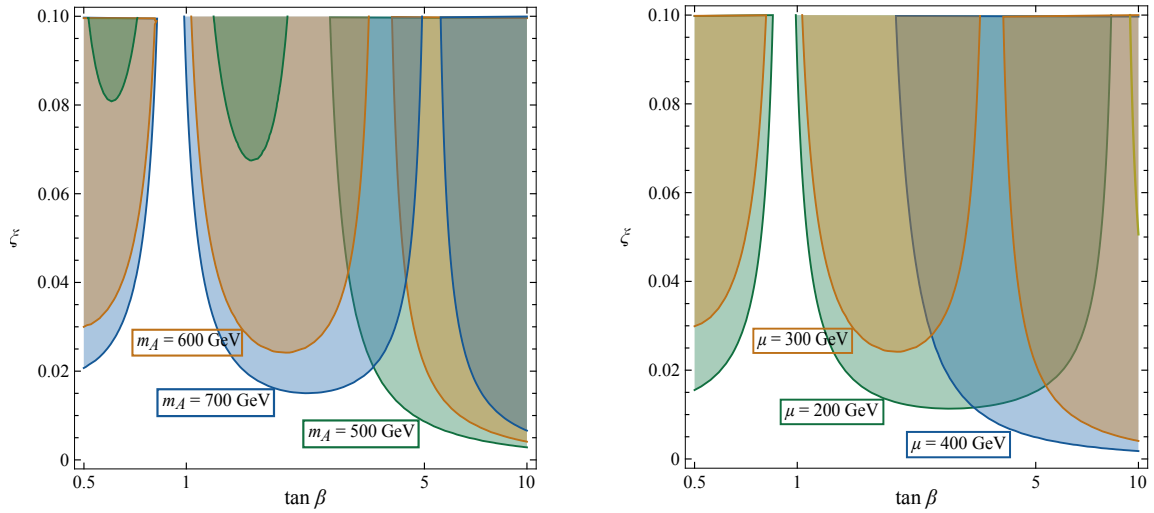


Figure 4.3: CP-violating phase $\xi$ versus $\tan\beta$ that is allowed by electron EDM measurements in the $CP$-violating Type II 2HDM. Shaded regions are excluded since the electron EDM in these regions is $|d_e| > 10^{-28}\ e{\cdot}\text{cm}$, in tension with the ACME constraint. In both plots we use the parameter values, $m_{\tilde{h}} = 125$ GeV, $m_{\tilde{H}} = 300$ GeV, $\beta - \alpha = \frac{\pi}{2}$. The funnels around $\tan\beta \sim 1$ are due to cancellations between the top- and $W$-loop contributions. A large $CP$-violating phase is also allowed for $m_{\tilde{A}} \simeq \bar{\mu}$. Left: Exclusion regions for different values of $m_{\tilde{A}}$. We set $\mu = 300$ GeV. Right: Exclusion regions for different values of $\mu$. We set $m_{\tilde{A}} = 600$ GeV.

We see that $\xi = 0.01 - 0.05$ (up to $\xi \simeq 0.1$ in some cases) is allowed in a 2HDM by the electron EDM bounds[10] for $\tan\beta < 5$. Note that for $\tan\beta > 5$, it is very hard to get a first-order phase transition (see Fig. 4.1.)

### *4.5 Baryogenesis in 2HDMs*

In Section 1.2.2 the mechanism of EW baryogenesis was discussed in the SM. 2HDM baryogenesis is very similar to that except in the source of $CP$ violation. We will not give any

[10]Note that this phase would not affect the $CP$ violation in $B$- and $K$- meson systems. The CKM phase is of $\mathcal{O}(1)$, and is still the main source of $CP$ violation in neutral meson systems. The CKM phase is not enough to explain the baryon asymmetry because the $CP$ violating processes involve all three generations of quarks, and hence are suppressed by small Yukawa couplings.

details here but introduce the general idea.

At temperatures much higher than the EW scale, the Higgs potential has a global minimum at zero (thermal) expectation value for the Higgs field(s) $\langle\phi\rangle = 0$. As the temperature falls, the potential acquires other minima at non-zero field expectation values. At some critical temperature $T_c$, a finite expectation value becomes the global minimum of the Higgs potential. It is shown that this EW transition can be a first-order phase transition in 2HDMs. In a first-order phase transition, the Universe responds to this change in minima by creating bubbles: Inside the bubbles is the broken phase where $\langle\phi\rangle \neq 0$ and outside the bubbles is the symmetric phase $\langle\phi\rangle = 0$. Smaller bubbles shrink due the pressure created by the difference between the free energies of the symmetric and broken phase. But larger bubbles can expand and eventually fill the whole Universe. As the bubbles expand fermions interact with the bubble wall and are either transmitted or reflected. The reflection rates of fermions and antifermions would differ if there is $CP$ violation in the interactions with the bubble wall. Neglecting the $CP$-violating phase in the CKM matrix (since it cannot produced the observed baryon asymmetry), the $CP$ violation comes through the Yukawa interactions

$$\mathcal{L}_f \supset i\,\bar{q}_R \not{D} q_R + y_q\,\bar{q}_L v_2(t) e^{i\theta(t)} q_R + \text{h.c.}\ , \tag{4.35}$$

where the top quark gives the most important contribution. Note that the phase $\theta$ and the *vev* $v_2$ are time dependent, since they change as the bubble expands. One can rotate the right-handed quark, $q_R \to e^{-i\theta(t)} q_R$ and get rid of the phase in the mass term. However than the kinetic term depends on the time-variation of the phase,

$$i\,\bar{q}_R \not{D} q_R \to i\,\bar{q}_R \not{D} q_R + \bar{q}_R \gamma^0 q_R\,\dot{\theta}\ , \tag{4.36}$$

where $\bar{q}_R \gamma^0 q_R$ is the right-handed quark current.

Inside the bubbles, there are baryon number violating sphaleron processes that happen out of equilibrium. The net baryon number produced by the wall

$$n_B \propto \int dt\,\Gamma_{\text{sph}}\,\dot{\theta}\ , \tag{4.37}$$

where $\Gamma_{\text{sph}}$ is the sphaleron rate (see Section 1.2.2 and Ref. [22] for details about sphalerons and baryon number violation). This gives a baryon-to-entropy ratio of

$$\eta \simeq 10^{-8} \Delta\theta. \tag{4.38}$$

Comparing this to the measured value of $\eta \simeq 10^{-10}$, we see that $\Delta\theta \sim \xi \sim 10^{-2}$ gives the right baryon–antibaryon asymmetry.

### *4.6 Conclusion*

The baryon asymmetry of the universe cannot be explained by the SM EW baryogenesis with a Higgs boson of mass 125 GeV since the EW transition is not a first-order phase transition. Furthermore, there is not enough $CP$ violation in the SM. 2HDMs are interesting extensions of the SM, since they allow a strongly first-order phase transition with a 125 GeV Higgs boson. Another feature of 2HDMs is that the scalar sector can have $CP$ violation. This $CP$ violation significantly complicates analyses by mixing $CP$-even and $CP$-odd Higgs fields. Due to EDM constraints, one expects only small $CP$ violation. I assumed a small $CP$ violating phase, $\xi$, in the Higgs sector, and expanded the Higgs mass states in terms of this small phase. This perturbative expansion makes it easier to incorporate $CP$ violation in the studies that scan the 2HDM parameter space to look for a strongly first order phase transition. A small $CP$ violation is not expected to affect the strength of the parameter transition. However, it can help constrain the phase space, since some portions of the parameter space that give a strongly first order parameter space would also give rise to large EDMs.

I also used the analytic results for the Higgs states to constrain the phase $\xi$ using electron EDM data. With the current experimental bounds ($|d_e| < 0.87 \times 10^{-28}\, e\,\text{cm}$) we can accommodate $\xi \simeq 0.01$ in most of the parameter space studied. Some studies suggest that one only needs $\xi \sim \mathcal{O}(10^{-2})$ to get sufficient baryon asymmetry. If a factor of two increase in the EDM sensitivity does not see a non-zero result, 2HDMs become fine-tuned. In addition, we need better estimates of the relation between the baryon asymmetry and the $CP$ violating phase.

Chapter 5

# BARYON ASYMMETRY: $CP$ VIOLATION IN PSEUDO-DIRAC GAUGINO OSCILLATIONS

Supersymmetric theories with a $U(1)_R$ symmetry have Dirac gauginos, solve the supersymmetric flavor and $CP$ problems, and have distinctive collider signatures. However when supergravity is included, the $U(1)_R$ must be broken, adding small Majorana mass terms which split the mass of the two components of the Dirac gaugino and lead to oscillations between $U(1)_R$ charge eigenstates. We present a general study of fermion-antifermion oscillations in this system, including the effects of decays and $CP$ violation. We consider the effects of such oscillations in the case where the two $U(1)_R$ charge eigenstates can decay into the same final state, and show that $O(1)$ $CP$ violation is allowed. In the case of decays into final states containing leptons such $CP$ violation can be observed as a same sign dilepton asymmetry.

## *5.1 Introduction*

The universe provides clear evidence for $CP$ violation beyond the standard model (SM). Assuming cosmological inflation erases any initial asymmetry, the asymmetry between matter and antimatter must arise due to a nonequilibrium microphysical process called baryogenesis, which requires $CP$ and baryon number violation, that creates the observed asymmetry of $10^{-8}$ between quarks and antiquarks. While the SM weak interactions violate baryon number via nonperturbative processes which are fairly rapid at high temperature [211], the effects of SM $CP$ violation are suppressed in the early Universe and new sources of $CP$ violation are needed to explain baryogenesis [26, 212]. However, any new sources of $CP$ violation are strongly constrained by searches for electric dipole moments (EDMs) (see, e.g., [32, 66, 213–218]). For example, in the minimal supersymmetric standard model (MSSM), electron and quark EDMs are generated at one loop level. Consequently, unless the superpartners are very heavy, the $CP$-violating phases in the soft supersymmetry-breaking terms of the MSSM

Lagrangian are tightly limited by the null results of EDM experiments [4, 206, 219]. Addressing this by assuming *CP* conservation in the SUSY-breaking terms is *ad hoc* and limits the possibilities for baryogenesis. Similar considerations apply for flavor-changing neutral currents.

One model that circumvents the fine-tuning of *CP*-violating and flavor-changing terms in the SUSY Lagrangian is the $R$-symmetric MSSM [220–222]. This model is an extension of the MSSM in which there is a global $U(1)_R$ symmetry [223]. The superpartners of fermions and gauge fields have $R$ charges of $+1$. This charge assignment forbids Majorana masses for the gauginos. Therefore, EDMs through neutralino exchange can only be induced at higher than one loop order, greatly reducing the constraints on the *CP*-violating phases in the Lagrangian. To give mass to the gauginos one needs to add an extra adjoint field with $R$ charge $-1$ for each of the MSSM gauginos to allow for Dirac masses. Each gaugino is then paired with its partner to form a Dirac spinor [224]. This scenario has a plausible short-distance origin. Mediating supersymmetry breaking to the MSSM by the nonvanishing expectation value of the $D$-term of a hidden $U(1)$ gauge field leads to $U(1)_R$-preserving Dirac gaugino masses [225, 226]. If the sector which mediates supersymmetry breaking does not contain a gauge singlet field with a non-vanishing $F$-term then Majorana gaugino masses and other $U(1)_R$ symmetry breaking soft supersymmetry breaking terms are suppressed.

The $U(1)_R$ symmetry is expected to be only an approximate symmetry in locally supersymmetric theories because it is always broken by the gravitino mass, and anomaly mediation will produce small $U(1)_R$-breaking Majorana mass terms for the gauginos [227, 228]. These Majorana masses produce a small mass splitting between different linear combinations of particle and antiparticle states (the eigenstates of $U(1)_R$ with opposite eigenvalues) that make up the Dirac spinor. Since the $U(1)_R$ symmetry is only approximate, the gaugino in this setup is therefore called a pseudo-Dirac fermion. The mass splitting causes oscillations between the two $R$ charge eigenstates in a way similar to neutral meson oscillations. Oscillations of pseudo-Dirac neutralinos have been considered in [229]. Another example of pseudo-Dirac fermion oscillation that arises in the context of $R$-symmetric SUSY is mesino-antimesino oscillation [230, 231]. Pseudo-Dirac fermion oscillations have also been extensively considered in the context of neutrinos [232–236]. However, the *CP* violation found in

these systems due to oscillations among the three (or more) generations of neutrinos [237] is different from the particle-antiparticle oscillations that we will consider.

*CP* violation in particle-antiparticle oscillations can occur if both states decay into common final states. In Ref. [229] *CP* violation in neutralino oscillations was not considered since it was assumed that there were no final states common to both $R$ charge eigenstates. However, there can be common final states when one allows for $U(1)_R$ violating interactions for both the neutralino and its Dirac partner.

In this paper we study *CP* violation in pseudo-Dirac fermion oscillations. For a concrete example with distinctive phenomenology we consider a pseudo-Dirac gluino which is the lightest MSSM superpartner (besides the gravitino), decaying via R-parity violation. We show that depending on the parameters of the model, there can be $O(1)$ *CP* violation in the oscillations. We also comment on ways to observe the *CP* violation from these oscillations, e.g. as a same sign dilepton asymmetry.

The organization of this paper is as follows. In Sec. 5.2 we set up the formalism to describe pseudo-Dirac fermion oscillations. In Sec. 5.3 we give the details of our model and compute the *CP* violation from interference between mixing and decay in pseudo-Dirac gluino oscillations in Sec. 5.4. A set of benchmark parameters of the model that lead to an interesting signal of *CP* violation is given in Sec. 5.5. Section 5.6 contains concluding remarks on this and variant scenarios.

### *5.2 Pseudo-Dirac Fermion Oscillations*

Before considering a specific model we demonstrate how the addition of a small Majorana mass to a theory with an otherwise Dirac fermion results in particle-antiparticle oscillations and obtain the Hamiltonian relevant to this two-state system. As *CP* violation in pseudo-Dirac fermion oscillations has not been previously discussed in the literature, we give a detailed treatment of the formalism here. In order to introduce these oscillations we use the two-component Weyl spinor techniques laid out in [238].

In a realistic supersymmetric theory, the pseudo-Dirac fermion could be a neutral mesino [230, 231], a neutralino as considered in [229], or a gluino. Reference [229] briefly mentions gluino oscillations, but claims that any macroscopic coherent oscillations would be destroyed due

to strong interactions with the detector. However, both the gluino and its Dirac partner are color octet fermions with identical strong interactions. Therefore, as explained in the Appendix, the coherence of the two $R$ charge states is not affected by scattering due to strong interactions or gluino hadronization, and such oscillations could be observable. For a concrete simple example of pseudo-Dirac fermion oscillations, we will consider the oscillations of a Dirac gluino here.

We start with a pair of left-handed, color octet Weyl spinors, $\lambda_\alpha$ and $\mathcal{O}_\alpha$ where $\alpha = 1, 2$ is the spinor index. We identify $\lambda$ with the usual gluino of the MSSM and $\mathcal{O}$ with the fermion component of a color adjoint chiral super field containing its Dirac partner, the octino. Under $U(1)_R$ symmetry, $\lambda$ and $\mathcal{O}$ have opposite charges, $R = +1$ and $-1$, respectively. If the $U(1)_R$ is exactly conserved by the mass terms, $\lambda$ and $\mathcal{O}$ pair up to form a Dirac fermion,

$$\begin{aligned} -\mathcal{L}_{\text{mass}} &= \frac{1}{2}\left(\lambda^\alpha \ \mathcal{O}^\alpha\right)\begin{pmatrix} 0 & m_D \\ m_D & 0 \end{pmatrix}\begin{pmatrix} \lambda_\alpha \\ \mathcal{O}_\alpha \end{pmatrix} + \text{h.c.} \\ &= \frac{1}{2} m_D \left(\lambda^\alpha \mathcal{O}_\alpha + \mathcal{O}^\alpha \lambda_\alpha\right) + \text{h.c.} \\ &= m_D \lambda \mathcal{O} + m_D^* \lambda^\dagger O^\dagger. \end{aligned} \tag{5.1}$$

We are free to rotate $\lambda$ and $\mathcal{O}$ such that the Dirac mass $m_D$ is real, and we do so. The Weyl spinors can be expressed in terms of creation and annihilation operators,

$$\lambda_\alpha(x) = \sum_s \int \frac{d^3\boldsymbol{p}}{(2\pi)^{3/2}\sqrt{2E_{\boldsymbol{p}}}}\left[x_\alpha(\boldsymbol{p}, s)\, a^s_{\boldsymbol{p}} e^{-ip\cdot x} + y_\alpha(\boldsymbol{p}, s)\, b^{s\dagger}_{\boldsymbol{p}} e^{ip\cdot x}\right], \tag{5.2a}$$

$$\mathcal{O}_\alpha(x) = \sum_s \int \frac{d^3\boldsymbol{p}}{(2\pi)^{3/2}\sqrt{2E_{\boldsymbol{p}}}}\left[x_\alpha(\boldsymbol{p}, s)\, b^s_{\boldsymbol{p}} e^{-ip\cdot x} + y_\alpha(\boldsymbol{p}, s)\, a^{s\dagger}_{\boldsymbol{p}} e^{ip\cdot x}\right], \tag{5.2b}$$

where $E_{\boldsymbol{p}} = \sqrt{\boldsymbol{p}^2 + m_D^2}$. $x$ and $y$ are momentum space solutions of the Dirac equation. Particle and antiparticle states are created by $a^{s\dagger}_{\boldsymbol{p}}$ and $b^{s\dagger}_{\boldsymbol{p}}$ respectively,

$$\begin{aligned} |\boldsymbol{p}, s; \psi\rangle &\equiv (2\pi)^{3/2}\, a^{s\dagger}_{\boldsymbol{p}}|0\rangle, \\ |\boldsymbol{p}, s; \bar{\psi}\rangle &\equiv (2\pi)^{3/2}\, b^{s\dagger}_{\boldsymbol{p}}|0\rangle. \end{aligned} \tag{5.3}$$

Suppressing the spin index, we use $|\psi\rangle$ and $|\bar{\psi}\rangle$ to label the states as $\boldsymbol{p} \to 0$. $|\psi\rangle$ carries $U(1)_R$ charge $R = -1$ while $|\bar{\psi}\rangle$ has $R = +1$.

### *5.2.1 Hamiltonian*

In the nonrelativistic limit, the Hamiltonian in the $\left(\psi, \bar{\psi}\right)$ basis can be written as

$$H_{ij}^{s',s} \equiv \langle \boldsymbol{p} \to 0, s'; i| - \mathcal{L}_{\text{mass}} |\boldsymbol{p} \to 0, s; j\rangle, \tag{5.4}$$

where $i, j = \psi, \bar{\psi}$ and $\mathcal{L}_{\text{mass}}$ is given in Eq. (5.1). Using the integral representations for $\lambda$ and $\mathcal{O}$ from Eq. (5.2) the Hamiltonian becomes

$$\boldsymbol{H}_D = \begin{pmatrix} m_D & 0 \\ 0 & m_D \end{pmatrix}, \tag{5.5}$$

using $y^\alpha(\boldsymbol{p}, s')x_\alpha(\boldsymbol{p}, s) = m_D \delta_{s,s'}$ and suppressing the trivial dependence on spin and color. We have used the subscript $D$ here to emphasize that this is the Hamiltonian in the Dirac (conserved $U(1)_R$) case.

Next, we allow for the $U(1)_R$ symmetry to be slightly broken. This allows for small Majorana mass terms in the Lagrangian

$$-\delta\mathcal{L}_{\text{mass}} = \frac{1}{2}\left(m_\lambda \lambda\lambda + m_{\mathcal{O}} \mathcal{O}\mathcal{O}\right) + \text{h.c.}, \tag{5.6}$$

where we have suppressed the spinor indices. The Hamiltonian resulting from the Majorana mass terms can be found in the same way as in the Dirac case. The full Hamiltonian in the nonrelativistic limit, corresponding to $\mathcal{L}_{\text{mass}} + \delta\mathcal{L}_{\text{mass}}$, is

$$\boldsymbol{H} = \boldsymbol{H}_D + \delta\boldsymbol{H} = \begin{pmatrix} m_D & m_M \\ m_M^* & m_D \end{pmatrix}, \tag{5.7}$$

where we have defined $m_M \equiv \left(m_\lambda^* + m_{\mathcal{O}}\right)/2$. The eigenvalues of this Hamiltonian are

$$M_{1,2} = m_D \pm |m_M|, \tag{5.8}$$

corresponding to the eigenstates

$$\frac{|\psi\rangle \pm e^{-i\phi}|\bar{\psi}\rangle}{\sqrt{2}}, \tag{5.9}$$

with $\phi = \arg\left(m_M\right)$.

### *5.2.2 Interactions*

Now we would like to examine what happens to the Hamiltonian when we allow for interactions of the Weyl fermions, in particular if they are allowed to decay. As a simple example, we consider a toy model which captures the essential physics. For now, we consider the case where $\lambda$ and $\mathcal{O}$ have Yukawa couplings to a fermion $\bar{d}$ and a complex scalar $\phi$ which are both fundamentals under color $SU(3)$,

$$\mathcal{L}_{\text{int}} = -\phi^* \left(y_\lambda \lambda^a + y_{\mathcal{O}} \mathcal{O}^a\right) t^a \bar{d} + \text{h.c.}, \tag{5.10}$$

where $t^a$ is a generator in the fundamental of $SU(3)$ normalized so that $\text{tr}\left(t^a t^b\right) = \delta^{ab}/2$ and $a$ labels the color of the adjoints. We will take $\bar{d}$ to be massless. If both $y_\lambda$ and $y_{\mathcal{O}}$ are nonzero, $\mathcal{L}_{\text{int}}$ breaks the $U(1)_R$.

With these interactions, the tree-level masses of $|\psi\rangle$ and $|\bar{\psi}\rangle$ ($M_{1,2}$) are modified (and possibly complex). As shown in [238], they are given by values of $\sqrt{s}$ that satisfy

$$\det\left[s\mathbf{1} - \left(\mathbf{1} - \boldsymbol{\Xi}^{\text{T}}\right)^{-1} \left(\boldsymbol{m} + \boldsymbol{\Omega}\right) \left(\mathbf{1} - \boldsymbol{\Xi}\right)^{-1} \left(\overline{\boldsymbol{m}} + \overline{\boldsymbol{\Omega}}\right)\right] = 0. \tag{5.11}$$

In the expression above $\boldsymbol{m}$ is the tree-level fermion mass matrix in the $\lambda, \mathcal{O}$ basis,

$$\boldsymbol{m} = \begin{pmatrix} m_\lambda & m_D \\ m_D & m_{\mathcal{O}} \end{pmatrix}, \tag{5.12}$$

and $\overline{\boldsymbol{m}} = \boldsymbol{m}^*$. $\boldsymbol{\Xi}$ and $\boldsymbol{\Omega}$ are chirality-preserving and -flipping self-energy functions, respectively. They are shown in Fig. 5.1 along with the related functions $\boldsymbol{\Xi}^{\text{T}}$ and $\overline{\boldsymbol{\Omega}}$. Note that these represent the finite pieces of the two-point functions (in some renormalization scheme); infinities in $\boldsymbol{\Omega}$ are absorbed by mass counterterms while those in $\boldsymbol{\Xi}$ are removed by wavefunction renormalization.

Corrections to the mass matrices are fixed by Eq. (5.11) at leading order to be

$$\begin{aligned} \boldsymbol{m}\big|_{1-\text{loop}} &= \boldsymbol{m} + \boldsymbol{\Omega} + \frac{1}{2}\left(\boldsymbol{m}\,\boldsymbol{\Xi} + \boldsymbol{\Xi}^{\text{T}}\boldsymbol{m}\right), \\ \overline{\boldsymbol{m}}\big|_{1-\text{loop}} &= \overline{\boldsymbol{m}} + \overline{\boldsymbol{\Omega}} + \frac{1}{2}\left(\overline{\boldsymbol{m}}\,\boldsymbol{\Xi}^{\text{T}} + \boldsymbol{\Xi}\,\overline{\boldsymbol{m}}\right). \end{aligned} \tag{5.13}$$

Armed with these expressions for the corrections to the mass matrices, we are ready to find the Hamiltonian for our toy model at one loop.

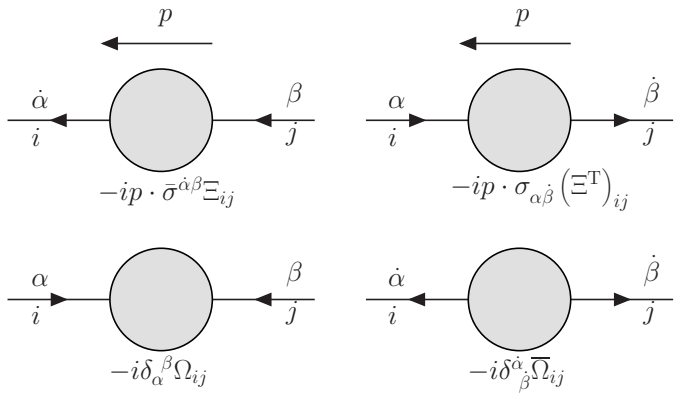


Figure 5.1: Definitions of the self-energy functions for $i, j = \lambda, \mathcal{O}$. The shaded circles represent the sum of all one-particle irreducible, connected Feynman diagrams. External legs are amputated. $\alpha$ and $\beta$ are spinor indices. Arrows (and dots) denote left- or right-handed chiralities.

In the toy model, $\mathbf{\Omega} \propto m_{\bar{d}}$ which we take to be vanishing so we are free to ignore $\mathbf{\Omega}$ and $\overline{\mathbf{\Omega}}$. In the $\overline{\mathrm{MS}}$ scheme, the elements of $\mathbf{\Xi}$, given by the diagram shown in Fig. 5.2, are

$$\Xi_{ij} = \frac{y_i y_j^*}{4\left(4\pi\right)^2}\left[\left(1-\frac{m_\phi^2}{p^2}\right)\int_0^1 dx \log\frac{\Delta}{Q^2} - \frac{m_\phi^2}{p^2}\left(1-\log\frac{m_\phi^2}{Q^2}\right)\right] \tag{5.14}$$

with

$$\Delta = x m_\phi^2 - x\left(1-x\right)p^2, \tag{5.15}$$

where $p$ is the momentum flowing through the diagram, $Q^2$ is the renormalization scale, and $i, j = \lambda, \mathcal{O}$.

If $m_\phi^2 < p^2$, there are on-shell intermediate states that give rise to an imaginary part in the loop integral for $\Xi_{ij}$,

$$\Im\left(\frac{\Xi_{ij}}{y_i y_j^*}\right) = \frac{1}{(4\pi)^2}\frac{\pi}{4}\left(1-\frac{m_\phi^2}{p^2}\right)^2 \theta\left(p^2 - m_\phi^2\right). \tag{5.16}$$

$(\Xi^{\mathrm{T}})_{ij}$ is obtained from $\Xi_{ij}$ through the relation $(\Xi^{\mathrm{T}})_{ij} = \Xi_{ij}^\star$, where $\star$ means taking the complex conjugate of the Lagrangian parameters but not of integrals over loop momenta.

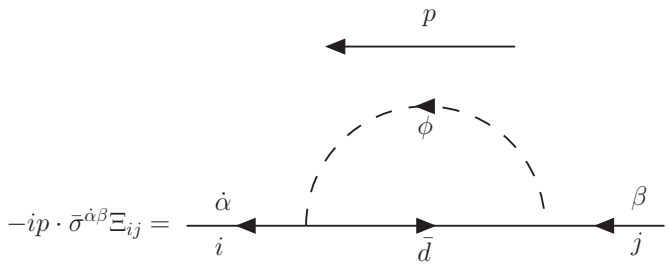


Figure 5.2: The one-loop contribution to $\boldsymbol{\Xi}$ for $i, j = \lambda, \mathcal{O}$ arising from the Yukawa interaction in Eq. (5.10). Contributions to the chirality-flipping two-point function $\boldsymbol{\Omega}$ are proportional to $m_{\bar{d}}$ which we neglect.

We express the one-loop mass matrices in Eq. (5.13) in terms of the elements of $\boldsymbol{\Xi}$ and $\boldsymbol{\Xi}^{\mathrm{T}}$ which we use to find the Hamiltonian at one loop and to leading order in $m_{\lambda,\mathcal{O}}/m_D$ using Eq. (5.7),

$$\boldsymbol{H} = \begin{pmatrix} m_D + \delta_D & m_M + \delta_M \\ m_M^* + \delta_M^* & m_D + \delta_D \end{pmatrix}, \tag{5.17}$$

with

$$\begin{aligned} \delta_D &= \frac{m_D}{4}\left(\Xi_{\lambda\lambda} + \Xi_{\mathcal{O}\mathcal{O}} + \Xi_{\lambda\lambda}^{\mathrm{T}} + \Xi_{\mathcal{O}\mathcal{O}}^{\mathrm{T}}\right), \\ \delta_M &= \frac{m_D}{2}\left(\Xi_{\mathcal{O}\lambda} + \Xi_{\lambda\mathcal{O}}^{\mathrm{T}}\right), \\ \delta_M^* &= \frac{m_D}{2}\left(\Xi_{\lambda\mathcal{O}} + \Xi_{\mathcal{O}\lambda}^{\mathrm{T}}\right), \end{aligned} \tag{5.18}$$

where we evaluate the one-loop diagrams at the scale of the fermion masses, $p^2 \simeq m_D^2$. The dispersive parts of $\delta_D$ and $\delta_M^{(*)}$ are corrections to the Dirac and Majorana masses, respectively, while the absorptive parts arising from on-shell intermediate states are related to the decays of the pseudo-Dirac fermions. As in the purely Dirac case, $m_D$ is multiplicatively renormalized while the Majorana masses pick up corrections proportional to the Dirac mass times a $U(1)_R$-breaking combination of couplings.

We can separate the Hamiltonian into its dispersive and absorptive parts in the standard

way,[1]

$$\boldsymbol{H} = \boldsymbol{M} - \frac{i}{2}\boldsymbol{\Gamma}, \tag{5.19}$$

where we set

$$\boldsymbol{M} = \begin{pmatrix} M_D & M_M \\ M_M^* & M_D \end{pmatrix}. \tag{5.20}$$

$M_D$ and $M_M$ are given by $m_D$ and $m_M$ plus the dispersive parts of the one-loop corrections in Eq. (5.18), with the renormalization condition that the pseudo-Dirac fermions have pole masses $M_D \pm |M_M|$ (in the limit that the width difference can be ignored). Since we have rotated $\lambda$ and $\mathcal{O}$ so that $m_D$ is real, $M_D$ is real. From the structure of the one-loop corrections in Eq. (5.18), $M_D \simeq m_D$ and we expect that in the absence of fine-tuning,

$$|M_M| \gtrsim \frac{|y_\lambda y_\mathcal{O}^*|}{(4\pi)^2} M_D. \tag{5.21}$$

The absorptive part of the Hamiltonian is

$$\boldsymbol{\Gamma} \simeq \frac{M_D}{64\pi}\left(1 - \frac{m_\phi^2}{M_D^2}\right)^2 \begin{pmatrix} |y_\lambda|^2 + |y_\mathcal{O}|^2 & 2y_\lambda y_\mathcal{O}^* \\ 2y_\lambda^* y_\mathcal{O} & |y_\lambda|^2 + |y_\mathcal{O}|^2 \end{pmatrix}. \tag{5.22}$$

As written, there are three phases in $\boldsymbol{H}$ but only one combination is physical since we have the freedom to remove two. For example, we can rotate one linear combination of $\lambda$ and $\mathcal{O}$ so that $M_M$ is real (another linear combination was rotated to make $M_D$ real) and by rotating $\phi^\dagger \bar{d}$ we can make $y_\lambda$ or $y_\mathcal{O}$ real but not necessarily both simultaneously.

### *5.2.3 Oscillations*

The form of $\boldsymbol{H}$ in Eq. (5.19) is the same as the two-state Hamiltonians relevant to neutral meson mixing. Therefore, we can simply adapt the same formalism to study the oscillations of the pseudo-Dirac fermions. We briefly review some of this formalism from Ref. [239]. For a more general treatment of oscillations see [240**?** ].

In terms of the states $|\psi\rangle$ and $|\bar{\psi}\rangle$ defined in Eq. (5.3), the eigenstates of $\boldsymbol{H}$ are

$$|\psi_H\rangle = p|\psi\rangle - q|\bar{\psi}\rangle, \quad |\psi_L\rangle = p|\psi\rangle + q|\bar{\psi}\rangle, \tag{5.23}$$

[1]The form of the Hamiltonian we will arrive at differs from the Hamiltonian in Eq. (7) of Ref. [229].

with eigenvalues $\omega_{H,L}$. The subscripts $H$ and $L$ refer to the heavy and light mass states respectively with masses $m_{H,L}$, and

$$\left(\frac{q}{p}\right)^2 = \frac{M_{12}^* - (i/2)\Gamma_{12}^*}{M_{12} - (i/2)\Gamma_{12}}. \tag{5.24}$$

where $M_{12}$ and $\Gamma_{12}$ are the 1-2 elements of $\boldsymbol{M}$ and $\boldsymbol{\Gamma}$. *CP* violation in mixing occurs when $|q/p| \neq 1$. The mass and width differences $\Delta m$ and $\Delta\Gamma$ between the two eigenstates are

$$\begin{aligned} \Delta m &= m_H - m_L = \Re(\omega_H - \omega_L), \\ \Delta\Gamma &= \Gamma_H - \Gamma_L = -2\Im(\omega_H - \omega_L), \end{aligned} \tag{5.25}$$

where

$$\omega_H - \omega_L = 2\sqrt{\left(M_{12} - \frac{i}{2}\Gamma_{12}\right)\left(M_{12}^* - \frac{i}{2}\Gamma_{12}^*\right)}. \tag{5.26}$$

A state that is initially pure $|\psi\rangle$ or $|\bar{\psi}\rangle$ evolves in time to a mixture of both states due to oscillations as follows[2]

$$\begin{aligned} |\psi(t)\rangle &= g_+(t)|\psi\rangle - \frac{q}{p}\, g_-(t)|\bar{\psi}\rangle, \\ |\bar{\psi}(t)\rangle &= g_+(t)|\bar{\psi}\rangle - \frac{p}{q}\, g_-(t)|\psi\rangle, \end{aligned} \tag{5.27}$$

where

$$g_\pm(t) = \frac{1}{2}\left(e^{-im_H t - \frac{1}{2}\Gamma_H t} \pm e^{-im_L t - \frac{1}{2}\Gamma_L t}\right). \tag{5.28}$$

To characterize the oscillations, it is often useful to define two dimensionless parameters,

$$x \equiv \frac{\Delta m}{\Gamma},\ y \equiv \frac{\Delta\Gamma}{2\Gamma}. \tag{5.29}$$

If $x \ll 1$, the states decay before oscillating while if $x \gg 1$, the states rapidly oscillate before decaying, making it difficult to observe oscillation signatures. The effects of oscillations are maximized for $x \sim 1$. For $|y|$ near unity (as defined $|y| \leq 1$) one of the two states can be rapidly depleted before the other decays, as is the case in the kaon system. If $|y| \ll 1$, neither state is preferentially depleted over the other.

---

[2]Note that in Ref. [229] the case of neutralino oscillations with fairly long lifetimes was discussed, and it was claimed that an oscillating decay rate could be an interesting consequence. Our analysis shows that in the absence of *CP* violation the decay rate does not oscillate in the rest frame, and therefore, by Lorentz invariance, will not oscillate for boosted particles either. Instead it is possible for the particle content of the final states to oscillate.

## 5.3 A Specific Example

### 5.3.1 UV Theory

We work with a nearly $U(1)_R$ symmetric SUSY model. The left-handed gauginos and the scalar superpartners of left-handed fermions have $R$ charge +1, while the SM particles have $R$ charge 0. We take the SM left-handed Weyl fermions $q_i, \bar{u}_i, \bar{d}_i, \ell_i, \bar{e}_i$ to be components of left chiral superfields $\Phi_{q_i}, \Phi_{\bar{u}_i}, \Phi_{\bar{d}_i}, \Phi_{\ell_i}, \Phi_{\bar{e}_i}$. The gluino $\lambda$ is the fermion component of the QCD field strength superfield $W_c^\alpha$. We assume the gluino to be the lightest superpartner other than the gravitino. In order for the gluino to get a $U(1)_R$ preserving Dirac mass, we introduce a left chiral, color adjoint superfield $\Phi_{\mathcal{O}}$ whose fermion component $\mathcal{O}$ is the Dirac partner of the gluino. For simplicity, we do not discuss the Higgs or the electroweak sectors in this work, but we note that it is possible to build a viable model with an extended Higgs sector and/or lepton number violation which preserves the $U(1)_R$ symmetry [220, 221, 241–246]. In order to allow non gauge interactions for $\Phi_{\mathcal{O}}$, we introduce superfields $\Phi_{\bar{D}}$ and $\Phi_D$, transforming under the SM gauge group in the same way as $\bar{d}$ and $\bar{d}^*$ respectively. We show the field content of the model that is most relevant to our study in Table 5.1.

These fields have a superpotential mass term and interactions

$$\int d^2\theta \; \mu_D \Phi_{\bar{D}} \Phi_D + y \Phi_{\bar{D}} \Phi_{\mathcal{O}} \Phi_D + g_i' \Phi_{\bar{d}_i} \Phi_{\mathcal{O}} \Phi_D + \text{h.c.}, \tag{5.30}$$

where $\mu_D$ is assumed to be very large, of order a TeV or higher. We neglect the possibility of mixing between the ordinary down quarks and the fermion components of $\Phi_{\bar{D}}, \Phi_D$.

We assume that the gluino is the lightest $R$-charged particle and decays via $U(1)_R$ symmetry violation. $U(1)_R$ symmetry must be broken by supergravity, and we will assume that R-parity is also broken. There is an extensive literature on R-parity violating interactions and their phenomenological constraints [247–249]. In this example, to ensure proton stability, we will assume that baryon number is conserved. We include the following R-parity and $U(1)_R$-symmetry–violating superpotential terms:

$$\int d^2\theta \; y_{ijk} \Phi_{\ell_i} \Phi_{q_j} \Phi_{\bar{d}_k} + y'_{ij} \Phi_{\ell_i} \Phi_{q_j} \Phi_{\bar{D}} + y''_{ij} \Phi_{\bar{e}_i} \Phi_{\bar{u}_j} \Phi_D + \text{h.c.} \tag{5.31}$$

The first two terms leave the linear combination $R - L$ unbroken, where $L$ is lepton number, and the third term leaves $R + L$ unbroken.

| Field | $SU(3)$ | $SU(2)$ | $U(1)$ | $U(1)_R$ |
|---|---|---|---|---|
| $q_i$ | 3 | 2 | 1/6 | 0 |
| $\bar{u}_i$ | $\bar{3}$ | 1 | $-2/3$ | 0 |
| $\bar{d}_i$ | $\bar{3}$ | 1 | 1/3 | 0 |
| $\ell_i$ | 1 | 2 | $-1/2$ | 0 |
| $\bar{e}_i$ | 1 | 1 | 1 | 0 |
| $\lambda$ | 8 | 1 | 0 | +1 |
| $\mathcal{O}$ | 8 | 1 | 0 | $-1$ |
| $\phi_{\bar{d}_i}$ | $\bar{3}$ | 1 | 1/3 | +1 |
| $\phi_{\bar{D}}$ | $\bar{3}$ | 1 | 1/3 | +1 |
| $\phi_D$ | 3 | 1 | $-1/3$ | +1 |

Table 5.1: Part of the particle content of the model with quantum numbers under the SM gauge group and $U(1)_R$. All fermions are left-handed Weyl spinors. $\lambda$ is the gluino, and $\mathcal{O}$ is the octino. The $\phi_{\bar{d}}$ fields are scalar superpartners of SM quarks, and $\phi_D, \phi_{\bar{D}}$ are superpartners of exotic heavy vector-like quarks. The fields $q_i, \bar{u}_i, \bar{d}_i, \ell_i, \bar{e}_i$ are SM fermions and $i$ is a generational index.

We do not discuss a specific SUSY-breaking model here, but assume that SUSY is broken in a hidden sector which communicates with the visible sector at the messenger scale $\Lambda_M$. Supersymmetry breaking is incorporated via spurions $W'_\alpha$ and $X$, where $W'_\alpha$ is the expectation value of a hidden sector $U(1)$ gauge field strength, and $X$ is the expectation value of a hidden sector chiral superfield. We set

$$\begin{aligned} W'_\alpha &= D\theta_\alpha, \\ X &= F\theta^2, \end{aligned} \tag{5.32}$$

where $D$ and $F$ are SUSY-breaking order parameters which are $U(1)_R$ neutral. We assume that $X$ transforms nontrivially under some symmetry of the SUSY-breaking sector. Because $X$ is not a singlet, there can be no $U(1)_R$-symmetry–violating Majorana gaugino mass terms from spurions such as $\int d^2\theta\, (X/\Lambda_M)\, W_\alpha W^\alpha$ where $W_\alpha$ is a SM gauge field strength

superfield. The Dirac gluino mass arises from the spurion term

$$\int d^2\theta \frac{c\, W'_\alpha}{\Lambda_M} W_c^\alpha \Phi_{\mathcal{O}} + \text{h.c.}, \tag{5.33}$$

where $c$ is a dimensionless parameter, giving

$$m_D = \frac{cD}{\Lambda_M} \ . \tag{5.34}$$

Majorana mass terms for the gauginos and scalar $\phi_D$, $\phi_{\bar{D}}$ mixing will be generated from anomaly mediation [227, 228], which gives, e.g. a Majorana gluino mass,

$$m_\lambda = \frac{\beta_s}{g_s} m_{3/2} \ , \tag{5.35}$$

and scalar mass mixing term,

$$m_{3/2} \mu_D \phi_D \phi_{\bar{D}} + \text{h.c.}, \tag{5.36}$$

where $\beta_s$ is the beta function for the QCD coupling $g_s$. $m_{3/2} \sim (D+F)/M_{\text{Pl}}$ is the gravitino mass with $M_{\text{Pl}}$ the Planck scale. Note that we must assume that $m_{3/2}$ is small in order to have an approximate $U(1)_R$ symmetry, so $\Lambda_M$ must be well below the Planck scale. The spurion $X$ can give rise to SUSY-breaking scalar masses via operators

$$\int d^4\theta \frac{X^\dagger X}{\Lambda_M^2} \left( c_{ij} \Phi^\dagger_{\bar{d}_i} \Phi_{\bar{d}_j} + c_i \Phi^\dagger_{\bar{D}} \Phi_{\bar{d}_i} + c_{\bar{D}} \Phi^\dagger_{\bar{D}} \Phi_{\bar{D}} + c_D \Phi^\dagger_D \Phi_D \right) \ , \tag{5.37}$$

where $c_{ij}, c_i, c_D, c_{\bar{D}}$ are dimensionless parameters. We will assume a modest hierarchy of supersymmetry breaking terms,

$$D < F, \tag{5.38}$$

so that in general scalar masses are larger than gaugino masses. A Majorana mass term for $\mathcal{O}$ could arise from a $U(1)_R$-violating superpotential term

$$\int d^2\theta \ m_{\mathcal{O}} \Phi_{\mathcal{O}}^2 + \text{h.c.} \tag{5.39}$$

Note that as we assume all $U(1)_R$-violating terms are small,

$$m_{\mathcal{O}} \ll m_D. \tag{5.40}$$

A possible explanation for the small size of this term is that $\mathcal{O}$ could be part of an approximately $\mathcal{N} = 2$ supersymmetric gauge or gauge/Higgs sector [224, 226, 250].

Supersymmetry breaking may also provide the supersoft terms [226]

$$\int d^2\theta \frac{W'^{\alpha} W'_{\alpha}}{\Lambda_M^2} \left( c_{\mathcal{O}\mathcal{O}} \Phi_{\mathcal{O}}^2 + c_{D\bar{D}} \Phi_D \Phi_{\bar{D}} + c_{D\bar{d}_i} \Phi_D \Phi_{\bar{d}_i} \right) + \text{h.c.}, \tag{5.41}$$

where $c_{\mathcal{O}\mathcal{O}}, c_{D\bar{D}}, c_{D\bar{d}_i}$ are dimensionless parameters. These give scalar mass mixing terms, including

$$\left( B^2_{D\bar{D}} \phi_D \phi_{\bar{D}} + B^2_{D\bar{d}_i} \phi_D \phi_{\bar{d}_i} \right) + \text{h.c.}, \tag{5.42}$$

with

$$B^2_{D\bar{D}} = \frac{c_{D\bar{D}} D^2}{\Lambda_M^2}, \quad B^2_{D\bar{d}_i} = \frac{c_{D\bar{d}_i} D^2}{\Lambda_M^2} \ . \tag{5.43}$$

Our assumption of relatively large $F$ term contributions to scalar masses solves the negative scalar mass squared problem [251–253], preserves the $U(1)_R$ solution to the SUSY $CP$ problem, but does not address the SUSY flavor problem. We assume the latter is addressed by an approximate flavor symmetry of the messenger interactions, leading to

$$c_{ij} = c_{\bar{d}} \delta_{ij} + \text{small} \tag{5.44}$$

and

$$c_i, c_{D\bar{d}_i} \ll c_{\bar{d}} \ . \tag{5.45}$$

Thus the $\phi_{\bar{d}_k}$ are nearly degenerate, with mass squared

$$m^2_{\phi_{\bar{d}_k}} \approx \frac{c_{\bar{d}} F^2}{\Lambda_M^2} \ . \tag{5.46}$$

We assume

$$\mu_D > \frac{F}{\Lambda_M} \tag{5.47}$$

so that $\phi_D, \phi_{\bar{D}}$ are nearly degenerate with mass $\mu_D$. We also note that there is a supersymmetry-breaking mixing term between the $\phi_{\bar{d}_k}$ and $\phi_{\bar{D}}$,

$$\mathcal{L} \supset -\tilde{m}_k^2 \phi_{\bar{d}_k} \phi^*_{\bar{D}} + \text{h.c.}, \tag{5.48}$$

with

$$\tilde{m}_k^2 = \frac{c_k F^2}{\Lambda_M^2} \tag{5.49}$$

assumed to be small.

The supersymmetric gauge interactions contain the Yukawa couplings

$$\mathcal{L} \supset -\sqrt{2} g_s \bar{d}_i \lambda^a t^a \phi^*_{\bar{d}_i} + \text{h.c.} \tag{5.50}$$

and the superpotential terms contain the interactions

$$\mathcal{L} \supset -g'_i \bar{d}_i \mathcal{O}^a t^a \phi_D - y_{ijk} \ell_i q_j \phi_{\bar{d}_k} - y'_{ij} \ell_i q_j \phi_{\bar{D}} - y''_{ij} \bar{e}^*_i \bar{u}^*_j \phi^*_D + \text{h.c.} \tag{5.51}$$

While the flavor-violating terms $B^2_{D\bar{d}_k}$ and $\tilde{m}^2_k$ can be suppressed at tree-level by a flavor symmetry as we assume, they are generated at one-loop and proportional to $y_{ijk} y'_{ij} B^2_{D\bar{D}}$ and $y_{ijk} y'_{ij}$, respectively.

### *5.3.2 Effective Four Fermion Theory for Gluino Decays*

Now we assume that all the squarks are heavy and can be integrated out. Using a mass insertion approximation for the small scalar mixing terms and neglecting the gravitino mass, the resulting effective 4-fermi Lagrangian for the gluino interactions is approximately

$$\mathcal{L}_{\text{eff}} = G_{ijk} \lambda \ell_i q_j \bar{d}_k + G'_{ijk} \mathcal{O} \ell_i q_j \bar{d}_k + G''_{ijk} \mathcal{O} \bar{e}^*_i \bar{u}^*_j \bar{d}_k + G'''_{ijk} \lambda \bar{e}^*_i \bar{u}^*_j \bar{d}_k + \text{h.c.}, \tag{5.52}$$

where we have suppressed color indices and

$$\begin{aligned} G_{ijk} &= \frac{\sqrt{2} g_s y_{ijk}}{m^2_{\phi_{\bar{d}}}} \ , \quad & G'_{ijk} &= \frac{g'_k y'_{ij} B^2_{D\bar{D}}}{\mu^4_D} \ , \\ G''_{ijk} &= \frac{g'_k y''_{ij}}{\mu^2_D} \ , & G'''_{ijk} &= \frac{\sqrt{2} g_s y''_{ij} (\tilde{m}^2_k B^2_{D\bar{D}} + \mu^2_D B^2_{D\bar{d}_k})}{m^2_{\phi_{\bar{d}}} \mu^4_D} \ . \end{aligned} \tag{5.53}$$

We have assumed a flavor symmetry such that $B^2_{D\bar{d}_k}$ and $\tilde{m}^2_k$ are loop-suppressed so we might expect that $G'''_{ijk}$ is somewhat smaller than the others.

### *5.3.3 Pseudo-Dirac Gluino Oscillations*

In this section we use the machinery from Sec. 5.2 with our specific model. In the toy model the scalar field $\phi$ was light so that the gluino decayed to a scalar and a fermion. However, in this specific model the squarks are heavier than the gluino so the relevant decays are to 3-body final states through the 4-fermi operators in Eq. (5.52). Therefore, the one-loop corrections to the gluino self-energy (as seen in Fig. 5.2) are real. Absorptive

contributions to the Hamiltonian occur at two-loop order through diagrams like the one shown in Fig. 5.3. We continue to ignore the chirality-flipping two-point functions, $\mathbf{\Omega}$, since they are proportional to light fermion masses.

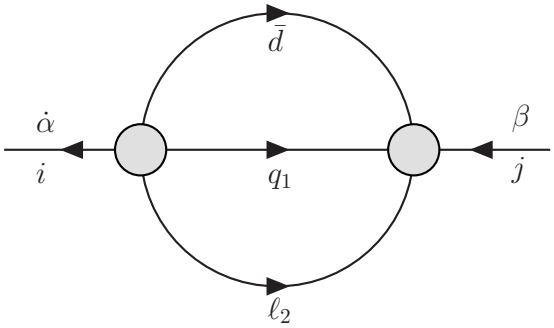


Figure 5.3: Two-loop corrections to the two-point functions, $\Xi_{ij}$, for $i, j = \lambda, \mathcal{O}$, that arise due to the couplings in Eq. (5.54).

For simplicity we will consider an example where there are only two relevant 4-fermi operators, assuming that $G_{211} \equiv \tilde{G}_\lambda$ and $G'_{211} \equiv \tilde{G}_\mathcal{O}$ dominate in Eq. (5.52),[3] leading to the effective Lagrangian

$$\mathcal{L}_{\text{eff}} = \tilde{G}_\lambda \lambda \bar{d} q_1 \ell_2 + \tilde{G}_\mathcal{O} \mathcal{O} \bar{d} q_1 \ell_2 + \text{h.c.}, \tag{5.54}$$

suppressing gauge indices.

The imaginary part of the diagram in Fig. 5.3 is found to be

$$\Im\left(\frac{\Xi_{ij}}{\tilde{G}_i \tilde{G}_j^*}\right) = \frac{2p^4}{3\,(16\pi)^3} \tag{5.55}$$

for $i, j = \lambda, \mathcal{O}$. Following the discussion in Sec. 5.2, in the presence of these interactions, the Hamiltonian for the pseudo-Dirac gluino is

$$\boldsymbol{H} = \boldsymbol{M} - \frac{i}{2}\boldsymbol{\Gamma} \tag{5.56}$$

[3]Due to our assumption of a flavor symmetry, we expect that $G'''_{ijk}$ is loop-suppressed. Since $CP$-violating effects involving the lepton singlet final state are proportional to $G''G'''$, this makes the lepton doublet final state that we have chosen more interesting.

with

$$\begin{aligned} \boldsymbol{M} &= \begin{pmatrix} M_D & M_M \\ M_M^* & M_D \end{pmatrix}, \\ \boldsymbol{\Gamma} &\simeq \begin{pmatrix} \Gamma_0 & 0 \\ 0 & \Gamma_0 \end{pmatrix} + \frac{M_D^5}{12\,(8\pi)^3} \begin{pmatrix} |\tilde{G}_\lambda|^2 + |\tilde{G}_\mathcal{O}|^2 & 2\tilde{G}_\lambda^* \tilde{G}_\mathcal{O} \\ 2\tilde{G}_\lambda \tilde{G}_\mathcal{O}^* & |\tilde{G}_\lambda|^2 + |\tilde{G}_\mathcal{O}|^2 \end{pmatrix}. \end{aligned} \tag{5.57}$$

$\Gamma_0$ represents possible contributions to the decay width that involve $\lambda$ (or possibly $\mathcal{O}$) that do not arise from operators in Eq. (5.54) and do not break the $U(1)_R$ symmetry, such as decays to a gluon and gravitino. The masses in $\boldsymbol{M}$ are the renormalized two-loop values such that the gluino and octino form nearly Dirac fermions with masses $M_D \pm |M_M|$ (ignoring any width difference). The Dirac mass is multiplicatively renormalized from its tree-level value in Eq. (5.34), leading to $M_D \simeq m_D$. At tree-level the Majorana mass, $M_M$, is $m_\lambda^* + m_\mathcal{O}$ from Eqs. (5.35) and (5.39). It also receives one-loop contributions proportional to the Dirac mass and $U(1)_R$-violating terms,

$$\delta_M \sim \frac{g_s g_k'}{(4\pi)^2} \left( \frac{\tilde{m}_k^2 B_{D\bar{D}}^2 + \mu_D^2 B_{D\bar{d}_k}^2}{\mu_D^4} \right) M_D. \tag{5.58}$$

Since we have assumed a flavor-symmetry so that $B_{D\bar{d}_k}^2$ and $\tilde{m}_k^2$ are loop-suppressed, this is effectively a two-loop contribution to the mass.

### *5.4 CP violation in pseudo-Dirac fermion oscillations*

Particle-antiparticle oscillations can enhance the observable effects of *CP*-violating phases, via interference between the phases in oscillations and decay amplitudes. Here we consider a possible charge asymmetry between like sign dimuons that may be produced in gluino decays as a possibly observable example. Like sign dileptons are a standard SUSY signal [254–257] and can exhibit a charge asymmetry at a *pp* collider like the LHC when the squarks are lighter than the gluino [256, 257], while in our scenario the gluino is lighter than the squarks. Since the interactions that produce a pair of pseudo-Dirac gluinos conserve $U(1)_R$, initially a pair of $R = +1$ and $R = -1$ states are produced. We denote the amplitude for a state with $U(1)_R$ charge $R$ to decay to $\mu^\pm$ as $\mathcal{M}_R^\pm$. Note that $\mathcal{M}_+^+$ can arise from the couplings $G_{2jk}, G_{2jk}'''$ in Eq. (5.52), while $\mathcal{M}_-^-$ can arise from their hermitian conjugates. At tree level,

and neglecting final state interactions, we expect no direct $CP$ violation, and may assume

$$\mathcal{M}_{-}^{-} = \mathcal{M}_{+}^{+*} \ . \tag{5.59}$$

Similarly, $\mathcal{M}_{-}^{+}$ is proportional to the couplings $G'_{2jk}, G''_{2jk}$ and $\mathcal{M}_{+}^{-}$ to their conjugates. Assuming no direct $CP$ violation gives

$$\mathcal{M}_{-}^{+} = \mathcal{M}_{+}^{-*} \ . \tag{5.60}$$

$CP$ violation due to interference between a decay with mixing and without mixing is only possible when either $R$ charge state can decay into an indistinguishable final state. Since the $G, G'$ operators tend to produce different helicities than the $G'', G'''$ operators, $CP$ violation from interference will be maximized when either the $G$-$G'$ or the $G''$-$G'''$ pair dominate, and when the quark flavor dependence of the different couplings is the same. In the following analysis we assume that the final states produced by the $\mathcal{M}_{+}^{+}$ decay amplitudes are indistinguishable from those produced by the $\mathcal{M}_{-}^{+}$ amplitudes, and the final states from $\mathcal{M}_{+}^{-}$ are indistinguishable from those due to $\mathcal{M}_{-}^{-}$.

Using Eq. (5.27), we find that a state with $R = +1$ at $t = 0$ decays into $\mu^{\pm}$ at time $t$ with an amplitude of

$$A_{+}^{\pm}(t) = g_{+}(t)\,\mathcal{M}_{+}^{\pm} - \frac{p}{q}\,g_{-}(t)\,\mathcal{M}_{-}^{\pm} \ , \tag{5.61}$$

and an initial $R = -1$ state decays into $\mu^{\pm}$ at time $t$ with an amplitude of

$$A_{-}^{\pm}(t) = g_{+}(t)\,\mathcal{M}_{-}^{\pm} - \frac{q}{p}\,g_{-}(t)\,\mathcal{M}_{+}^{\pm} \ . \tag{5.62}$$

It is possible that the oscillation length is too short to be directly observable for gluino decays. However, interference between decays with and without mixing can still produce sizable observable $CP$ violation when the oscillation and decay times are similar. Assuming initial incoherent production of a pair of gluinos with opposite $R$ charges, the number of resulting like-sign pairs of positively charged muons, $N^{++}$, versus negatively charged muons, $N^{--}$, where

$$N^{\pm\pm} \propto \left[\int_0^\infty dt\,\left|A_{+}^{\pm}(t)\right|^2\right] \times \left[\int_0^\infty dt\,\left|A_{-}^{\pm}(t)\right|^2\right], \tag{5.63}$$

can exhibit a nonzero asymmetry,

$$A \equiv \frac{N^{++} - N^{--}}{N^{++} + N^{--}}. \tag{5.64}$$

Also of interest is the total fraction of same sign muon decays,

$$R \equiv \frac{N^{++} + N^{--}}{N^{+-} + N^{-+} + N^{++} + N^{--}}, \tag{5.65}$$

where we calculate the number of opposite sign muon decays in an analogous way to Eq. (5.63). Below, we show approximate expressions for $A$ and $R$ in some physically relevant limits.

If the total decay width of the pseudo-Dirac particles is dominated by final states that do not include muons and do not break the $U(1)_R$, then we can ignore the width difference between the states, $\Delta\Gamma$, and take $|q/p| = 1$. This corresponds to $\Gamma_0 \gg \Gamma$ in Eq. (5.57). Then the asymmetry can be expressed as

$$A \simeq \frac{4xr(1-r^2)\sin\beta}{(1+x^2)^2(1+r^2)^2 - (1-r^2)^2 - 4x^2r^2\sin^2\beta}, \tag{5.66}$$

where $x$ is related to the mass difference as in Eq. (5.29) and we assume no direct $CP$ violation as in Eqs. (5.59) and (5.60). We have defined a reparameterization-invariant phase,

$$\beta \equiv \arg\left(\frac{q}{p}\frac{\mathcal{M}_+^+}{\mathcal{M}_-^+}\right), \tag{5.67}$$

and a ratio of amplitudes,

$$r \equiv \frac{|\mathcal{M}_+^+|}{|\mathcal{M}_-^+|}\,. \tag{5.68}$$

In the same limit the ratio of same sign muon decays is

$$R \simeq \frac{1}{2}\left[1 - \frac{\left(1-r^2\right)^2}{\left(1+x^2\right)^2\left(1+r^2\right)^2 - 4x^2r^2\sin^2\beta}\right]. \tag{5.69}$$

For $x \gtrsim r$, as we would expect without fine-tuning, the product of the asymmetry and the fraction of same sign decays is approximately

$$A \times R \simeq \frac{2xr\sin\beta}{\left(x^2+1\right)^2}. \tag{5.70}$$

In the benchmark model we will consider in Sec. 5.5, the final states involving muons common to both $R = \pm 1$ states dominate the total width, which corresponds to $\Gamma_0 \ll \Gamma$ in Eq. (5.57), and we can no longer ignore the width difference or the deviation of $|p/q|$ from unity. In this case, $\Delta\Gamma$, $|p/q| - 1 \propto r$. For $r < 2M_M/\Gamma$, which we expect is the case in the absence of fine-tuning, we can write the asymmetry as

$$A \simeq \frac{4r}{x}\left(\frac{x^2+3}{x^2+2}\right)\sin\beta, \tag{5.71}$$

and the fraction of same sign decays as

$$R \simeq \frac{x^2}{2}\frac{x^2+2}{(x^2+1)^2}. \tag{5.72}$$

The asymmetries that we have expressed above can be significant for a fairly wide range of parameters, and the product of the asymmetry and the fraction of same sign decays is typically of order $x\,r\sin\beta$. We also note that when $r$ is close to one, $A$ is suppressed for any value of $\Delta\Gamma$ and $|p/q|$.

### *5.5 Benchmark Model Estimates*

Here we give sample parameters which allow for sizable *CP* violation in gluino decays. The distinctive final state that the gluino decays into through $\mathcal{L}_{\text{eff}}$ in Eq. (5.54), $\mu jj$ is subject to leptoquark searches at the LHC [258].[4] The very strong constraints from CMS on second generation leptoquarks using 20 fb$^{-1}$ of 8 TeV data [261] suggest that a gluino that decays with an $O(1)$ branching fraction to this final state should be heavy enough to be out of reach at 8 TeV. We therefore choose a benchmark gluino mass of 1.6 TeV, out of the reach of this search as well as standard SUSY searches involving missing energy. At next-to-leading order in QCD including next-to-leading-logarithmic threshold corrections, assuming the squarks are decoupled, the cross section for a 1.6 TeV Dirac gluino pair production in $pp$ collisions is 16 fb (0.4 fb) at 13 TeV (8 TeV) center-of-mass energy, with an uncertainty on the order of 15-20% [262–266], which is in agreement with the limit from [261] given a 100% branching to $\mu jj$.

[4]This scenario could lead to a $\ell\ell$ + jets signal for $\ell = e$, $\mu$, $\tau$, an intriguing possibility in light of recent excesses in leptoquark [259] and right-handed charged gauge boson [260] searches.

The following estimate shows that we do not expect an observably long lifetime for the gluino unless $x \gg 1$, in which case $CP$ violation from interference between mixing and decay becomes suppressed. The mass splitting from anomaly mediation is proportional to the gravitino mass, while the rate for decay into a gluon and gravitino is inversely proportional to the square of the gravitino mass. We cannot take the mass splitting to be small without taking the gravitino light or fine-tuning, however if we take the gravitino mass to be too small the gluino will decay too fast to oscillate. The rate for a gluino of mass $M_D$ to decay to a gluon and gravitino is [267]

$$\Gamma_{g\tilde{G}} = \frac{M_D^5}{12 M_{\rm Pl}^2 m_{3/2}^2} \tag{5.73}$$

which gives $\Gamma_{g\tilde{G}} \sim 60$ eV for a 1.6 TeV gluino mass and 10 eV gravitino. From Eq. (5.35), a gravitino mass of 10 eV would give a mass splitting from anomaly mediation of about 0.4 eV. We therefore can only have comparable oscillation and decay rates when the gravitino is heavier than a few eV and the gluino width is greater than about an eV.

We consider a gluino width of 300 eV and assume the gravitino branching fraction is small, so that the decays are dominated by the effective operators of Eq. (5.54). For a 1.6 TeV gluino this width corresponds to

$$\sqrt{|\tilde{G}_\lambda|^2 + |\tilde{G}_{\mathcal{O}}|^2} \sim \frac{1}{(21\ \text{TeV})^2}. \tag{5.74}$$

Taking $\mu_D = 5$ TeV, $m_{\phi_{\bar{d}}} = 4$ TeV, $|g_1'| = |y_{21}'| = 0.3$, $y_{211} = 0.02$, and $|B_{D\bar{D}}^2| = (1.25\ \text{TeV})^2$ gives

$$|\tilde{G}_\lambda| = \frac{1}{(21\ \text{TeV})^2},\ |\tilde{G}_{\mathcal{O}}| = \frac{1}{(56\ \text{TeV})^2}\ . \tag{5.75}$$

Given scalar masses of this size, these values of the $R$-parity–violating couplings $y_{211}$ and $y_{21}'$ are in agreement with limits from charged pion decays and neutrino scattering [249]. The ratio $r$ is

$$r = \frac{|\mathcal{M}_+^+|}{|\mathcal{M}_-^+|} = \frac{|\tilde{G}_{\mathcal{O}}|}{|\tilde{G}_\lambda|} = 0.14. \tag{5.76}$$

We work in a basis where we have rotated the Majorana mass to be real. The phase $\phi_\Gamma \equiv \arg \Gamma_{12}$ is a free parameter and is related to the physical phase in this basis as

$\phi_\Gamma \simeq \beta + \pi$. Loop corrections to the $U(1)_R$-breaking gaugino mass splitting are effectively at the two loop level, due to our assumption of a flavor symmetry suppressing $\tilde{m}_k$ and $B_{D\bar{d}_k}$, and are of order $r\Gamma$. This means that without fine-tuning, $M_M \simeq x\Gamma/2 \gtrsim r\Gamma$. The particular value, however, depends on the gravitino mass and is a free parameter. Taking the mass splitting to be 200 eV and $\phi_\Gamma = -\pi/3$ gives a dimuon asymmetry

$$A \simeq 0.8, \tag{5.77}$$

and a fraction of same sign events of $R \simeq 0.25$. Given the production cross sections above, we therefore expect about 400 (2) same sign muon pair events in 100 fb$^{-1}$ of data at 13 TeV (20 fb$^{-1}$ at 8 TeV). This event rate could allow for $O(10\%)$ asymmetries to be probed.

In Fig. 5.4, we show the asymmetry for the parameters specified above, allowing the mass splitting to vary, as well as the approximate expression for the asymmetry from Eq. (5.71). We also show the product of the asymmetry and the ratio of same sign decays and the product of the approximate expressions in Eqs. (5.71) and (5.72).

Note that assuming this gluino mass splitting is dominated by the anomaly-mediated contribution gives a gravitino mass of about 5 keV, which could make the gravitino an interesting warm dark matter candidate. A 5 keV gravitino mass gives a branching fraction for the gluino to gluon plus gravitino of $0.8 \times 10^{-6}$.

### *5.6 Summary and Outlook*

This paper is the first to study the possibility of *CP* violation in the decays of oscillating pseudo-Dirac fermions. We set up the effective Hamiltonian, and show that it takes the same form as the one used for decays of oscillating mesons. We then consider a particular example, chosen to have the distinctive signature of an asymmetry between pairs of positively and negatively charged muons produced from gluino decays. Similar phenomena are possible for a pseudo-Dirac neutralino. We note that order one asymmetries in like sign dilepton events are possible.

Another possibility for heavy decaying pseudo-Dirac fermions is a supersymmetric theory (not necessarily containing an approximate $U(1)_R$ symmetry or pseudo-Dirac gauginos) with squarks as the lightest superpartners, in which case the squarks may hadronize as mesinos

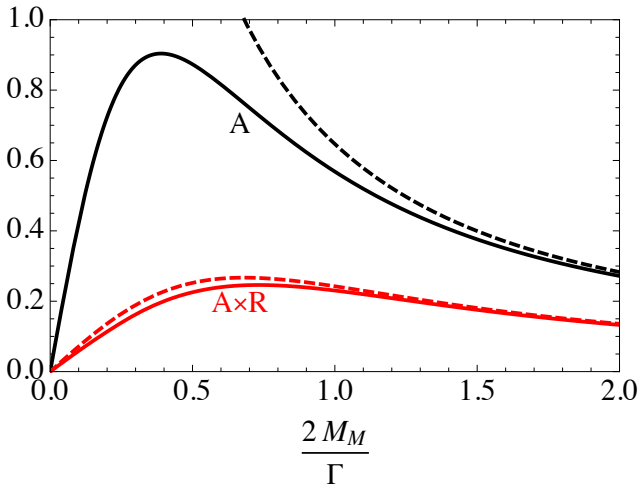


Figure 5.4: The same sign dimuon asymmetry, $A$, of pseudo Dirac gluino decays as defined in Eq. (5.64) (upper/black solid curve) and the approximate expression for $A$ in Eq. (5.71) (upper/black dashed curve) along with the product of $A$ and the ratio of same sign muon decays, $R$, defined in Eq. (5.65) (lower/red solid curve) and the product of the approximate expressions for $A$ [Eq. (5.71)] and $R$ [Eq. (5.72)] (lower/red dashed curve) as functions of $2M_M/\Gamma \simeq x = \Delta m/\Gamma$. We have taken $\Gamma = 300$ eV, $r = 0.14$, and $\phi_\Gamma = -\pi/3$.

before they decay via R-parity violation. *CP* violation from interference between oscillation and decays would be a generic feature of mesino decays as well.

Besides the unusual signature, our example was motivated by the $U(1)_R$ symmetry solution to the SUSY *CP* problem, and the potential to obtain large *CP* violation for baryogenesis which is not constrained by electric dipole moments. If the lightest particle of the MSSM (besides the gravitino) is a pseudo-Dirac fermion which decays primarily via R-parity violation, *CP* violation in the decays could produce either a baryon asymmetry or a lepton asymmetry which gets converted by anomalous weak processes into a baryon asymmetry. If such a particle could also be produced in a collider, then the *CP* violation responsible for baryogenesis could potentially be directly observed.

# Chapter 6

# WHAT IS BEYOND THE STANDARD MODEL?

The discovery of the Higgs boson at the LHC in 2012 was a milestone in completing the Standard Model of elementary particles. The SM, built over many decades, explains interactions of the known elementary particles via the strong, weak, and electromagnetic forces. However, there are many phenomena that it cannot explain. A comprehensive list of the problems of the SM was given in Section 1 preceded by a brief review of the history and the basics of the model. This thesis, compiling my doctoral work, focused on two observations that cannot be explained within the SM: **(1)** The particle nature of dark matter, and **(2)** the origin of the matter–antimatter asymmetry of the Universe.

In Chapters 2-3 I investigated two different new physics models to explain different indirect hints of dark matter–SM interactions. One such signal comes from the Galactic Center as an excess of gamma rays with $O(\text{GeV})$ energy. This can be explained with DM particles of 30 GeV mass that decay to $b$ quarks via a pseudoscalar exchange. These interactions can be generated with a two-Higgs-doublet model in the SM sector and a dark pseudoscalar that mixes with the $CP$-odd Higgs of the two-Higgs-doublet model. The implications of and constraints on this model were discussed in Chapter 2.

Another hint towards dark matter–SM interactions is a discrepancy between the number of observed satellite galaxies and that are predicted by simulations with cold, collisionless dark matter. The simulations predict that there should be thousands of small dark matter subhalos while there are only $O(20)$ observed satellite galaxies with the smallest object of mass $\sim 10^8\ M_\odot$. In Chapter 3 it is shown that if the DM interacts with neutrinos, it stays in equilibrium with the relativistic plasma till later times, $T \sim$ keV. The formation of structures with masses smaller than $10^8\ M_\odot(\text{keV}/T_d)^3$ is suppressed. We introduce a model that gives the required DM-neutrino interactions. This requires a light DM with mass $O(10\text{ MeV})$ and a heavy sterile neutrino (of mass $O(100\text{ MeV})$). Several aspects of

this model were investigated, including constraints on the sterile neutrino mixing matrix element from neutrino experiments and implications on the neutrino spectrum of a future supernova.

Another very important existential problem of the SM is that it cannot explain why there are more baryons than anti baryons in the Universe. This is due to two reasons: **(i)** There is not enough $CP$ violation and **(ii)** there is no out-of-equilibrium process in the SM. Different new physics models that can produce this asymmetry were studied in Chapters 4-5. The first approach I took was to study the two-Higgs-doublet models since they are shown to exhibit a first-order EW phase transition. In Chapter 4 $CP$-violation in the extended Higgs sector of the two-Higgs-doublet models was discussed. The amount of $CP$ violation is constrained by null results from electric dipole moment experiments. Small $CP$ violation was used to analyze the mixing of the $CP$-even and $CP$-odd neutral Higgs bosons perturbatively. A $CP$-violating phase of $10^{-2}$ is shown to be allowed by electric dipole moment measurements, which could be enough to explain the baryon asymmetry of the Universe.

Chapter 5 gives a different approach to producing this baryon asymmetry: out-of-equilibrium decays of a pseudo-Dirac gauginos. In the minimal supersymmetric SM, large electric dipole moments for the electron and the neutron can be produced. However, if the gauginos are Dirac particles with a conserved global $U(1)$ charge, this problem can be solved. This global symmetry is broken by supergravity, and the Dirac gauging acquire small Majorana masses, making them pseudo-Dirac particles. Pseudo-Dirac gauginos exhibit particle–antiparticle oscillations, much like neutral mesons. Effects of possible $CP$ violation in these oscillations is investigated in Chapter 5. One possible collider signature of $CP$ violation in pseudo-Dirac gaugino oscillations is a same-sign dilepton asymmetry. It is also shown that these decays (due to oscillations) can produce more leptons than antileptons.

It is sometimes wrongfully thought that after the Higgs boson discovery our understanding of the Universe is complete and we should stop searching for new physics. The SM does not give us a full understanding of the Universe. There are many unanswered questions that we need new physics for. I hopefully demonstrated with this work that there is plenty

of new physics scenarios that can help to explain Universe's mysteries. Fortunately we also have many experiments that are searching for new physics models. Especially with the LHC starting its second run with increased energy and luminosity we will probe new physics at a few TeV scale. It is a very exciting era as we push our theoretical and experimental boundaries ever forward in the quest for knowledge.

# BIBLIOGRAPHY


[1] C. Burgess and G. Moore, *The standard model: A primer*. Cambridge University Press, 2007.

[2] M. Srednicki, *Quantum field theory*. Cambridge University Press, 2007.

[3] S. Coleman, *Aspects of Symmetry*. Cambridge University Press, 1988.

[4] C. Baker, D. Doyle, P. Geltenbort, K. Green, M. van der Grinten, et al., *An Improved experimental limit on the electric dipole moment of the neutron*, *Phys.Rev.Lett.* **97** (2006) 131801, [hep-ex/0602020].

[5] R. Peccei and H. R. Quinn, *CP Conservation in the Presence of Instantons*, *Phys.Rev.Lett.* **38** (1977) 1440–1443.

[6] P. W. Higgs, *Broken Symmetries and the Masses of Gauge Bosons*, *Phys.Rev.Lett.* **13** (1964) 508–509.

[7] F. Englert and R. Brout, *Broken Symmetry and the Mass of Gauge Vector Mesons*, *Phys.Rev.Lett.* **13** (1964) 321–323.

[8] **CMS** Collaboration, S. Chatrchyan et al., *Observation of a new boson at a mass of 125 GeV with the CMS experiment at the LHC*, *Phys.Lett.* **B716** (2012) 30–61, [arXiv:1207.7235].

[9] **ATLAS** Collaboration, G. Aad et al., *Observation of a new particle in the search for the Standard Model Higgs boson with the ATLAS detector at the LHC*, *Phys.Lett.* **B716** (2012) 1–29, [arXiv:1207.7214].

[10] **Particle Data Group** Collaboration, K. Olive et al., *Review of Particle Physics*, *Chin.Phys.* **C38** (2014) 090001.

[11] J. Christenson, J. Cronin, V. Fitch, and R. Turlay, *Evidence for the 2 pi Decay of the k(2)0 Meson*, *Phys.Rev.Lett.* **13** (1964) 138–140.

[12] M. Kobayashi and T. Maskawa, *CP Violation in the Renormalizable Theory of Weak Interaction*, *Prog.Theor.Phys.* **49** (1973) 652–657.

[13] N. Cabibbo, *Unitary Symmetry and Leptonic Decays*, *Phys.Rev.Lett.* **10** (1963) 531–533.

[14] **CDF** Collaboration, T. Aaltonen et al., *Evidence for a Mass Dependent Forward-Backward Asymmetry in Top Quark Pair Production*, *Phys.Rev.* **D83** (2011) 112003, [arXiv:1101.0034].

[15] **D0** Collaboration, V. M. Abazov et al., *Forward-backward asymmetry in top quark-antiquark production*, *Phys.Rev.* **D84** (2011) 112005, [arXiv:1107.4995].

[16] S. Ipek, *Light Axigluon Contributions to $b\bar{b}$ and $c\bar{c}$ Asymmetry and Constraints on Flavor Changing Axigluon Currents*, *Phys.Rev.* **D87** (2013), no. 11 116010, [arXiv:1301.3990].

[17] **Planck** Collaboration, P. Ade et al., *Planck 2015 results. XIII. Cosmological parameters*, arXiv:1502.0158.

[18] F. Zwicky, *On the Masses of Nebulae and of Clusters of Nebulae*, *Astrophys.J.* **86** (1937) 217–246.

[19] **WMAP** Collaboration, D. Spergel et al., *First year Wilkinson Microwave Anisotropy Probe (WMAP) observations: Determination of cosmological parameters*, *Astrophys.J.Suppl.* **148** (2003) 175–194, [astro-ph/0302209].

[20] D. Clowe, M. Bradac, A. H. Gonzalez, M. Markevitch, S. W. Randall, et al., *A direct empirical proof of the existence of dark matter*, *Astrophys.J.* **648** (2006) L109–L113, [astro-ph/0608407].

[21] T. van Albada, J. N. Bahcall, K. Begeman, and R. Sancisi, *The Distribution of Dark Matter in the Spiral Galaxy NGC-3198*, *Astrophys.J.* **295** (1985) 305–313.

[22] D. S. Gorbunov and V. A. Rubakov, *Introduction to the theory of the early universe: Hot big bang theory*, .

[23] J. P. Kneller and G. Steigman, *BBN for pedestrians*, *New J.Phys.* **6** (2004) 117, [astro-ph/0406320].

[24] A. Sakharov, *Violation of CP Invariance, c Asymmetry, and Baryon Asymmetry of the Universe*, *Pisma Zh.Eksp.Teor.Fiz.* **5** (1967) 32–35.

[25] M. D'Onofrio, K. Rummukainen, and A. Tranberg, *Sphaleron Rate in the Minimal Standard Model*, *Phys.Rev.Lett.* **113** (2014), no. 14 141602, [arXiv:1404.3565].

[26] P. Huet and E. Sather, *Electroweak baryogenesis and standard model CP violation*, *Phys.Rev.* **D51** (1995) 379–394, [hep-ph/9404302].

[27] M. Gavela, P. Hernandez, J. Orloff, and O. Pene, *Standard model baryogenesis*, hep-ph/9407403.

[28] N. Goldenfeld, *Lectures on phase transitions and the renormalization group*, .

[29] V. Kuzmin, V. Rubakov, and M. Shaposhnikov, *On anomalous electroweak baryon-number non-conservation in the early universe*, *Physics Letters B* **155** (1985), no. 1-2 36 – 42.

[30] S. Ipek, D. McKeen, and A. E. Nelson, *A Renormalizable Model for the Galactic Center Gamma Ray Excess from Dark Matter Annihilation*, *Phys.Rev.* **D90** (2014), no. 5 055021, [arXiv:1404.3716].

[31] B. Bertoni, S. Ipek, D. McKeen, and A. E. Nelson, *Constraints and consequences of reducing small scale structure via large dark matter-neutrino interactions*, *JHEP* **1504** (2015) 170, [arXiv:1412.3113].

[32] S. Ipek, *Perturbative analysis of the electron electric dipole moment and CP violation in two-Higgs-doublet models*, *Phys.Rev.* **D89** (2014), no. 7 073012, [arXiv:1310.6790].

[33] S. Ipek, D. McKeen, and A. E. Nelson, *CP Violation in Pseudo-Dirac Fermion Oscillations*, *Phys.Rev.* **D90** (2014), no. 7 076005, [arXiv:1407.8193].

[34] J. L. Feng, *Dark matter candidates from particle physics and methods of detection*, *Ann. Rev. Astron. Astrophys.* **48** (2010) 495, [arXiv:1003.0904].

[35] **LAT Collaboration** Collaboration, M. Ackermann et al., *Fermi LAT Search for Dark Matter in Gamma-ray Lines and the Inclusive Photon Spectrum*, *Phys.Rev.* **D86** (2012) 022002, [arXiv:1205.2739].

[36] **Fermi-LAT** Collaboration, M. Ackermann et al., *Search for gamma-ray spectral lines with the Fermi large area telescope and dark matter implications*, *Phys.Rev.* **D88** (2013) 082002, [arXiv:1305.5597].

[37] **Fermi-LAT Collaboration** Collaboration, M. Ackermann et al., *Dark Matter Constraints from Observations of 25 Milky Way Satellite Galaxies with the Fermi Large Area Telescope*, *Phys.Rev.* **D89** (2014) 042001, [arXiv:1310.0828].

[38] T. Daylan, D. P. Finkbeiner, D. Hooper, T. Linden, S. K. N. Portillo, et al., *The Characterization of the Gamma-Ray Signal from the Central Milky Way: A Compelling Case for Annihilating Dark Matter*, arXiv:1402.6703.

[39] D. Hooper, I. Cholis, T. Linden, J. Siegal-Gaskins, and T. Slatyer, *Millisecond pulsars Cannot Account for the Inner Galaxy's GeV Excess*, *Phys.Rev.* **D88** (2013) 083009, [arXiv:1305.0830].

[40] D. Hooper and L. Goodenough, *Dark Matter Annihilation in The Galactic Center As Seen by the Fermi Gamma Ray Space Telescope*, *Phys.Lett.* **B697** (2011) 412–428, [arXiv:1010.2752].

[41] L. Goodenough and D. Hooper, *Possible Evidence For Dark Matter Annihilation In The Inner Milky Way From The Fermi Gamma Ray Space Telescope*, arXiv:0910.2998.

[42] D. Hooper and T. Linden, *On The Origin Of The Gamma Rays From The Galactic Center*, *Phys.Rev.* **D84** (2011) 123005, [arXiv:1110.0006].

[43] K. N. Abazajian and M. Kaplinghat, *Detection of a Gamma-Ray Source in the Galactic Center Consistent with Extended Emission from Dark Matter Annihilation and Concentrated Astrophysical Emission*, *Phys.Rev.* **D86** (2012) 083511, [arXiv:1207.6047].

[44] C. Gordon and O. Macias, *Dark Matter and Pulsar Model Constraints from Galactic Center Fermi-LAT Gamma Ray Observations*, *Phys.Rev.* **D88** (2013) 083521, [arXiv:1306.5725].

[45] K. N. Abazajian, N. Canac, S. Horiuchi, and M. Kaplinghat, *Astrophysical and Dark Matter Interpretations of Extended Gamma Ray Emission from the Galactic Center*, arXiv:1402.4090.

[46] D. Hooper and T. R. Slatyer, *Two Emission Mechanisms in the Fermi Bubbles: A Possible Signal of Annihilating Dark Matter*, *Phys.Dark Univ.* **2** (2013) 118–138, [arXiv:1302.6589].

[47] W.-C. Huang, A. Urbano, and W. Xue, *Fermi Bubbles under Dark Matter Scrutiny. Part I: Astrophysical Analysis*, arXiv:1307.6862.

[48] V. Barger, Y. Gao, M. McCaskey, and G. Shaughnessy, *Light Higgs Boson, Light Dark Matter and Gamma Rays*, *Phys. Rev.* **D82** (2010) 095011, [arXiv:1008.1796].

[49] E. Hardy, R. Lasenby, and J. Unwin, *Annihilation Signals from Asymmetric Dark Matter*, *JHEP* **07** (2014) 049, [arXiv:1402.4500].

[50] K. P. Modak, D. Majumdar, and S. Rakshit, *A Possible Explanation of Low Energy $\gamma$-ray Excess from Galactic Centre and Fermi Bubble by a Dark Matter Model with Two Real Scalars*, *JCAP* **1503** (2015) 011, [arXiv:1312.7488].

[51] G. Marshall and R. Primulando, *The Galactic Center Region Gamma Ray Excess*

*from A Supersymmetric Leptophilic Higgs Model*, *JHEP* **05** (2011) 026, [arXiv:1102.0492].

[52] M. R. Buckley, D. Hooper, and J. L. Rosner, *A Leptophobic Z' And Dark Matter From Grand Unification*, *Phys. Lett.* **B703** (2011) 343–347, [arXiv:1106.3583].

[53] T. Lacroix, C. Boehm, and J. Silk, *Fitting the Fermi-LAT GeV excess: On the importance of including the propagation of electrons from dark matter*, *Phys. Rev.* **D90** (2014), no. 4 043508, [arXiv:1403.1987].

[54] A. Berlin, D. Hooper, and S. D. McDermott, *Simplified Dark Matter Models for the Galactic Center Gamma-Ray Excess*, arXiv:1404.0022.

[55] P. Agrawal, B. Batell, D. Hooper, and T. Lin, *Flavored Dark Matter and the Galactic Center Gamma-Ray Excess*, *Phys. Rev.* **D90** (2014), no. 6 063512, [arXiv:1404.1373].

[56] **LUX Collaboration** Collaboration, D. Akerib et al., *First results from the LUX dark matter experiment at the Sanford Underground Research Facility*, arXiv:1310.8214.

[57] C. Boehm, M. J. Dolan, C. McCabe, M. Spannowsky, and C. J. Wallace, *Extended gamma-ray emission from Coy Dark Matter*, arXiv:1401.6458.

[58] A. Alves, S. Profumo, F. S. Queiroz, and W. Shepherd, *The Effective Hooperon*, arXiv:1403.5027.

[59] C. P. Burgess, M. Pospelov, and T. ter Veldhuis, *The Minimal model of nonbaryonic dark matter: A Singlet scalar*, *Nucl. Phys.* **B619** (2001) 709–728, [hep-ph/0011335].

[60] M. J. Strassler and K. M. Zurek, *Echoes of a hidden valley at hadron colliders*, *Phys. Lett.* **B651** (2007) 374–379, [hep-ph/0604261].

[61] B. Patt and F. Wilczek, *Higgs-field portal into hidden sectors*, hep-ph/0605188.

[62] M. J. Strassler and K. M. Zurek, *Discovering the Higgs through highly-displaced vertices*, *Phys. Lett.* **B661** (2008) 263–267, [hep-ph/0605193].

[63] M. Pospelov and A. Ritz, *Higgs decays to dark matter: beyond the minimal model*, *Phys. Rev.* **D84** (2011) 113001, [arXiv:1109.4872].

[64] Y. Bai, V. Barger, L. L. Everett, and G. Shaughnessy, *Two-Higgs-doublet-portal dark-matter model: LHC data and Fermi-LAT 135 GeV line*, *Phys.Rev.* **D88** (2013) 015008, [arXiv:1212.5604].

[65] D. G. E. Walker, *Unitarity Constraints on Higgs Portals*, arXiv:1310.1083.

[66] D. McKeen, M. Pospelov, and A. Ritz, *Modified Higgs branching ratios versus CP and lepton flavor violation*, *Phys.Rev.* **D86** (2012) 113004, [arXiv:1208.4597].

[67] CMS Collaboration Public Note *CMS-PAS-HIG-13-021,* (2013). http://cds.cern.ch/record/1623367/files/HIG-13-021-pas.pdf.

[68] J. R. Ellis, A. Ferstl, and K. A. Olive, *Reevaluation of the elastic scattering of supersymmetric dark matter*, *Phys.Lett.* **B481** (2000) 304–314, [hep-ph/0001005].

[69] D. Malling, D. Akerib, H. Araujo, X. Bai, S. Bedikian, et al., *After LUX: The LZ Program*, arXiv:1110.0103.

[70] D. Curtin, R. Essig, S. Gori, P. Jaiswal, A. Katz, et al., *Exotic Decays of the 125 GeV Higgs Boson*, arXiv:1312.4992.

[71] **CMS Collaboration** Collaboration, S. Chatrchyan et al., *Search for the standard model Higgs boson produced in association with a W or a Z boson and decaying to bottom quarks*, *Phys.Rev.* **D89** (2014) 012003, [arXiv:1310.3687].

[72] P. P. Giardino, K. Kannike, I. Masina, M. Raidal, and A. Strumia, *The universal Higgs fit*, arXiv:1303.3570.

[73] W. Skiba and J. Kalinowski, *$B_s \to \tau^+\tau^-$ decay in a two Higgs doublet model*, *Nucl.Phys.* **B404** (1993) 3–19.

[74] **LHCb Collaboration** Collaboration, R. Aaij et al., *First Evidence for the Decay $B_s^0 \to \mu^+\mu^-$*, *Phys.Rev.Lett.* **110** (2013) 021801, [arXiv:1211.2674].

[75] **CMS** Collaboration, S. Chatrchyan et al., *Measurement of the B(s) to mu+ mu- branching fraction and search for B0 to mu+ mu- with the CMS Experiment*, *Phys.Rev.Lett.* **111** (2013) 101804, [arXiv:1307.5025].

[76] **LHCb, CMS** Collaboration, CMS and L. Collaborations, *Combination of results on the rare decays $B^0$_(s) $\to \mu^+\mu^-$ from the CMS and LHCb experiments*, .

[77] C. Bobeth, M. Gorbahn, T. Hermann, M. Misiak, E. Stamou, and M. Steinhauser, *B_s,d -¿ l+ l- in the Standard Model with Reduced Theoretical Uncertainty*, *Phys. Rev. Lett.* **112** (2014) 101801, [arXiv:1311.0903].

[78] A. J. Buras, R. Fleischer, J. Girrbach, and R. Knegjens, *Probing New Physics with the $B_s \to \mu^+\mu^-$ Time-Dependent Rate*, *JHEP* **1307** (2013) 77, [arXiv:1303.3820].

[79] M. Beltran, D. Hooper, E. W. Kolb, Z. A. Krusberg, and T. M. Tait, *Maverick dark matter at colliders*, *JHEP* **1009** (2010) 037, [arXiv:1002.4137].

[80] J. Goodman, M. Ibe, A. Rajaraman, W. Shepherd, T. M. Tait, et al., *Constraints on Dark Matter from Colliders*, *Phys.Rev.* **D82** (2010) 116010, [arXiv:1008.1783].

[81] A. Rajaraman, W. Shepherd, T. M. Tait, and A. M. Wijangco, *LHC Bounds on Interactions of Dark Matter*, *Phys.Rev.* **D84** (2011) 095013, [arXiv:1108.1196].

[82] P. J. Fox, R. Harnik, J. Kopp, and Y. Tsai, *Missing Energy Signatures of Dark Matter at the LHC*, *Phys.Rev.* **D85** (2012) 056011, [arXiv:1109.4398].

[83] I. M. Shoemaker and L. Vecchi, *Unitarity and Monojet Bounds on Models for DAMA, CoGeNT, and CRESST-II*, *Phys.Rev.* **D86** (2012) 015023, [arXiv:1112.5457].

[84] P. J. Fox, R. Harnik, R. Primulando, and C.-T. Yu, *Taking a Razor to Dark Matter Parameter Space at the LHC*, *Phys.Rev.* **D86** (2012) 015010, [arXiv:1203.1662].

[85] **CMS Collaboration** Collaboration, S. Chatrchyan et al., *Search for dark matter and large extra dimensions in monojet events in pp collisions at $\sqrt{s} = 7$ TeV*, *JHEP* **1209** (2012) 094, [arXiv:1206.5663].

[86] **ATLAS Collaboration** Collaboration, G. Aad et al., *Search for dark matter candidates and large extra dimensions in events with a jet and missing transverse momentum with the ATLAS detector*, *JHEP* **1304** (2013) 075, [arXiv:1210.4491].

[87] T. Lin, E. W. Kolb, and L.-T. Wang, *Probing dark matter couplings to top and bottom at the LHC*, *Phys.Rev.* **D88** (2013) 063510, [arXiv:1303.6638].

[88] J. Alwall, M. Herquet, F. Maltoni, O. Mattelaer, and T. Stelzer, *MadGraph 5 : Going Beyond*, *JHEP* **1106** (2011) 128, [arXiv:1106.0522].

[89] T. Sjostrand, S. Mrenna, and P. Z. Skands, *PYTHIA 6.4 Physics and Manual*, *JHEP* **0605** (2006) 026, [hep-ph/0603175].

[90] S. Ovyn, X. Rouby, and V. Lemaitre, *DELPHES, a framework for fast simulation of a generic collider experiment*, arXiv:0903.2225.

[91] B. Moore, S. Ghigna, F. Governato, G. Lake, T. R. Quinn, et al., *Dark matter substructure within galactic halos*, *Astrophys. J.* **524** (1999) L19–L22, [astro-ph/9907411].

[92] G. Kauffmann, S. D. White, and B. Guiderdoni, *The Formation and Evolution of Galaxies Within Merging Dark Matter Haloes*, *Mon. Not. Roy. Astron. Soc.* **264** (1993) 201.

[93] B. Moore, *Evidence against dissipationless dark matter from observations of galaxy haloes*, *Nature* **370** (1994) 629.

[94] R. A. Flores and J. R. Primack, *Observational and theoretical constraints on singular dark matter halos*, *Astrophys. J.* **427** (1994) L1–4, [astro-ph/9402004].

[95] A. A. Klypin, A. V. Kravtsov, O. Valenzuela, and F. Prada, *Where are the missing Galactic satellites?*, *Astrophys. J.* **522** (1999) 82–92, [astro-ph/9901240].

[96] M. Boylan-Kolchin, J. S. Bullock, and M. Kaplinghat, *Too big to fail? The puzzling darkness of massive Milky Way subhaloes*, *Mon. Not. Roy. Astron. Soc.* **415** (2011) L40, [arXiv:1103.0007].

[97] M. G. Walker, *Dark Matter in the Milky Way's Dwarf Spheroidal Satellites*, arXiv:1205.0311.

[98] D. H. Weinberg, J. S. Bullock, F. Governato, R. K. de Naray, and A. H. G. Peter, *Cold dark matter: controversies on small scales*, arXiv:1306.0913.

[99] A. Brooks, *Re-Examining Astrophysical Constraints on the Dark Matter Model*, *Annalen Phys.* **526** (2014), no. 7-8 294–308, [arXiv:1407.7544].

[100] J. S. Bullock, *Notes on the Missing Satellites Problem*, *ArXiv e-prints* (Sept., 2010) [arXiv:1009.4505].

[101] A. S. Font, A. J. Benson, R. G. Bower, C. F. Frenk, A. P. Cooper, et al., *The population of Milky Way satellites in the $\Lambda$CDM cosmology*, *Mon. Not. Roy. Astron. Soc.* **417** (2011) 1260, [arXiv:1103.0024].

[102] S. Dodelson and L. M. Widrow, *Sterile neutrinos as dark matter*, *Phys. Rev. Lett.* **72** (1994) 17–20, [hep-ph/9303287].

[103] S. Colombi, S. Dodelson, and L. M. Widrow, *Large scale structure tests of warm dark matter*, *Astrophys. J.* **458** (1996) 1, [astro-ph/9505029].

[104] D. N. Spergel and P. J. Steinhardt, *Observational evidence for selfinteracting cold dark matter*, *Phys. Rev. Lett.* **84** (2000) 3760–3763, [astro-ph/9909386].

[105] S. Tulin, H.-B. Yu, and K. M. Zurek, *Resonant Dark Forces and Small Scale Structure*, *Phys. Rev. Lett.* **110** (2013), no. 11 111301, [arXiv:1210.0900].

[106] S. Tulin, H.-B. Yu, and K. M. Zurek, *Beyond Collisionless Dark Matter: Particle Physics Dynamics for Dark Matter Halo Structure*, *Phys. Rev. D* **87** (2013), no. 11 115007, [arXiv:1302.3898].

[107] M. Kaplinghat, S. Tulin, and H.-B. Yu, *Self-interacting Dark Matter Benchmarks*, arXiv:1308.0618.

[108] L. G. van den Aarssen, T. Bringmann, and C. Pfrommer, *Is dark matter with long-range interactions a solution to all small-scale problems of ΛCDM cosmology?*, *Phys. Rev. Lett.* **109** (2012) 231301, [arXiv:1205.5809].

[109] I. M. Shoemaker, *Constraints on Dark Matter Protohalos in Effective Theories and Neutrinophilic Dark Matter*, *Phys. Dark Univ.* **2** (2013) 157–162, [arXiv:1305.1936].

[110] T. Bringmann, J. Hasenkamp, and J. Kersten, *Tight bonds between sterile neutrinos and dark matter*, *JCAP* **1407** (2014) 042, [arXiv:1312.4947].

[111] P. Ko and Y. Tang, *νΛMDM: A Model for Sterile Neutrino and Dark Matter Reconciles Cosmological and Neutrino Oscillation Data after BICEP2*, *Phys. Lett. B* **739** (2014) 62–67, [arXiv:1404.0236].

[112] M. Archidiacono, S. Hannestad, R. S. Hansen, and T. Tram, *Cosmology with self-interacting sterile neutrinos and dark matter - A pseudoscalar model*, arXiv:1404.5915.

[113] J. F. Cherry, A. Friedland, and I. M. Shoemaker, *Neutrino Portal Dark Matter: From Dwarf Galaxies to IceCube*, arXiv:1411.1071.

[114] A. M. Green, S. Hofmann, and D. J. Schwarz, *The First wimpy halos*, *JCAP* **0508** (2005) 003, [astro-ph/0503387].

[115] A. Loeb and M. Zaldarriaga, *The Small-scale power spectrum of cold dark matter*, *Phys. Rev. D* **71** (2005) 103520, [astro-ph/0504112].

[116] T. Bringmann, *Particle Models and the Small-Scale Structure of Dark Matter*, *New J. Phys.* **11** (2009) 105027, [arXiv:0903.0189].

[117] L. E. Strigari, J. S. Bullock, M. Kaplinghat, J. D. Simon, M. Geha, et al., *A common mass scale for satellite galaxies of the Milky Way*, *Nature* **454** (2008) 1096–1097, [arXiv:0808.3772].

[118] M. Viel, G. D. Becker, J. S. Bolton, and M. G. Haehnelt, *Warm dark matter as a solution to the small scale crisis: New constraints from high redshift Lyman-$\alpha$ forest data*, *Phys. Rev. D* **88** (2013) 043502, [arXiv:1306.2314].

[119] S. Vegetti, D. Lagattuta, J. McKean, M. Auger, C. Fassnacht, et al., *Gravitational detection of a low-mass dark satellite at cosmological distance*, arXiv:1201.3643.

[120] S. Vegetti, L. Koopmans, M. Auger, T. Treu, and A. Bolton, *Inference of the Cold Dark Matter substructure mass function at z=0.2 using strong gravitational lenses*, arXiv:1405.3666.

[121] J. F. Navarro, C. S. Frenk, and S. D. White, *A Universal density profile from hierarchical clustering*, *Astrophys. J.* **490** (1997) 493–508, [astro-ph/9611107].

[122] S.-H. Oh, W. de Blok, E. Brinks, F. Walter, and J. Kennicutt, Robert C., *Dark and luminous matter in THINGS dwarf galaxies*, *Astron. J.* **141** (2011) 193, [arXiv:1011.0899].

[123] **Planck** Collaboration, P. Ade et al., *Planck 2013 results. XVI. Cosmological parameters*, *Astron. Astrophys.* (2014) [arXiv:1303.5076].

[124] F. Iocco, G. Mangano, G. Miele, O. Pisanti, and P. D. Serpico, *Primordial Nucleosynthesis: from precision cosmology to fundamental physics*, *Phys. Rept.* **472** (2009) 1–76, [arXiv:0809.0631].

[125] P. D. Serpico and G. G. Raffelt, *MeV-mass dark matter and primordial nucleosynthesis*, *Phys. Rev. D* **70** (2004) 043526, [astro-ph/0403417].

[126] R. J. Wilkinson, C. Boehm, and J. Lesgourgues, *Constraining Dark Matter-Neutrino Interactions using the CMB and Large-Scale Structure*, *JCAP* **1405** (2014) 011, [arXiv:1401.7597].

[127] C. Boehm, M. J. Dolan, and C. McCabe, *A Lower Bound on the Mass of Cold Thermal Dark Matter from Planck*, *JCAP* **1308** (2013) 041, [arXiv:1303.6270].

[128] K. M. Nollett and G. Steigman, *BBN And The CMB Constrain Neutrino Coupled Light WIMPs*, arXiv:1411.6005.

[129] D. Britton, S. Ahmad, D. Bryman, R. Burnham, E. Clifford, et al., *Improved search for massive neutrinos in $\pi^+ \to e^+\nu$ decay*, *Phys. Rev. D* **46** (1992) 885–887.

[130] **PIENU** Collaboration, M. Aoki et al., *Search for Massive Neutrinos in the Decay $\pi \to e\nu$*, *Phys. Rev. D* **84** (2011) 052002, [arXiv:1106.4055].

[131] D. Britton, S. Ahmad, D. Bryman, R. Burnbam, E. Clifford, et al., *Measurement of the $\pi^+ \to e^+\nu$ branching ratio*, *Phys. Rev. Lett.* **68** (1992) 3000–3003.

[132] G. Czapek, A. Federspiel, A. Fluckiger, D. Frei, B. Hahn, et al., *Branching ratio for the rare pion decay into positron and neutrino*, *Phys. Rev. Lett.* **70** (1993) 17–20.

[133] W. J. Marciano and A. Sirlin, *Radiative corrections to $\pi_{\ell 2}$ decays*, *Phys. Rev. Lett.* **71** (1993) 3629–3632.

[134] **MuLan Collaboration** Collaboration, V. Tishchenko et al., *Detailed Report of the MuLan Measurement of the Positive Muon Lifetime and Determination of the Fermi Constant*, *Phys. Rev. D* **87** (2013), no. 5 052003, [arXiv:1211.0960].

[135] R. Abela, M. Daum, G. Eaton, R. Frosch, B. Jost, et al., *Search for an Admixture of Heavy Neutrino in Pion Decay*, *Phys. Lett. B* **105** (1981) 263–266.

[136] R. Hayano, T. Taniguchi, T. Yamanaka, T. Tanimori, R. Enomoto, et al., *Heavy-Neutrino Search Using $K_{\mu 2}$ Decay* , *Phys. Rev. Lett.* **49** (1982) 1305.

[137] A. Artamonov, B. Bassalleck, B. Bhuyan, E. Blackmore, D. Bryman, et al., *Search for heavy neutrinos in $K^+ \to \mu^+\nu_H$ decays*, arXiv:1411.3963.

[138] **TWIST** Collaboration, R. Bayes et al., *New Experimental Constraints for the Standard Model from Muon Decay*, arXiv:1010.4998.

[139] S. N. Gninenko, *A resolution of puzzles from the LSND, KARMEN, and MiniBooNE experiments*, *Phys. Rev. D* **83** (2011) 015015, [arXiv:1009.5536].

[140] **ALEPH** Collaboration, R. Barate et al., *An Upper limit on the tau-neutrino mass from three-prong and five-prong tau decays*, *Eur. Phys. J. C* **2** (1998) 395–406.

[141] **Belle** Collaboration, K. Belous et al., *Measurement of the $\tau$-lepton lifetime at Belle*, *Phys. Rev. Lett.* **112** (2014), no. 3 031801, [arXiv:1310.8503].

[142] A. Pich, *Precision Tau Physics*, *Prog. Part. Nucl. Phys.* **75** (2014) 41–85, [arXiv:1310.7922].

[143] J. C. Helo, S. Kovalenko, and I. Schmidt, *On sterile neutrino mixing with $\nu_\tau$*, *Phys. Rev. D* **84** (2011) 053008, [arXiv:1105.3019].

[144] M. Gonzalez-Garcia, M. Maltoni, and T. Schwetz, *Updated fit to three neutrino mixing: status of leptonic CP violation*, arXiv:1409.5439.

[145] L. Wolfenstein, *Neutrino Oscillations in Matter*, *Phys. Rev. D* **17** (1978) 2369–2374.

[146] S. Mikheev and A. Y. Smirnov, *Resonance Amplification of Oscillations in Matter and Spectroscopy of Solar Neutrinos*, *Sov. J. Nucl. Phys.* **42** (1985) 913–917.

[147] B. Pontecorvo, *Neutrino Experiments and the Problem of Conservation of Leptonic Charge*, *Sov. Phys. JETP* **26** (1968) 984–988.

[148] **Daya Bay** Collaboration, F. An et al., *Spectral measurement of electron antineutrino oscillation amplitude and frequency at Daya Bay*, *Phys. Rev. Lett.* **112** (2014) 061801, [arXiv:1310.6732].

[149] R. J. Wilkes, *New results from super-k and k2k*, *ECONF* **C020805** (2002) TTH02, [hep-ex/0212035].

[150] **MINOS** Collaboration, P. Adamson et al., *Measurement of the neutrino mass splitting and flavor mixing by MINOS*, *Phys. Rev. Lett.* **106** (2011) 181801, [arXiv:1103.0340].

[151] **KamLAND** Collaboration, K. Eguchi et al., *First results from kamland: Evidence for reactor anti- neutrino disappearance*, *Phys. Rev. Lett.* **90** (2003) 021802, [hep-ex/0212021].

[152] **SNO** Collaboration, B. Aharmim et al., *Combined Analysis of all Three Phases of Solar Neutrino Data from the Sudbury Neutrino Observatory*, *Phys. Rev. C* **88** (2013) 025501, [arXiv:1109.0763].

[153] **Borexino** Collaboration, G. Bellini et al., *Measurement of the solar 8B neutrino rate with a liquid scintillator target and 3 MeV energy threshold in the Borexino detector*, *Phys. Rev. D* **82** (2010) 033006, [arXiv:0808.2868].

[154] **Borexino** Collaboration, D. D'Angelo et al., *Recent Borexino results and prospects for the near future*, arXiv:1405.7919.

[155] A. M. Serenelli, W. Haxton, and C. Pena-Garay, *Solar models with accretion. I. Application to the solar abundance problem*, *Astrophys. J.* **743** (2011) 24, [arXiv:1104.1639].

[156] S. Dev and S. Kumar, *Constraints on weakly mixed sterile neutrinos in the light of SNO salt phase and 766.3 Ty KamLAND data*, *Mod. Phys. Lett. A* **20** (2005) 2957–2968, [hep-ph/0504237].

[157] M. Cirelli, G. Marandella, A. Strumia, and F. Vissani, *Probing oscillations into sterile neutrinos with cosmology, astrophysics and experiments*, *Nucl. Phys. B* **708** (2005) 215–267, [hep-ph/0403158].

[158] **Super-Kamiokande** Collaboration, K. Abe et al., *Limits on Sterile Neutrino Mixing using Atmospheric Neutrinos in Super-Kamiokande*, arXiv:1410.2008.

[159] A. Esmaili and A. Y. Smirnov, *Probing Non-Standard Interaction of Neutrinos with IceCube and DeepCore*, *JHEP* **1306** (2013) 026, [arXiv:1304.1042].

[160] E. Akhmedov, A. Kartavtsev, M. Lindner, L. Michaels, and J. Smirnov, *Improving Electro-Weak Fits with TeV-scale Sterile Neutrinos*, *JHEP* **1305** (2013) 081, [arXiv:1302.1872].

[161] S. Schael et al., *Precision electroweak measurements on the Z resonance*, *Phys. Rept.* **427** (2006) 257–454, [hep-ex/0509008].

[162] J. Orloff, A. N. Rozanov, and C. Santoni, *Limits on the mixing of tau neutrino to heavy neutrinos*, *Phys. Lett. B* **550** (2002) 8–15, [hep-ph/0208075].

[163] **NOMAD** Collaboration, P. Astier et al., *Search for heavy neutrinos mixing with tau neutrinos*, *Phys. Lett. B* **506** (2001) 27–38, [hep-ex/0101041].

[164] **DELPHI** Collaboration, P. Abreu et al., *Search for neutral heavy leptons produced in Z decays*, *Z. Phys. C* **74** (1997) 57–71.

[165] B. Batell, M. Pospelov, and A. Ritz, *Exploring Portals to a Hidden Sector Through Fixed Targets*, *Phys. Rev. D* **80** (2009) 095024, [arXiv:0906.5614].

[166] P. deNiverville, M. Pospelov, and A. Ritz, *Observing a light dark matter beam with neutrino experiments*, *Phys. Rev. D* **84** (2011) 075020, [arXiv:1107.4580].

[167] P. deNiverville, D. McKeen, and A. Ritz, *Signatures of sub-GeV dark matter beams at neutrino experiments*, *Phys. Rev. D* **86** (2012) 035022, [arXiv:1205.3499].

[168] B. Batell, P. deNiverville, D. McKeen, M. Pospelov, and A. Ritz, *Leptophobic Dark Matter at Neutrino Factories*, arXiv:1405.7049.

[169] D. Hooper, M. Kaplinghat, L. E. Strigari, and K. M. Zurek, *MeV Dark Matter and Small Scale Structure*, *Phys. Rev. D* **76** (2007) 103515, [arXiv:0704.2558].

[170] P. Gondolo, J. Hisano, and K. Kadota, *The Effect of quark interactions on dark matter kinetic decoupling and the mass of the smallest dark halos*, *Phys. Rev. D* **86** (2012) 083523, [arXiv:1205.1914].

[171] T. Bringmann and S. Hofmann, *Thermal decoupling of WIMPs from first principles*, *JCAP* **0407** (2007) 016, [hep-ph/0612238].

[172] C. Boehm, J. Schewtschenko, R. Wilkinson, C. Baugh, and S. Pascoli, *Using the Milky Way satellites to study interactions between cold dark matter and radiation*, *Mon. Not. Roy. Astron. Soc.* **445** (2014) L31–L35, [arXiv:1404.7012].

[173] M. R. Buckley, J. Zavala, F.-Y. Cyr-Racine, K. Sigurdson, and M. Vogelsberger, *Scattering, Damping, and Acoustic Oscillations: Simulating the Structure of Dark Matter Halos with Relativistic Force Carriers*, *Phys. Rev. D* **90** (2014) 043524, [arXiv:1405.2075].

[174] H.-T. Janka, K. Langanke, A. Marek, G. Martinez-Pinedo, and B. Mueller, *Theory of Core-Collapse Supernovae*, *Phys. Rept.* **442** (2007) 38–74, [astro-ph/0612072].

[175] H.-T. Janka, *Explosion Mechanisms of Core-Collapse Supernovae*, *Ann. Rev. Nucl. Part. Sci.* **62** (2012) 407–451, [arXiv:1206.2503].

[176] D. A. Dicus, S. Nussinov, P. B. Pal, and V. L. Teplitz, *Implications of Relativistic Gas Dynamics for Neutrino-neutrino Cross-sections*, *Phys. Lett. B* **218** (1989) 84.

[177] P. Fayet, D. Hooper, and G. Sigl, *Constraints on light dark matter from core-collapse supernovae*, *Phys. Rev. Lett.* **96** (2006) 211302, [hep-ph/0602169].

[178] B. Bertoni, D. McKeen, A. E. Nelson, and S. Reddy, *in preparation*, .

[179] G. Mangano, A. Melchiorri, P. Serra, A. Cooray, and M. Kamionkowski, *Cosmological bounds on dark matter-neutrino interactions*, *Phys. Rev. D* **74** (2006) 043517, [astro-ph/0606190].

[180] Y. Farzan and S. Palomares-Ruiz, *Dips in the Diffuse Supernova Neutrino Background*, *JCAP* **1406** (2014) 014, [arXiv:1401.7019].

[181] K. Blum, A. Hook, and K. Murase, *High energy neutrino telescopes as a probe of the neutrino mass mechanism*, arXiv:1408.3799.

[182] F. Governato, C. Brook, L. Mayer, A. Brooks, G. Rhee, et al., *At the heart of the matter: the origin of bulgeless dwarf galaxies and Dark Matter cores*, *Nature* **463** (2010) 203–206, [arXiv:0911.2237].

[183] F. Governato, A. Zolotov, A. Pontzen, C. Christensen, S. Oh, et al., *Cuspy No More: How Outflows Affect the Central Dark Matter and Baryon Distribution in Lambda*

*CDM Galaxies*, *Mon. Not. Roy. Astron. Soc.* **422** (2012) 1231–1240, [arXiv:1202.0554].

[184] R. Teyssier, A. Pontzen, Y. Dubois, and J. Read, *Cusp-core transformations in dwarf galaxies: observational predictions*, arXiv:1206.4895.

[185] A. Zolotov, A. M. Brooks, B. Willman, F. Governato, A. Pontzen, et al., *Baryons Matter: Why Luminous Satellite Galaxies Have Reduced Central Masses*, *Astrophys. J.* **761** (2012) 71, [arXiv:1207.0007].

[186] P. Madau, S. Shen, and F. Governato, *Dark Matter Heating and Early Core Formation in Dwarf Galaxies*, *Astrophys. J.* **789** (2014) L17, [arXiv:1405.2577].

[187] A. Pontzen and F. Governato, *How supernova feedback turns dark matter cusps into cores*, *Mon. Not. Roy. Astron. Soc.* **421** (2012) 3464, [arXiv:1106.0499].

[188] J. Penarrubia, A. Pontzen, M. G. Walker, and S. E. Koposov, *The coupling between the core/cusp and missing satellite problems*, *Astrophys. J.* **759** (2012) L42, [arXiv:1207.2772].

[189] G. Ogiya and A. Burkert, *Re-examining the Too-Big-To-Fail Problem for Dark Matter Haloes with Central Density Cores*, *ArXiv e-prints* (Aug., 2014) [arXiv:1408.6444].

[190] M. Boylan-Kolchin, J. S. Bullock, and M. Kaplinghat, *The Milky Way's bright satellites as an apparent failure of LCDM*, *Mon. Not. Roy. Astron. Soc.* **422** (2012) 1203–1218, [arXiv:1111.2048].

[191] S. Garrison-Kimmel, M. Rocha, M. Boylan-Kolchin, J. Bullock, and J. Lally, *Can Feedback Solve the Too Big to Fail Problem?*, arXiv:1301.3137.

[192] I. M. Nugent, *Determination of $|V_{us}|$ from $\tau$ Decays*, arXiv:1301.0637.

[193] S. Choubey and T. Ohlsson, *Bounds on Non-Standard Neutrino Interactions Using PINGU*, *Phys. Lett. B* **739** (2014) 357–364, [arXiv:1410.0410].

[194] R. Alonso, S. Antusch, M. Blennow, P. Coloma, A. de Gouvea, et al., *Summary report of MINSIS workshop in Madrid*, arXiv:1009.0476.

[195] A. E. Nelson and S. Barr, *Upper bound on baryogenesis scale from neutrino masses*, *Physics Letters B* **246** (Aug., 1990) 141–143.

[196] C. Jarlskog, *Commutator of the quark mass matrices in the standard electroweak model and a measure of maximal CP nonconservation*, *Physical Review Letters* **55** (Sept., 1985) 1039–1042.

[197] A. I. Bochkarev, S. V. Kuzmin, and M. E. Shaposhnikov, *Model dependence of the cosmological upper bound on the higgs-boson mass*, *Physical Review D* **43** (Jan., 1991) 369–374.

[198] G. Dorsch, S. Huber, and J. No, *A strong electroweak phase transition in the 2HDM after LHC8*, *JHEP* **1310** (2013) 029, [arXiv:1305.6610].

[199] J. Shu and Y. Zhang, *Impact of a CP violating higgs: from LHC to baryogenesis*, arXiv:1304.0773.

[200] A. Pich and P. Tuzon, *Yukawa Alignment in the Two-Higgs-Doublet Model*, *Phys. Rev.* **D80** (2009) 091702, [arXiv:0908.1554].

[201] G. Branco, P. Ferreira, L. Lavoura, M. Rebelo, M. Sher, et al., *Theory and phenomenology of two-Higgs-doublet models*, *Phys.Rept.* **516** (2012) 1–102, [arXiv:1106.0034].

[202] J. F. Gunion, H. E. Haber, G. L. Kane, and S. Dawson, *The Higgs Hunter's Guide*, *Front. Phys.* **80** (2000) 1–448.

[203] C.-Y. Chen, S. Dawson, and M. Sher, *Heavy Higgs Searches and Constraints on Two Higgs Doublet Models*, *Phys.Rev.* **D88** (2013) 015018, [arXiv:1305.1624].

[204] M. Pospelov and A. Ritz, *Electric dipole moments as probes of new physics*, *Annals of Physics* **318** (July, 2005) 119–169.

[205] M. Jung and A. Pich, *Electric dipole moments in two-higgs-doublet models*, arXiv:1308.6283.

[206] **ACME** Collaboration, J. Baron et al., *Order of Magnitude Smaller Limit on the Electric Dipole Moment of the Electron*, *Science* **343** (2014) 269–272, [arXiv:1310.7534].

[207] T. Fukuyama, *Searching for new physics beyond the standard model in electric dipole moment*, arXiv:1201.4252.

[208] S. M. Barr and A. Zee, *Electric dipole moment of the electron and of the neutron*, *Physical Review Letters* **65** (July, 1990) 21–24.

[209] S. M. Barr and A. Zee, *Erratum: Electric dipole moment of the electron and of the neutron*, *Physical Review Letters* **65** (Dec., 1990) 2920–2920.

[210] T. Hermann, M. Misiak, and M. Steinhauser, *$\bar{B}\to x_s \gamma$ in the two higgs doublet model up to next-to-next-to-leading order in QCD*, arXiv:1208.2788. JHEP 1211 (2012) 036.

[211] V. Kuzmin, V. Rubakov, and M. Shaposhnikov, *On the Anomalous Electroweak Baryon Number Nonconservation in the Early Universe*, *Phys. Lett. B* **155** (1985) 36.

[212] M. Gavela, P. Hernandez, J. Orloff, O. Pene, and C. Quimbay, *Standard model CP violation and baryon asymmetry. Part 2: Finite temperature*, *Nucl. Phys. B* **430** (1994) 382–426, [hep-ph/9406289].

[213] M. Pospelov and A. Ritz, *Electric dipole moments as probes of new physics*, *Annals Phys.* **318** (2005) 119–169, [hep-ph/0504231].

[214] V. Cirigliano, S. Profumo, and M. J. Ramsey-Musolf, *Baryogenesis, Electric Dipole Moments and Dark Matter in the MSSM*, *JHEP* **0607** (2006) 002, [hep-ph/0603246].

[215] L. Fromme, S. J. Huber, and M. Seniuch, *Baryogenesis in the two-Higgs doublet model*, *JHEP* **0611** (2006) 038, [hep-ph/0605242].

[216] D. E. Morrissey and M. J. Ramsey-Musolf, *Electroweak baryogenesis*, *New J. Phys.* **14** (2012) 125003, [arXiv:1206.2942].

[217] D. McKeen, M. Pospelov, and A. Ritz, *Electric dipole moment signatures of PeV-scale superpartners*, *Phys. Rev. D* **87** (2013), no. 11 113002, [arXiv:1303.1172].

[218] J. R. Ellis, J. S. Lee, and A. Pilaftsis, *Electric Dipole Moments in the MSSM Reloaded*, *JHEP* **0810** (2008) 049, [arXiv:0808.1819].

[219] W. Griffith, M. Swallows, T. Loftus, M. Romalis, B. Heckel, et al., *Improved Limit on the Permanent Electric Dipole Moment of Hg-199*, *Phys. Rev. Lett.* **102** (2009) 101601.

[220] L. Hall and L. Randall, *U(1)-R symmetric supersymmetry*, *Nucl. Phys. B* **352** (1991) 289–308.

[221] G. D. Kribs, E. Poppitz, and N. Weiner, *Flavor in supersymmetry with an extended R-symmetry*, *Phys. Rev. D* **78** (2008) 055010, [arXiv:0712.2039].

[222] E. Dudas, M. Goodsell, L. Heurtier, and P. Tziveloglou, *Flavour models with Dirac and fake gluinos*, *Nucl. Phys. B* **884** (2014) 632–671, [arXiv:1312.2011].

[223] P. Fayet, *Supergauge Invariant Extension of the Higgs Mechanism and a Model for the electron and Its Neutrino*, *Nucl. Phys. B* **90** (1975) 104–124.

[224] P. Fayet, *Fermi-Bose Hypersymmetry*, *Nucl. Phys. B* **113** (1976) 135.

[225] M. Dine and D. MacIntire, *Supersymmetry, naturalness, and dynamical supersymmetry breaking*, *Phys. Rev. D* **46** (1992) 2594–2601, [hep-ph/9205227].

[226] P. J. Fox, A. E. Nelson, and N. Weiner, *Dirac gaugino masses and supersoft supersymmetry breaking*, *JHEP* **0208** (2002) 035, [hep-ph/0206096].

[227] L. Randall and R. Sundrum, *Out of this world supersymmetry breaking*, *Nucl. Phys. B* **557** (1999) 79–118, [hep-th/9810155].

[228] G. F. Giudice, M. A. Luty, H. Murayama, and R. Rattazzi, *Gaugino mass without singlets*, *JHEP* **9812** (1998) 027, [hep-ph/9810442].

[229] Y. Grossman, B. Shakya, and Y. Tsai, *Neutralino Oscillations at the LHC*, *Phys. Rev. D* **88** (2013) 035026, [arXiv:1211.3121].

[230] U. Sarid and S. D. Thomas, *Mesino - anti-mesino oscillations*, *Phys. Rev. Lett.* **85** (2000) 1178–1181, [hep-ph/9909349].

[231] J. Berger, C. Csaki, Y. Grossman, and B. Heidenreich, *Mesino Oscillation in MFV SUSY*, *Eur. Phys. J. C* **73** (2013) 2408, [arXiv:1209.4645].

[232] S. M. Bilenky and S. T. Petcov, *Massive neutrinos and neutrino oscillations*, *Rev. Mod. Phys.* **59** (Jul, 1987) 671–754.

[233] L. Wolfenstein, *Different varieties of massive dirac neutrinos*, *Nuclear Physics B* **186** (1981), no. 1 147 – 152.

[234] S. Petcov, *On pseudo-dirac neutrinos, neutrino oscillations and neutrinoless double $\beta$-decay*, *Physics Letters B* **110** (1982), no. 3–4 245 – 249.

[235] M. Kobayashi and C. Lim, *Pseudo Dirac scenario for neutrino oscillations*, *Phys. Rev. D* **64** (2001) 013003, [hep-ph/0012266].

[236] J. Schechter and J. W. F. Valle, *Neutrino masses in su(2) $\bigotimes$ u(1) theories*, *Phys. Rev. D* **22** (Nov, 1980) 2227–2235.

[237] S. Bray, J. S. Lee, and A. Pilaftsis, *Resonant CP violation due to heavy neutrinos at the LHC*, *Nucl. Phys. B* **786** (2007) 95–118, [hep-ph/0702294].

[238] H. K. Dreiner, H. E. Haber, and S. P. Martin, *Two-component spinor techniques and feynman rules for quantum field theory and supersymmetry*, *Physics Reports* **494** (Sept., 2010) 1–196.

[239] **Particle Data Group** Collaboration, J. Beringer et al., *Review of Particle Physics (RPP)*, *Phys. Rev. D* **86** (2012) 010001.

[240] M. Martone and D. J. Robinson, *Flavor Oscillation from the Two-Point Function*, *Phys. Rev. D* **85** (2012) 045006, [arXiv:1103.3486].

[241] C. Frugiuele, T. Gregoire, P. Kumar, and E. Ponton, *'L=R' – $U(1)_R$ Lepton Number at the LHC*, *JHEP* **1305** (2013) 012, [arXiv:1210.5257].

[242] E. Bertuzzo, C. Frugiuele, T. Gregoire, and E. Ponton, *Dirac gauginos, R symmetry and the 125 GeV Higgs*, arXiv:1402.5432.

[243] R. Davies, J. March-Russell, and M. McCullough, *A Supersymmetric One Higgs Doublet Model*, *JHEP* **1104** (2011) 108, [arXiv:1103.1647].

[244] C. Frugiuele and T. Gregoire, *Making the Sneutrino a Higgs with a $U(1)_R$ Lepton Number*, *Phys. Rev. D* **85** (2012) 015016, [arXiv:1107.4634].

[245] C. Frugiuele, T. Gregoire, P. Kumar, and E. Ponton, *'L=R' - $U(1)_R$ as the Origin of Leptonic 'RPV'*, *JHEP* **1303** (2013) 156, [arXiv:1210.0541].

[246] F. Riva, C. Biggio, and A. Pomarol, *Is the 125 GeV Higgs the superpartner of a neutrino?*, *JHEP* **1302** (2013) 081, [arXiv:1211.4526].

[247] J. R. Ellis, G. Gelmini, C. Jarlskog, G. G. Ross, and J. Valle, *Phenomenology of Supersymmetry with Broken R-Parity*, *Phys. Lett. B* **150** (1985) 142.

[248] G. G. Ross and J. Valle, *Supersymmetric Models Without R-Parity*, *Phys. Lett. B* **151** (1985) 375.

[249] R. Barbier, C. Berat, M. Besancon, M. Chemtob, A. Deandrea, et al., *R-parity violating supersymmetry*, *Phys. Rept.* **420** (2005) 1–202, [hep-ph/0406039].

[250] P. Fayet, *Spontaneously Broken Supersymmetric GUTs With Gauge Boson / Higgs Boson Unification*, *Phys. Lett. B* **142** (1984) 263.

[251] C. Csaki, J. Goodman, R. Pavesi, and Y. Shirman, *The $m_D - b_M$ Problem of Dirac Gauginos and its Solutions*, *Phys. Rev. D* **89** (2014) 055005, [arXiv:1310.4504].

[252] K. Benakli and M. Goodsell, *Dirac Gauginos in General Gauge Mediation*, *Nucl. Phys. B* **816** (2009) 185–203, [arXiv:0811.4409].

[253] K. Benakli and M. Goodsell, *Dirac Gauginos, Gauge Mediation and Unification*, *Nucl. Phys. B* **840** (2010) 1–28, [arXiv:1003.4957].

[254] R. M. Barnett, J. F. Gunion, and H. E. Haber, *Discovering supersymmetry with like sign dileptons*, *Phys. Lett. B* **315** (1993) 349–354, [hep-ph/9306204].

[255] M. Guchait and D. Roy, *Like sign dilepton signature for gluino production at CERN LHC including top quark and Higgs boson effects*, *Phys. Rev. D* **52** (1995) 133–141, [hep-ph/9412329].

[256] H. Baer, X. Tata, and J. Woodside, *Multi - lepton signals from supersymmetry at hadron super colliders*, *Phys. Rev. D* **45** (1992) 142–160.

[257] H. Baer, C.-h. Chen, F. Paige, and X. Tata, *Signals for minimal supergravity at the CERN large hadron collider. 2: Multi - lepton channels*, *Phys. Rev. D* **53** (1996) 6241–6264, [hep-ph/9512383].

[258] J. A. Evans and Y. Kats, *LHC searches examined via the RPV MSSM*, arXiv:1311.0890.

[259] CMS Collaboration Public Note, *Search for Pair-production of First Generation Scalar Leptoquarks in pp Collisions at sqrt s = 8 TeV*, *CMS-PAS-EXO-12-041,* (2014). http://cds.cern.ch/record/1742179/files/EXO-12-041-pas.pdf.

[260] **CMS Collaboration** Collaboration, V. Khachatryan et al., *Search for heavy neutrinos and W bosons with right-handed couplings in proton-proton collisions at sqrt(s) = 8 TeV*, arXiv:1407.3683.

[261] CMS Collaboration Public Note, *Search for pair-production of second generation leptoquarks in 8 tev proton-proton collisions*, *CMS-PAS-EXO-12-042,* (2013). http://cds.cern.ch/record/1542374/files/EXO-12-042-pas.pdf.

[262] W. Beenakker, R. Hopker, M. Spira, and P. Zerwas, *Squark and gluino production at hadron colliders*, *Nucl. Phys. B* **492** (1997) 51–103, [hep-ph/9610490].

[263] A. Kulesza and L. Motyka, *Threshold resummation for squark-antisquark and gluino-pair production at the LHC*, *Phys. Rev. Lett.* **102** (2009) 111802, [arXiv:0807.2405].

[264] A. Kulesza and L. Motyka, *Soft gluon resummation for the production of gluino-gluino and squark-antisquark pairs at the LHC*, *Phys. Rev. D* **80** (2009) 095004, [arXiv:0905.4749].

[265] W. Beenakker, S. Brensing, M. Kramer, A. Kulesza, E. Laenen, et al., *Soft-gluon resummation for squark and gluino hadroproduction*, *JHEP* **0912** (2009) 041, [arXiv:0909.4418].

[266] W. Beenakker, S. Brensing, M. Kramer, A. Kulesza, E. Laenen, et al., *Squark and Gluino Hadroproduction*, *Int. J. Mod. Phys. A* **26** (2011) 2637–2664, [arXiv:1105.1110].

[267] M. D. Goodsell and P. Tziveloglou, *Dirac Gauginos in Low Scale Supersymmetry Breaking*, arXiv:1407.5076.

# VITA

Seyda Ipek was born and raised in Karabük, Turkey. If you do not know where Karabük is, do not worry, even most Turkish people cannot spot it on the map. (It is 500 km east of Istanbul, close to the Black Sea coast, to give a more familiar reference point.) Seyda finished high school in Karabük in 2004.

She moved to Ankara to study at Bilkent University in the physics department. She graduated with a B.Sc. degree in 2008. Wanting to learn more theoretical physics she started a master's degree at Koc University in the great city of Istanbul, working with Tekin Dereli. She defended her M.Sc. thesis, titled "2+1 Dimensional Gravity Theories", in 2010. She also moved to Seattle to start her Ph.D. in physics at the University of Washington, Seattle that year. She finished her graduate studies, which is the subject of this thesis, in 2015.